HEAT TRANSFER ANALYSIS DURING THE PROCESS OF INJERA BAKING BY FINITE ELEMENT METHOD

By

Gashaw Getenet

A Thesis Submitted to the School of Graduate Studies of Addis Ababa University in Partial Fulfillment of the Requirements for the Degree of Masters of Science in Mechanical Engineering (With Specialization in Thermal Engineering)

Advisor: Dr.Ing. Demiss Alemu

November 2011

Acknowledgment

I would like to express my deepest gratitude to my advisor Dr.Ing Demiss Alemu for sharing his wealth of knowledge and making himself available for guidance at various stages of this work.

I would also like to thank my co-advisor Ato Abdulkadir Aman for his friendly approach and invaluable support both in material and idea.

My last but not least appreciation goes to mechanical engineering department staff members; Addis Tesfaye, Ermias Sisay, and Yesuf Detemo for sharing their office with me.

Gashaw Getenet

Addis Ababa institute of technology

November 2011

ABSTRACT

The main objective of this study was the modeling and simulation of the heat transfer during the process of injera baking. In doing these, mathematical models and finite element formulations for baking pan and injera during baking was developed. In this study, thermo physical properties of injera were studied analytically and were used for the temperature profile prediction using the numerical model. The main properties of interest were specific heat capacity, thermal conductivity, and density.

The mathematical model of injera during baking employs the coupled partial differential equations proposed by Luikov. Resulting system of non linear partial differential equations in time and two space dimensions were reduced to algebraic system by applying the finite element numerical method. The fundamental two-dimensional axisymmetric transient finite element model with triangular elements to predict the heat transfer for the baking pan and heat and mass transfer that occur during baking of injera was solved using the Finite Element Method by MATLAB. The backward difference time stepping technique was used for the transient analysis.

The simulation was done in terms of temperature profile during heat up, and cyclic injera baking. Simulation was carried out for four different input heated oil temperatures (250, 275, 300, and $325°C$) and for four different electric power sources (1.867, 2.2, 2.5, and $3kW$). Two types of baking pans (clay and ceramic) with different thicknesses were investigated. Experiments on conventional clay baking pan were conducted to measure heat up time, and mass balance of batter and injera. The heat up time obtained from simulation was compared with experimental test; from the comparison a relatively good agreement was obtained.

The energy utilization and efficiency of electric baking pans were determined based on the amount of energy baking pans use in a baking session for a given power input. A relatively better efficiency was obtained for $10mm$ thick clay and $8mm$ thick ceramic baking pans with a power source of $2.5kW$. While the $10mm$ pan was not practically realized, the $8mm$ ceramic pan manufactured by Tabor ceramic factory is currently under study.

Key Words: Finite element method, Injera, Heat and Mass Transfer, Simulation, Efficiency.

Table of contents

List of Tables

List of Figures

Nomenclature

Symbol	Meaning	SI unit
A	Area	(m^2)
V	Average fluid velocity	(m/s)
h_b	Boiling heat transfer coefficient	$(W/m^2.K)$
L	Characteristic dimension	(m)
h_c	Convective heat transfer coefficient	$(W/m^2.K)$
I	Current through the resistor	(A)
ρ	Density	(kg/m^3)
D	Diffusion coefficient	(m^2/s)
μ	Dynamic viscosity	$(N.s/m^2)$
Γ	Element boundary	-
ε	Emissivity	-
h	Enthalpy	(kJ/kg)
g	Gravitational acceleration	(m/s^2)
$\dot{Q}_v$	Heat generation per unit area	(W/m^2)
Q	Heat lost or gained	(J)
v	Kinematic viscosity	$(N.s/m^2)$
h_{fg}	Latent heat	(J/kg)
m	Mass	(kg)
x_i	Mass fraction of i^{th} component	-
Nu	Nusselt number	-
P	Power developed in the resistor	(W)
h_r	Radiative heat transfer coefficient	$(W/m^2.K)$
q	Rate of heat input	(W)
ε_r	Ratio of vapor diffusion coefficient to the coefficient of total	

	moisture diffusion	-
Ra	Rayleigh number	-
R	Resistance of the resistor	(Ω)
Re	Reynolds number	-
c_p	Specific heat	$(J/kg.K)$
δ	Stefan-Boltzmann constant	-
ΔT	Temperature change	(K)
k	Thermal conductivity	$(W/m.K)$
δ_t	Thermo-gradient coefficient	(J/kg)
α	Thermal diffusivity	(m^2/s)
t	Time	(s)
β	Volumetric expansion coefficient	$(1/K)$
N_i	Weighting function	-

Subscripts and superscripts

ap	Apparent
a	Ash
ave	Average
c	Carbohydrate
eff	Effective
e	Element
f	Fat
o	Initial
p	Protein
s	Surface
∞	Surrounding /ambient
w	Water

CHAPTER ONE
INTRODUCTION

Food processing involves heating or cooling of food materials of various compositions over a broad range of temperatures. The optimal design of processes requires knowledge of engineering properties of the food materials including thermal and physical properties as a function of variables that are relevant to processing conditions. Design of baking processes is possible through the use of mathematical models. Mathematical modeling enables a mathematical definition to the baking process and allows quantifying the interactions between the product and the baking pan environment.

According to Luikov, baking is modeled generally as a simultaneous heat and mass transfer process. Lukov's heat and mass transfer model in capillary porous media has been employed to simulate temperature and moisture movement during baking of various food stuffs [12, 16, 21, 40, 45, 50, 51, and 52]. Knowledge of accurate heat and mass transfer parameters is important for modeling processes during which simultaneous heat and mass transfer take place. Baking is one such process which is performed by putting the food material on hot pan until it is cooked.

During the baking process, heat is transferred from the hot pan to the surface of the food material, while moisture is transferred from the interior to the surface of the product. As a result, change in *temperature* and *moisture* conditions develop as cooking proceeds, and bring about the desirable characteristics (color, texture, and flavor) of the food.

1.1 Background of the study

Injera is the most popular baked product in Ethiopia and some parts of east Africa. Preparation of injera usually takes two to four days from mixing to cooking. It can be produced from teff and other powdered cereals. The main components of teff injera are carbohydrate, protein, fat, ash, fiber, and moisture constituting the major part. The injera batter is poured on top of a hot baking pan at sizes of two to three millimeters. Injera is said to be baked when its surface temperature changes from the initial temperature to the boiling point of water around that area (90-94^{o}C) [13, 14].

Injera baking pan ("mittad") is a house hold equipment used for the baking of Ethiopian traditional food ("injera").The most widely used types of baking pans use electric and biomass as a source of energy. Baking pans are responsible for the majority of house hold energy consumption [13, 14].

The conventional electric baking pan ("mittad") consists of clay cooking plate (measuring 0.50-0.60m in diameter and 0.02m in thickness) with electric heating elements(resistors) embedded on the grooves at the back side of the baking pan. After the heating elements are buried inside the grooves the bottom of the pan is covered with gypsum for insulation. The pan is supported at the bottom by a flat galvanized iron sheet and on the sides by a cylindrical galvanized iron. The surface of the pan is smooth to create non-sticky surface, so that injera will be easily separated from the pan after baking.

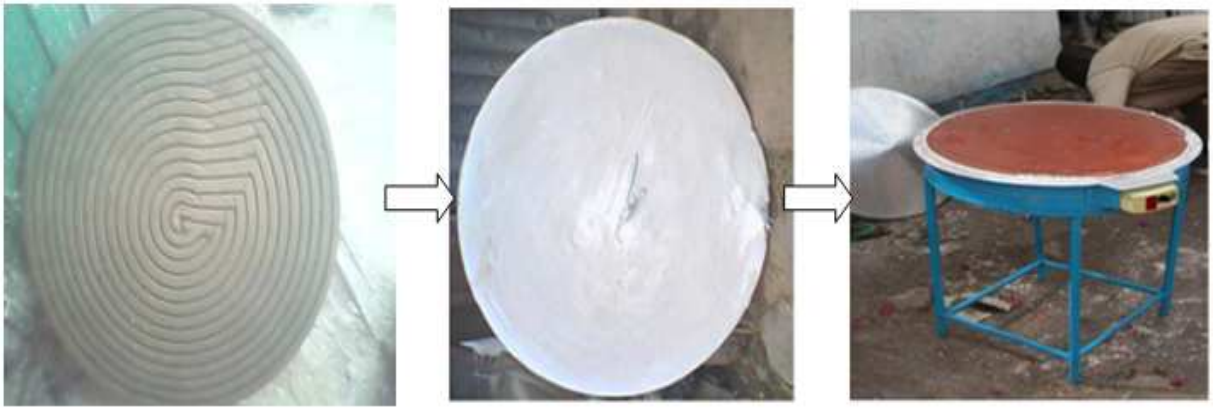

(a) (b) (c)

Figure 1-1: a) Back side of baking pan and its groove b) Baking pan with resistors embedded and molded with gypsum c) Assembled conventional baking pan

The heat transfer during injera baking involves the following processes, heat transfer from different sources (electric or solar sources) to the baking pan ("mittad") , and from the "mittad" to the injera and to the sides of the baking pan through a combination of different modes of heat transfer(radiation , convection, and conduction). A significant amount of energy is lost during the process of injera baking.

A limited research has been done on the heat transfer analysis of injera baking pans (and injera baking in general). An experimental work and modeling of the transient heat transfer analysis of

electric injera baking pan was done by Assefa [2] to obtain optimized geometry of the baking pan ("mittad") and the appropriate power source. Moreover the study of a baking pan with alternative energy source (solar energy using oil as heat transfer medium) was also studied. Assefa in his work proposed $0.01m$ plate thickness with $2.5kW$ power input as an efficient baking pan. Considering the potential use of analyzing the heat transfer during injera baking, where a significant amount of electrical as well as other sources of energy are used, this study will be carried out to obtain preliminary information on the performance of baking pans and power sources.

1.2 Objectives

1.2.1 General objectives

The general objective of this thesis was the modeling and simulation of heat transfer in injera and baking pan during baking. To achieve this objective a transient heat transfer mathematical model for the baking pan, and a simultaneous heat and mass transfer model for injera during baking was developed followed by finite element formulations. The formulated empirical model was simulated with the appropriate boundary conditions and thermo-physical properties of baking pan and injera.

1.2.2 Specific objectives

The Specific objectives of this thesis are:

- Review of literatures related with:
  - The determination of thermo-physical properties.
  - Modeling of different food processing.
- Study geometry of the baking pan, injera, and prepare a simplified model for the analysis.
- Determination of thermo-physical property of injera.
- Determination of boundary conditions.
- Perform experimental investigation on existing electric injera baking pans.
- Conduct simulations during heat up and cyclic injera baking for different types of baking pans (clay, and ceramic), and different power sources.
- Determination of efficiency, and proposing energy efficient baking pan.

CHAPTER TWO
LITRATURE REVIEW

A substantial number of studies have been reported in the literature on food processing (drying, baking, frying etc). Some of them are reviewed in this section. The literature review part of this thesis consists of two sections. The first section is a review of thermo-physical properties of food stuffs and their determination. The second section reviews the heat transfer theories, models, and the relevant numerical techniques used in food processing.

2.1 Thermo-physical Properties

Thermo-physical properties of foods are important for modeling and optimization of processes involving heating and cooling. The properties used in a mathematical model of heat transfer are usually thermal conductivity (k), specific heat (c_p), and density (ρ). An improved knowledge of these thermo-physical properties of foods is essential in accurately predicting temperature changes, process duration, and energy consumption during processing. Among these properties, specific heat and density are significant in analyzing mass energy balances; thermal conductivity is the key property in determining the rate of thermal energy transfer within a material by conduction; and the combination of these three properties, thermal diffusivity, is a key property in the analysis of transient heat transfer. In the past years, much research have been involved to determine thermo-physical property of different food stuffs: soy been [43], chick pea [34], bread dough [12, 21, 40, 45, 49, 50, 51], Indian flat bread (chapatti)[18], cereal flours[17] are some of them.

The thermo-physical properties of a food depends on the temperature, the material chemical composition (i.e. carbohydrate, fat, protein, ash, fiber and water contents), and physical structure. Since foodstuffs are composite materials, it is apparent that the relevant information is the average value. This value is clearly some function of those of the components [1, 23, 25, 34, and 42].

Thermo-physical properties of food stuffs can either be obtained experimentally or using analytical methods based on composition. In this thesis, the analytical method based on

composition is used for the determination of thermo-physical property of injera. The analytical method uses composition data in conjunction with temperature dependent mathematical models of the thermal properties of individual components. The percentage composition of the major components of fermented cereals is given in the FAO report [15]. The percentage composition of teff injera taken from the FAO report is shown in Table 2-1.

Table2-1: Percentage composition of injera

Major components	Percentage by mass, (%)
Carbohydrate	33.9
Protein	4.2
Fiber	1.7
Ash	1.5
Fat	0.6
Moisture	58.1

2.1.1 Specific Heat Capacity

The specific heat of food stuff is defined as the quantity of thermal energy associated with a unit mass of the food and a unit of change in temperature. This thermo-physical property is often referred to as heat capacity and is an essential component of a thermal energy analysis on a food product, a thermal process, or processing equipment used for heating or cooling of a food.

Specific heat capacity depends on the nature of the heat addition process in terms of either at constant pressure or at constant volume. However, since pressure change in heat transfer problems of food materials are usually very small, the specific heat at constant pressure is most often considered [1, 2].

Specific heat is the ratio of heat losses or gained to temperature change for a unit mass [24, 33, 37, 41, and 46]:

$$c_p = \frac{Q}{m\Delta T} \tag{2.1}$$

Where:

c_p = specific heat$(J/kg.K)$,

Q=heat loss or gained (J),

ΔT =temperature change(K), and

m= mass of the food(kg).

In the past, different empirical equations have been proposed by different researchers to determine specific heat. One of the earliest models to calculate specific heat was proposed by Siebel (1892) [33]:

$$c_p = 0.837+3.349x_w \tag{2.2}$$

Where:

x_w= mass fraction of water.

The influence of product components was expressed in an empirical equation proposed by charm (1978) as [23, 33]:

$$c_p = 4187x_w+2093x_f+1256x_s \tag{2.3}$$

Where:

x_f= mass fraction of fat, and, x_s= mass fraction of solids.

Choi and okos (1983) gave a more generalized equation for specific heat which takes into account the composition of food [1, 33] as:

$$c_p = 4180x_w+1711x_p+1928x_f+1547x_c+0.908x_a \tag{2.4}$$

Where:

x=mass fraction of each component, and

The subscripts are:

w=water, p =protein, f =fat, c =carbohydrate, and a =ash.

An additional dimension of the dependence of specific heat on composition was suggested by heldman and singh [23]:

$$c_p = 4187x_w + 1549x_p + 1675x_f + 1424x_c + 0.837x_a \quad (2.5)$$

Gupta (1990) suggested the following equation to determine the specific heat of food products as a function of temperature and water content in a range of 303-336K and in a moisture content range of 0.1%-80%.

$$c_p = 2477 + 2356x_w + 3.79T \quad (2.6)$$

A more comprehensive model for the prediction of specific heat of food was published by Choi and okos [17, 23, 25, 42, and 46]:

$$c_p = \sum_{j=1}^{n} x_j c_{pj} \quad (2.7)$$

$$= x_w c_{pw} + x_p c_p + x_f c_{pf} + x_c c_{pc} + x_a c_{pa} + x_{fib} c_{pfib}$$

Where:

c_p= specific heat($J/kg.K$),

c_{pj}= specific heat of the components of the food($J/kg.K$), and

x_j= percentage composition of the components.

Empirical equations used for the determination of the specific heat of the major components of a food (c_{pj}) are given in Table 2-2 [1, 23, 25, and 42].

Table2-2: Models of specific heat for major components of foods

	Components	Equations
$c_p(J/kg.K)$	Carbohydrate	$c_p = 1.5488 + 1.9625\times10^{-3}T - 9399\times10^{-6}T^2$
	Ash	$c_p = 1.0926 + 1.8896\times10^{-3}T - 3.6817\times10^{-6}T^2$
	Fiber	$c_p = 1.8459 + 1.8306\times10^{-3}T - 4.6509\times10^{-6}T^2$
	Fat	$c_p = 1.9842 + 1.4733\times10^{-3}T - 4.8008\times10^{-6}T^2$
	Protein	$c_p = 2.0082 + 1.2089\times10^{-3}T - 1.3129\times10^{-6}T^2$
	Water(0<T<150)	$c_p = 4.1762 - 9.0864\times10^{-5}T + 5.4731\times10^{-6}T^2$

2.1.2 Thermal Conductivity

Thermal conductivity of a food is the quantity of heat that flows per unit time through a food of unit thickness and unit area having unit temperature difference. Thermal conductivity can be either determined experimentally or through mathematical estimation. A simplified approximation for thermal conductivity is given as [1, 24, 26, 37, and 41]:

$$k = \frac{\dot{Q}x}{A\Delta T} \tag{2.8}$$

Where:

k= thermal conductivity ($W/m.K$),

$\dot{Q}$= rate of heat input (W),

x= material thickness parallel to heat flow(m),

ΔT=temperature change (^oC), and

A=contact area normal to direction of heat flow(m^2).

A number of physical models have been proposed to predict thermal conductivity of foods. The most common models are those assuming that different components are arranged in layers either parallel or normal to the heat flow, resulting in the following expressions based on the electric analogy of heat transmission [25, 42].

Series model:- in this model, layers of components placed normal to the heat flow, in a series arrangement of resistances and the effective thermal conductivity k can be calculated as follows:

$$k = \frac{1}{\sum_{i=1}^{n} \varepsilon_i / k_i} \tag{2.9}$$

Where:

k= thermal conductivity ($W/m.K$),

ε_i= volume fraction of i^{th} component phase(m^3), and

k_i= thermal conductivity of i^{th} phase ($W/m.K$).

Parallel model: - in this model, layers of components are placed in the direction of the heat flow, in parallel arrangements of resistances. The effective thermal conductivity is given by:

$$k = \sum_{i=1}^{n} k_i \varepsilon_i \tag{2.10}$$

The volume fractions in Eq. (2.9) and Eq. (2.10) can be calculated from the mass fractions x_i and intrinsic densities ρ_i as:

$$\varepsilon_i = \frac{x_i/\rho_i}{\sum_{i=1}^{n} x_i/\rho_i} \tag{2.11}$$

Where:

ε_i = volume fraction of each food composition(m^3),

ρ_i= density of each food composition(kg/m^3), and

x_i= mass or weight fraction of each food composition.

Random model: Woodside and messmer (1961) proposed an intermediate model, which is the weighted geometric mean of the component phases and can be written as [25, 42]:

$$k = k_1^{\varepsilon_1} k_2^{\varepsilon_2} k_3^{\varepsilon_3} \dots\dots k_n^{\varepsilon_n} \tag{2.12}$$

Another empirical equation is developed by sweert for solid and liquid foods [34]:

$$k = 0.58x_w + 0.155x_p + 0.16x_f + 0.25x_c + 0.135x_a \tag{2.13}$$

Marakami and okos (1989) considered thermal properties of 15 different food powders from literature and observed that all data points fall on the range defined by values predicted by series and parallel models. It was observed that the parallel model defined the upper limit while the series model defined the lower limit of the predictions [1].

An empirical relation for the determination of thermal conductivity of major components of foods is given in Table 2-3, [1, 23, 25, and 42].

Table 2-3: Models for thermal conductivity of major components of foods

	Components	Equations
$k(W/m.K)$	Carbohydrate	$k = 0.20141+1.3874\times10^{-3}T - 4.3312\times10^{-6}T^2$
	Ash	$k = 0.32962+1.4011\times10^{-3}T - 2.9069\times10^{-6}T^2$
	Fiber	$k = 0.18331+1.2497\times10^{-3}T - 3.1683\times10^{-6}T^2$
	Fat	$k = 0.18071+2.7604\times10^{-4}T - 1.7749\times10^{-7}T^2$
	Protein	$k = 0.17881+1.1958\times10^{-3}T - 2.7178\times10^{-6}T^2$
	Water	$k = 0.57109+1.7625\times10^{-3}T - 6.7036\times10^{-6}T^2$

2.1.3 Density

Density is the ratio of mass to volume of a material. Density of food products is an important property in analyzing food processing operations. Density is closely related to porosity and moisture content of food. The structure of food materials can be characterized by density (apparent and true), porosity, specific volume, particle density shrinkage and so on. Among these, density and porosity are the most common structural properties.

Apparent density (ρ_{ap}): concerns powdered and porous materials and it is determined by the mass of the sample and its apparent volume.

$$\rho_{ap} = \frac{m_t}{V_t} \tag{2.14}$$

Where: m_t is the total mass, and V_t is the total volume of the sample including the pores.

True density (ρ_T): is the density excluding all pores and it is determined by the mass of the sample and its true volume.

$$\rho_T = \frac{m_t}{V_p} \tag{2.15}$$

Where: $V_p = V_s+V_w$, is the total volume of the sample excluding pores (volume of dry solids and water).

Density is an intensive property it depends directly on the mass fractions of the major components of the food and can be found from [7, 23, 25, and 42]:

$$\rho = \frac{1}{\sum_{i=1}^{n} x_i/\rho_i} \tag{2.16}$$

Where:

ρ= density of the product (kg/m^3),

ρ_i= density of each food composition(kg/m^3), and

x_i= mass or weight fraction of each food composition.

An empirical relation for the determination of density of major food components as a function of temperature is given in Table 2-4 [1, 23, 25, and 42].

Table 2-4: Models for density of major components of foods

	Components	Equations
$\rho(kg/m^3)$	Carbohydrate	$\rho = 1.5991\times10^3$-$0.31046T$
	Ash	$\rho = 2.4238\times10^3$-$28063T$
	Fiber	$\rho = 1.3115\times10^3 - 0.36589T$
	Fat	$\rho = 9.2559\times10^2 - 0.41757T$
	Protein	$\rho = 1.3299\times10^3 - 0.51840T$
	Water(0<T<150)	$\rho = 997.18+3.1439\times10^{-3}T - 3.7574\times10^{-3}T^2$

2.1.4 Thermal Diffusivity

Thermal diffusivity indicates how fast heat propagates through a sample while heating or cooling. Thermal diffusivity is a parameter used in the heat transfer calculation by conduction. The rate at which heat diffuses by conduction through a material depends on the thermal diffusivity and can be defined as:

$$\alpha = \frac{k}{\rho c_p} \tag{2.17}$$

Where:

α=thermal diffusivity (m^2/s),

ρ =density(kg/m^3),

c_p =specific heat capacity($J/kg.K$)), and

k= thermal conductivity ($W/m.K$).

Thermal diffusivity can be determined either by direct experiment or estimated from the thermal conductivity, specific heat, and density data using Eq. (2.17).

2.1.5 Moisture Diffusivity

Moisture diffusivity, D is the rate at which moisture diffuses through a material. Moisture diffusivity is an important transport property necessary for the design and optimization of all the processes that involve internal moisture movement. Fick's second law is used in liquid diffusion theory to establish moisture diffusion as a function of the concentration gradient [25, 42]:

$$\frac{\partial w}{\partial t} = \frac{\partial}{\partial x}\left(D\frac{\partial w}{\partial x}\right) \tag{2.18}$$

Where:

w = concentration(kg/m^3),

t = time(s),

x = material thickness along direction of mass transfer(m), and

D = diffusion coefficient (m^2/s).

2.2 Heat Transfer Theories, Models, and their Application in Food Processing

This section reviews the heat transfer theories with phase change, the models to which the heat transfer theories apply, and the different types of numerical techniques used in food processing.

2.2.1 Heat Transfer with Phase Change Theories

The analysis of heat and mass transfer in a food system is very important because food properties change with temperature and moisture movement during the process. A mathematical model used to describe simultaneous heat and mass transfer during drying and baking was proposed by Luikov [30]. The concepts of irreversible thermodynamics and the concept of moisture transfer potential for water movement in a capillary porous body are applied in the model. The Lukov's mathematical model employs the following two assumptions. Pressure gradients within the porous body are very small, and external resistance to heat and mass transfer is negligible [58].

The interrelation between liquid and heat transfer becomes closer when liquid evaporates inside the porous body. In this case mass inside the capillary porous body transfers not only in the form of liquid but in the form of vapor as well. For this reason using separately differential equations (Fourier's equation for heat transfer and Fick's equation for mass transfer), the interrelated differential equations are employed for heat and mass transfer in capillary porous bodies [30].

2.2.2 Heat Transfer Models and their Application in Food Processing

Various mathematical models have been developed for different types of food stuffs and are applied for different types of food processing (frying, drying, and baking). Some of the models are reviewed as follows.

Adefemi Farinu [1] shows the relationship between heat transfer coefficient and mass transfer coefficient in determining the rate of heat and mass transfer during frying of potato chips under turbulent condition of frying. Comini and Lewis [9] use the finite element method for the numerical solution of two dimensional heat and mass transfer problems in porous medium. A model for simultaneous heat, water and vapor diffusion was developed by Thorvaldsen, and Janestad, [24] to use for the prediction of the diffusion of water inside foods during heat processing. The model was based on Fourier's and Fick's laws applied for drying process.

A model for convective oven cake baking process was investigated [31] by experimental and numerical methods as a simultaneous heat and mass transfer process. The heat and mass transfer mechanisms were defined by Fourier's and Fick's second laws respectively. A heat and moisture transfer model was developed by Sabapathy [34] to predict the heat and moisture transfer within chickpea during cooking.

A set of coupled heat, mass and pressure transfer equations proposed by Luikov [1975] was employed by Irudyaraj [46] to model the heat, Mass and pressure transfer phenomenon in a composite food system during drying. A lot of research has been done on bread baking [12, 16, 21, 40, 45, 50, 51, and 52] to investigate simultaneous heat and mass transfer analysis.

2.2.3 Numerical Techniques Used in Food processing

Numerical solution techniques are usually easier than analytical techniques since engineering problems involve ordinary or partial differential equations which may not be solved with the analytical solution techniques. In food process modeling, the finite element and finite difference methods are commonly used especially in solving partial differential equations. The finite difference method is the oldest discretization method for the numerical solution of differential equations. The latest numerical technique, the finite element method has been successfully used to model several food processing operations, among this, frying [1, 51], bread baking [9, 16], and drying [46] are some of them.

The most attractive feature of the finite element method is its ability to handle complex geometries (and boundaries) with relative ease. While finite difference method in its basic form is restricted to handle simple shapes. The handling of geometries in finite element method is theoretically straightforward although the problem of computational time is strongly influenced by the ability to precondition the problem. More over the finite element method can handle non – homogeneous materials easily. In comparison with the finite element method the finite difference method is very easy to implement. Because of its advantage to handle complex geometries and composite materials the finite element method is used for this study.

CHAPTER THREE

MATHEMATICAL MODELING AND FINITE ELEMENT FORMULATION

A mathematical model representing heat and mass transfer for injera and transient heat transfer for the baking pan during baking was developed in this chapter. The model for the injera employs the coupled partial differential equations proposed by Luikov; where as the model for the baking pan is a two dimensional transient heat conduction in a solid. The resulting system of non linear partial differential equations in time and two space dimensions are reduced to algebraic system by applying the finite element method.

3.1 Assumptions and Heat Balance Models

The following modeling assumptions and heat balance models with regard to the baking pan and injera were made to simplify the mathematical modeling and finite element formulation.

- The initial temperature and moisture distribution of batter are uniform.
- Heat transfer is two dimensional, unsteady, and in the radial and axial directions.
- Both the baking pan and injera are modeled as axisymmetric.
- Thickness of injera is assumed to be uniform.
- The effect of pressure gradient is negligible.

Heat flows from the heating units (electric, oil) to the different components, and to the injera in the following paths [13].

- From the heating elements to the baking pan via conduction and convection.
- Heat transfer at the plate surface is assumed to be via radiation and convection to constant temperature surroundings when the plate is empty, and directly via conduction (associated with nucleate boiling) when injera batter is present. When the batter is present it is assumed that the batter will be heated up to the boiling temperature of water in that area.
- From the baking pan to the sides through conduction. Heat is then lost through convection from the sides to the surrounding.

- Heat is lost through the sand gravels at the bottom of the baking pan via conduction and lost via convection to the surrounding.
- Heat is lost to the surrounding through the lid cover of the baking pan via convection and radiation.

3.2 Mathematical Modeling for Baking Pan

The transient heat conduction through the baking pan can be given as [11, 29, 37, 40, 44, and 47]:

$$\rho c_p \frac{\partial T}{\partial t} = div(k\nabla T) + \dot{Q}_v \tag{3.1}$$

Where:

ρ=density (kg/m^3), c_p = specific heat capacity ($J/kg.K$), T= temperature (K), t= time (s) and k = thermal conductivity ($W/m.K$), and $\dot{Q}_v$=volumetric heat generation(W/m^3).

For a constant thermal conductivity and cylindrical coordinate system Eq. (3.1) can be written as:

$$\frac{\partial T}{\partial t} = \alpha\left(\frac{\partial^2 T}{\partial r^2} + \frac{1}{r}\frac{\partial T}{\partial r} + \frac{\partial^2 T}{\partial z^2}\right) + \frac{\dot{Q}_v}{k} \tag{3.2}$$

Where:

$\alpha = \frac{k}{\rho c_p}$, is the thermal diffusivity, and $\nabla^2 = \frac{\partial^2 T}{\partial r^2} + \frac{1}{r}\frac{\partial T}{\partial r} + \frac{\partial^2 T}{\partial z^2}$, is the Laplacian operator in cylindrical coordinate system.

3.2.1 Initial, Boundary, and Symmetry Conditions

Initial Condition:

The baking pan is initially at a constant room temperature.

$$T_{room} = T(r,z)|_{t=0} = 20℃ \tag{3.3}$$

Boundary Conditions:

The boundary condition at the top surface of baking pan is:

$$-\left(k\frac{\partial T}{\partial n}\right)_{(r,z,t)} = h_{c1}\times(T_s - T_\infty) \tag{3.5}$$

Where:

$h_{c1} = h_c + h_r$ -is the convective and radiative heat transfer coefficient at the surface of the pan($W/m^2.K$).

The boundary condition at the bottom surface of the electric baking pan is:

$$-\left(k\frac{\partial T}{\partial n}\right)_{(r,0,t)} = h_{c2}\times(T_s - T_\infty) \tag{3.4}$$

Where:

$k\frac{\partial T}{\partial n}$= amount of heat passing into the body,

h_{c2} = convective heat transfer coefficient at the bottom surface of the pan($W/m^2.K$),

T_s=surface temperature of the pan (^oC), and

T_∞=ambient temperature (^oC).

The boundary condition at the bottom of the oil baking pan is:

$$-\left(k\frac{\partial T}{\partial n}\right)_{(r,0,t)} = h_{c3}\times(T_s - T) \tag{3.6}$$

Where:

h_{c3}=convective heat transfer coefficient of the oil($W/m^2.K$), and

T=temperature of the oil (^oC).

In addition to the above boundary conditions there is a heat generation load for electric baking pans at the heating coil position [2]. The heat generation load varies depending on the type of heating unit used ($\dot{Q}_{(r,z/2,t)} = 1.867$, 2.2, 2.5, and $3kW$).

Symmetry Condition:

Symmetry can be used to reduce the size of the finite element models significantly. It must be remembered that symmetry is not simply a geometric occurrence. For symmetry, geometry, loading, material properties, and boundary conditions must all be symmetric about an axis to reduce the model.

In the case of the baking pan, the pan is a cylindrical solid, so it is a solid of revolution with the longitudinal axis (z-axis) as the axis of revolution. The baking pan therefore fulfills the geometry symmetry condition.

The loading and boundary conditions of the baking pan are all symmetric to the axis of symmetry. The heating load from the electric resistors is located at $z/2$ of the baking pan, and the difference in distance between successive loops is constant. The boundary conditions; convective boundary conditions, radiative boundary condition, and the initial conditions are all symmetric with the axis of revolution and are independent of the circumferential coordinate θ.

The material properties (density, thermal conductivity, and specific heat etc) are symmetric with the axis of revolution. The baking pan and injera fulfills all the preconditions for symmetry. So they can be modeled with one quarter of the pan and injera, reducing the computational time and space. The axis of symmetry can be taken as insulated boundary condition$\left(\left(k\frac{\partial T}{\partial n}\right)_{(0,z,t)} = 0\right)$.

3.3 Mathematical Modeling for Injera during Baking

In this section, the mathematical modeling for transient heat transfer analysis of injera during baking was done based on the simultaneous heat and mass transfer theory of Luikov. The effect of phase change on the temperature gradient is considered, whereas the effect of pressure is neglected in the modeling.

The *thermal energy* balance for a capillary porous body can be written as [30, 46]:

$$\rho c_p \frac{\partial T}{\partial t} = -div(j_q) - \sum_{j=1}^{3} h_i I_i \tag{3.7}$$

Where:

$\sum_{i=1}^{3} h_i I_i$= heat source or sink, i=1, for moisture in vapor form, 2, for moisture in liquid form, and 3, for moisture in solid form.

j_q = heat flux(W/m^2).

The heat flux can be written using Fourier's law as:

$$j_q = -k\nabla T = -k\left(\frac{\partial T}{\partial r}n_r + \frac{\partial T}{\partial z}n_z\right) \tag{3.8}$$

The source of heat is due to the phase change of the water contained within the body. By neglecting the effect of moisture potential and pressure the heat source can be expressed as:

$$\sum_{j=1}^{2} h_i I_i = I(h_1 - h_2) = Ih_{fg} = \varepsilon_r \rho h_{fg} \frac{\partial m}{\partial t} \tag{3.9}$$

Where$I = \varepsilon_r \rho \frac{\partial m}{\partial t}$, and ε_r=ratio of vapor diffusion coefficient to total moisture diffusion.

Substituting Eqs.(3.8), and (3.9) into Eq. (3.7):

$$\rho c_p \frac{\partial T}{\partial t} = k\nabla^2 T + \varepsilon_r \rho h_{fg} \frac{\partial m}{\partial t} \tag{3.10}$$

The *mass balance* for a capillary porous body can be obtained from the laws of mass conservation

$$\rho \frac{\partial m}{\partial t} = -div(j_m) + I_m \tag{3.11}$$

Where, j_m=mass flux

In addition to the moisture gradient the mass flux can be related with the temperature gradient as follows, this effect is known as the Soret effect:

$$j_m = -D\rho(\nabla m + \delta_t \nabla T) \tag{3.12}$$

Assuming there is no moisture gain during baking and moisture exists as vapor and liquid.

$$I_m = 0 \tag{3.13}$$

Substituting Eqs.(3.12), and (3.13) into Eq. (3.11):

$$\frac{\partial m}{\partial t} = D\nabla^2 m + D\delta_t \nabla^2 T \tag{3.14}$$

Where, D= moisture diffusivity, δ_t=thermo-gradient coefficient.

The simultaneous partial differential equation for heat and mass transfer will be obtained by substituting Eq. (3.14) into Eq. (3.10):

$$\frac{\partial T}{\partial t} = \frac{\left(k+\varepsilon_r \rho h_{fg} \delta_t D\right)}{\rho C_p} \nabla^2 T + \frac{\varepsilon_r \rho h_{fg} D}{\rho C_p} \nabla^2 m \tag{3.15}$$

Neglecting the effect of moisture gradient and rearranging equation (3.15):

$$\frac{\partial T}{\partial t} = \left(\frac{k}{\rho c_p} + \frac{\varepsilon_r h_{fg} \delta_t D}{c_p}\right) \nabla^2 T \tag{3.16}$$

$$\frac{\partial T}{\partial t} = \left(\frac{k+\varepsilon_r h_{fg} \rho \delta_t D}{\rho c_p}\right) \left(\frac{\partial^2 T}{\partial r^2} + \frac{1}{r}\frac{\partial T}{\partial r} + \frac{\partial^2 T}{\partial z^2}\right) \tag{3.17}$$

$$\frac{\partial T}{\partial t} = \alpha_{eff} \left(\frac{\partial^2 T}{\partial r^2} + \frac{1}{r}\frac{\partial T}{\partial r} + \frac{\partial^2 T}{\partial z^2}\right) \tag{3.18}$$

Where: $\alpha_{eff} = \left(\frac{k+\varepsilon_r h_{fg} \rho \delta_t D}{\rho c_p}\right)$=effective thermal diffusivity

3.3.1 Initial and Boundary Conditions

Initial condition:

The initial condition of the injera batter is:

$$T(r,z)|_{t=0} = 20^{o}C \tag{3.19}$$

Boundary conditions:

The boundary condition for the complete domain of the injera can be expressed as:

$$k\frac{\partial T}{\partial n} = h_b \times (T_\infty - T_s) - j_q \tag{3.20}$$

Where:

h_b=boiling heat transfer coefficient$(W/m^2.K)$,

$(T_\infty - T_s)$, and j_q are heat supplied at the surface, and

$k\frac{\partial T}{\partial n}$ = amount of heat passing into the body.

The boundary condition at the top surface of injera is:

$$k\frac{\partial T}{\partial n} = h_c \times (T_\infty - T_s) - j_q \tag{3.21}$$

Where:

h_c= convective plus radiative heat transfer coefficient over the surface of injera$(W/m^2.K)$,

The boundary condition at the bottom of injera is [2]:

$$T = T_s(t) \tag{3.22}$$

Where:

T_s= contact surface temperature between batter and pan. It can be considered as the boiling point of injera batter.

3.4 Finite Element Formulations

Once the governing partial differential equations are obtained from the mathematical modeling, a series of finite element formulations are performed to obtain a numerical solution of the governing partial differential equations using Galerkin's weighted residual method. The finite element equations were formulated based on the methodologies adopted in different literatures [2, 11, 30, 37, 44, 46, and 47].

Step-1 Identify the Governing Equation

The governing equation for a cylindrical axisymmetric transient heat transfer problem is:

$$\frac{\partial T}{\partial t} = \alpha\left(\frac{\partial^2 T}{\partial r^2} + \frac{1}{r}\frac{\partial T}{\partial r} + \frac{\partial^2 T}{\partial z^2}\right) + \frac{\dot{Q}_v}{k} \tag{3.23}$$

Step-2 Weighted Residual Formulation

The weighted residual equations can easily be obtained by multiplying Eq. (3.23) with the weighting function:

$$\int_{\Omega^e}\left[N_i\left(\frac{1}{\alpha}\frac{\partial T}{\partial t}-\left(\frac{\partial^2 T}{\partial r^2}+\frac{1}{r}\frac{\partial T}{\partial r}+\frac{\partial^2 T}{\partial z^2}\right)+\frac{\dot{Q}_v}{k}\right)d\Omega^e\right] \quad (3.24)$$

Where: N_i- is the weighting function.

Expanding the domain integral:

$$2\pi\int_{A^{(e)}}\left[N_i\left(\frac{1}{\alpha}\frac{\partial T}{\partial t}-\left(\frac{\partial^2 T}{\partial r^2}+\frac{1}{r}\frac{\partial T}{\partial r}+\frac{\partial^2 T}{\partial z^2}\right)+\frac{\dot{Q}_v}{k}\right)rdrdz\right] \quad (3.25)$$

Where: $A^{(e)}$= the area of the element in the rz plane.

Rearranging Eq. (3.25)

$$\iint_{A^e} rN_i\frac{1}{\alpha}\frac{\partial T}{\partial t}drdz-\iint_{A^{(e)}}\left(N_i\frac{\partial}{\partial r}\left(\frac{\partial T}{\partial r}\right)+N_i\frac{\partial}{\partial z}\left(\frac{\partial T}{\partial z}\right)\right)drdz\iint_{A^e} rN_i\frac{\dot{Q}_v}{k}rdrdz=0 \quad (3.26)$$

Applying the chain rule to the second term in equation (3.26):

$$\frac{\partial}{\partial r}\left(rN_i\frac{\partial T}{\partial r}\right)=N_i\frac{\partial}{\partial r}\left(r\frac{\partial T}{\partial r}\right)+r\frac{\partial T}{\partial r}\frac{\partial N_i}{\partial r}\Rightarrow N_i\frac{\partial}{\partial r}\left(r\frac{\partial T}{\partial r}\right)$$

$$=\frac{\partial}{\partial r}\left(rN_i\frac{\partial T}{\partial r}\right)-r\frac{\partial T}{\partial r}\frac{\partial N_i}{\partial r} \quad (3.27)$$

Noting that equation (3.27) is also applicable to the z variable, the residual equations represented by equation (3.26) can be written as:

$$\iint_{A^e} rN_i\frac{1}{\alpha}\frac{\partial T}{\partial t}drdz-\iint_{A^{(e)}}\left(\frac{\partial}{\partial r}\left(rN_i\frac{\partial T}{\partial r}\right)+\frac{\partial}{\partial z}\left(rN_i\frac{\partial T}{\partial z}\right)\right)drdz-\iint_{A^e} rN_i\frac{\dot{Q}_v}{k}rdrdz=0 \quad (3.28)$$

Integrating the second term by parts:

$$\iint_{A^e} rN_i\frac{1}{\alpha}\frac{\partial T}{\partial t}drdz+\iint_{A^{(e)}}\left(\frac{\partial N_i}{\partial r}\frac{\partial T}{\partial r}+\frac{\partial N_i}{\partial z}\frac{\partial T}{\partial z}\right)\mathrm{r}\,drdz-\oint_{\Gamma^e}\left(\frac{\partial T}{\partial r}n_r+\frac{\partial T}{\partial z}n_z\right)rN_i dr-$$

$$\int_{A^{(e)}} rN_i\frac{\dot{Q}_v}{k}rdrdz=0 \quad (3.29)$$

Where Γ is the boundary of the element and n_r and n_z are the radial and axial components of the outward unit vector normal to the boundary. Defining q_Γ using Fourier's law in cylindrical coordinates as:

$$q_\Gamma=q_r+q_z$$

$$= -k\left(\frac{\partial T}{\partial r}n_r - \frac{\partial T}{\partial z}n_z\right) \tag{3.30}$$

Equation (3.29) can now be rewritten as:

$$\iint_{A^e} rN_i \frac{1}{\alpha}\frac{\partial T}{\partial t}drdz + \iint_{A^{(e)}}\left(\frac{\partial N_i}{\partial r}\frac{\partial T}{\partial r} + \frac{\partial N_i}{\partial z}\frac{\partial T}{\partial z}\right) \mathrm{r}\, drdz + \oint_{\Gamma e}\frac{q_\Gamma}{k} rN_i d\Gamma - \int_{A^{(e)}} rN_i \frac{\dot{Q}_v}{k} rdrdz = 0 \tag{3.31}$$

Step -3 Interpolations of Functions

The finite element discretizations reduce the given region (domain) into a finite number of triangular elements. The elements are connected to each other at points called nodes. The nodal points depict the field variable (T) or the unknown defined in terms of approximating or *interpolating functions* within each element. The field variable and its derivatives with respect to position and time as a function of the interpolation functions are given below.

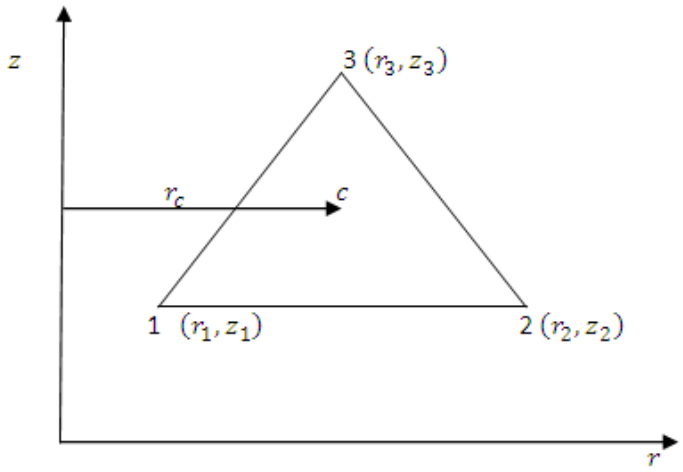

Figure 3-1: Triangular axisymmetric element

$$T(r,z,t) = \sum_{j=0}^{n} N_j\,(r,z)T_j \tag{3.32a}$$

$$\frac{\partial T}{\partial z}(r,z,t) = \sum_{j=0}^{n} N_j\,(r,z)\frac{\partial T_j(t)}{\partial z} \tag{3.32b}$$

$$\frac{\partial T}{\partial r}(r,z,t) = \sum_{j=0}^{n} N_j\,(r,z)\frac{\partial T_j(t)}{\partial r} \tag{3.32c}$$

$$\frac{\partial T}{\partial t}(r,z,t) = \sum_{j=0}^{n} N_j\,(r,z)\frac{\partial T_j(t)}{\partial t} \tag{3.32d}$$

Where n is the total number of node.

Step-4 Evaluation of Element Equations and Assembly

Substituting the interpolation functions into equation (3.31):

$$\iint_{A^e}\left[\left(\frac{1}{\alpha}\right)\sum_{j=0}^{n}N_j\frac{\partial T_j}{\partial t}rdrdz\right]+\iint_{A^{(e)}}\left[\frac{\partial N_i}{\partial r}\sum_{j=0}^{n}N_j\frac{\partial T_j}{\partial r}+\sum_{j=0}^{n}N_j\frac{\partial T_j}{\partial r}\right]\mathrm{r}\,drdz+\int_{\Gamma^e}\frac{q_\Gamma}{k}rN_i d\Gamma-$$

$$\iint_{A^{(e)}}rN_i\frac{\dot{Q}_v}{k}rdrdz=0 \tag{3.33}$$

Simplifying equation (3.33):

$$\underbrace{\left[\iint_{A^e}\frac{1}{\alpha}[N_j][N_i]^T rdrdz\right]}_{[C]^{(e)}}\left\{\frac{\partial T}{\partial t}\right\}+\underbrace{\left[\iint_{A^{(e)}}\left(\left[\frac{\partial N_j}{\partial r}\right]\left[\frac{\partial N_i}{\partial r}\right]^T+\left[\frac{\partial N_j}{\partial z}\right]\left[\frac{\partial N_i}{\partial z}\right]^T\right)\mathrm{r}\,drdz\right]}_{[K]^{(e)}}\{T\}=$$

$$\underbrace{\iint_{A^{(e)}}rN_i\frac{\dot{Q}_v}{k}rdrdz-\int_{\Gamma^e}\frac{q_\Gamma}{k}rN_i d\Gamma}_{\{F\}^{(e)}} \tag{3.33*}$$

Equation (3.33*) can also be written in matrix form as:

$$[C]^{(e)}\{\dot{T}\}+[K]^{(e)}\{T\}=\{F\}^{(e)} \tag{3.34}$$

Where:

$[C]^{(e)}$= mass matrix,

$[K]^{(e)}$ =stiffness matrix, and

$\{F\}^{(e)}$ = thermal load vector.

Step-5 Imposing boundary conditions and further discretizations of element matrices in equation (3.33).

The elemental mass matrix (Eq. (3.34)) can be descritized by representing r using the interpolation function (Eq. (3.36)), and using Eq. (3.37) to integrate area coordinates over the area of a triangular element:

$$[C]^{(e)}=\iint_{A^e}\frac{1}{\alpha}[N_j][N_i]^T rdrdz \tag{3.35}$$

$$r=\sum_{i=0}^{3}N_i r_i \tag{3.36}$$

$$\int_{A^e} N_1^{\theta} N_2^{\beta} N_3^{\gamma} dA^e = \frac{\theta\beta\gamma}{(\theta+\beta+\gamma+2)} 2A \tag{3.37}$$

Where: A is the area of a triangular element.

Substituting equation (3.36) into equation (3.35) and integrating using equation (3.37):

$$[C]^{(e)} = \frac{1}{\alpha}\frac{A}{60}\begin{bmatrix} 6r_1+2r_2+2r_3 & 2r_1+2r_2+r_3 & 2r_1+r_2+2r_3 \\ 2r_1+2r_2+r_3 & 2r_1+6r_2+2r_3 & r_1+2r_2+2r_3 \\ 2r_1+r_2+2r_3 & r_1+2r_2+2r_3 & 2r_1+2r_2+6r_3 \end{bmatrix} \tag{3.37}$$

Similarly the stiffness matrix can be descritized as follows:

$$[K]^{(e)} = \iint_{A^{(e)}} \left(\left[\frac{\partial N_j}{\partial r}\right] \left[\frac{\partial N_i}{\partial r}\right]^T + \left[\frac{\partial N_j}{\partial z}\right] \left[\frac{\partial N_i}{\partial z}\right]^T \right) \mathrm{r}\, drdz \tag{3.39}$$

The shape function for a triangular linear element is given as:

$$N_i = \frac{1}{2A}(a_i+b_i r+c_i r) \tag{3.40}$$

Where a_i ,b_i , and c_i are constants which can be expressed for a triangular element as:

$$\left.\begin{array}{lll} a_1 = r_2 z_3 - r_3 z_2, & a_2 = r_3 z_1 - r_1 z_1 \ , & a_1 = r_1 z_2 - r_2 z_1, \\ b_1 = z_2 - z_3, & b_2 = z_3 - z_1 \ , & b_3 = z_1 - z_2, \\ c_1 = r_3 - r_2, & c_2 = r_1 - r_3, & c_3 = r_2 - r_1. \end{array}\right\} \tag{3.41}$$

The double integral of r is equal to:

$$\iint_{A^{(e)}} \mathrm{r}\, drdz = \iint_{r\ z} rdrdz = Ar_c \tag{3.42}$$

Where r_c = r coordinate value of the centroid defined as:

$$r_c = 1/3\ (r_1+r_2+r_3) \tag{3.43}$$

By substituting equations (3.40), (3.42) and (3.43) into equation (3.39) the element stiffness matrix will then be:

$$[K]^{(e)} = (Ar_c)\left(\left[\frac{b_i}{2A}\right]^T + \left[\frac{c_i}{2A}\right] \left[\frac{c_i}{2A}\right]^T \right)$$

$$= \frac{r_c}{4A}\begin{bmatrix} b_1^2+c_1^2 & b_1b_2+c_1c_2 & b_1b_3+c_1c_3 \\ & b_2^2+c_2^2 & b_3b_2+c_3c_2 \\ & & b_3^2+c_3^2 \end{bmatrix} \quad (3.44)$$

The discretization of the thermal load vector is done as follows:

$$\{F\}^{(e)} = \iint_{A^{(e)}} rN_i \frac{\dot{Q}_v}{k} rdrdz - \oint_{\Gamma^e} \frac{q_\Gamma}{k} rN_i d\Gamma \quad (3.45)$$

Applying the convective plus radiative boundary condition, i.e. substituting Eq. (3.5) into Eq. (3.45) we will get:

$$\{F\}^{(e)} = \iint_{A^{(e)}} rN_i \frac{\dot{Q}_v}{k} rdrdz - \frac{h}{k}\oint_{\Gamma^e} \mathrm{T_s}\, rN_i d\Gamma + \frac{h}{k}\oint_{\Gamma^e} \mathrm{T_\infty}\, rN_i d\Gamma \quad (3.46)$$

The third term in the right hand side of Eq. (3.46) is the stiffness due to convection.

The new thermal load vector now becomes

$$\{F\}^{(e)} = \iint_{A^{(e)}} rN_i \frac{\dot{Q}_v}{k} rdrdz + \frac{h}{k}\oint_{\Gamma^e} \mathrm{T_\infty}\, rN_i d\Gamma \quad (3.47)$$

When there is a flux boundary condition in addition to the convective boundary condition, the thermal load vector will then be:

$$\{F\}^{(e)} = \iint_{A^{(e)}} rN_i \frac{\dot{Q}_v}{k} rdrdz + \frac{h}{k}\oint_{\Gamma^e} \mathrm{T_\infty}\, rN_i d\Gamma - \oint_{\Gamma^e} N_i \frac{\mathrm{q}}{\mathrm{k}} \mathrm{r} d\Gamma \quad (3.48)$$

In general the thermal load vector is the sum of the load due to heat generation$\left(\{F_Q\}^{(e)}\right)$, convection$\left(\{F_h\}^{(e)}\right)$, and the load due to flux$\left(\{F_q\}^{(e)}\right)$.

$$\{F\}^{(e)} = \{F_Q\}^{(e)} + \{F_h\}^{(e)} + \{F_q\}^{(e)} \quad (3.49)$$

When there is a uniform convection on the boundary of the triangular element:

$$\{F_h\}^{(e)} = \frac{h\mathrm{T_\infty l}}{3k}\begin{Bmatrix} 2r_i+r_j \\ r_i+2r_j \end{Bmatrix} \quad (3.50)$$

Where r_i and r_j are the coordinate values of boundary nodes$i\ and\ j$, and l is the side length of the element.

For a constant heat generation rate:

$$\{F_Q\}^{(e)} = \iint_{A^{(e)}} rN_i \frac{\dot{Q}_v}{k} rdrdz = \frac{\dot{Q}_v}{k} \iint_{r\ z} [N_1 \quad N_2 \quad N_3]^T\, rdrdz$$

$$= \frac{\dot{Q}_v}{k}\frac{A}{6}\begin{Bmatrix} 2r_1+r_2+r_3 \\ r_1+2r_2+r_3 \\ r_1+r_2+2r_3 \end{Bmatrix} \tag{3.51}$$

When there is a flux boundary condition:

$$\{F_q\}^{(e)} = -\oint_{\Gamma^e} N_i \frac{\mathrm{q}}{\mathrm{k}} \mathrm{r} d\Gamma = \frac{\mathrm{q}l_{12}}{6\mathrm{k}}\begin{Bmatrix} 2r_1+r_2 \\ r_1+2r_2 \end{Bmatrix} \tag{3.52}$$

Where= l_{12} is the length of the element boundary.

The elemental stiffness matrix is the sum of the stiffness due to conduction and convection:

$$[K]^{(e)} = [K_{cond}]^{(e)}+[K_{conv}]^{(e)} \tag{3.53}$$

Where the stiffness due to convection is given by:

$$[K_{conv}]^{(e)} = \frac{h}{k}\oint_{\Gamma^e} N_i\, N_j r d\Gamma^e \tag{3.54}$$

The assembled matrix with the boundary conditions applied becomes:

$$\underbrace{\left[\iint_{A^e} \frac{1}{\alpha}[N][N]^T rdrdz\right]}_{[C]}\left\{\frac{\partial T}{\partial t}\right\} \underbrace{\left[\iint_{A^{(e)}} \left(\left[\frac{\partial N}{\partial r}\right]\left[\frac{\partial N}{\partial r}\right]^T + \left[\frac{\partial N}{\partial z}\right]\left[\frac{\partial N}{\partial z}\right]^T\right) \mathrm{r}\, drdz\right]}_{[K_{cond}]} + \underbrace{\left[\frac{h}{k}\oint_{\Gamma^e} N_i\, N_j r d\Gamma^e\right]}_{[K_{conv}]} \{T\}$$

$$= \underbrace{\iint_{A^{(e)}} rN_i \frac{\dot{Q}_v}{k} rdrdz}_{\{F_Q\}^{(e)}} + \underbrace{\frac{h}{k}\oint_{\Gamma^e} \mathrm{T}_\infty\, rN_i d\Gamma}_{\{F_h\}^{(e)}} - \underbrace{\oint_{\Gamma^e} N_i \frac{\mathrm{q}}{\mathrm{k}} \mathrm{r} d\Gamma}_{\{F_q\}^{(e)}} \tag{3.55}$$

$$[C]\{\dot{T}\}+([K_{cond}]+[K_{conv}])\{T\} = \{F_Q\}^{(e)}+\{F_h\}^{(e)}+\{F_q\}^{(e)} \tag{3.56}$$

$$[C]\{\dot{T}\}+[K]\{T\} = \{F\} \tag{3.57}$$

Step-6 Solution of the Assembled Equations

Once the systems of matrix equations are properly set they have to be solved with appropriate solution techniques. Four solution techniques are available (forward difference, backward difference, Crank-Nicolson, and Galerkin's method). The backward difference technique is used in this study because of its unconditional stability. In the backward difference method any size of time step can be used without worrying about stability.

In the backward difference technique equation (3.57) can be written as:

$$[C]\{\dot{T}\}^{t+\Delta t}+[K]\{T\}^{t+\Delta t} = \{F\}^{t+\Delta t} \tag{3.58}$$

The time derivative in the backward difference technique is:

$$\{\dot{T}\}^{t+\Delta t} = \frac{\{T\}^{t+\Delta t}-\{T\}^{t}}{\Delta t} \tag{3.59}$$

Substituting Eq. (3.59) into Eq. (3.58) and rearranging:

$$([C]+\Delta t[K])\{T\}^{t+\Delta t} = \Delta t\{F\}^{t+\Delta t}+[C]\{T\}^{t} \tag{3.60}$$

$$\{T\}^{t+\Delta t} = [A]^{-1}\{V\}^{t} \tag{3.61}$$

Where:

$[A] = [C]+\Delta t[K]$, and

$\{V\}^{t} = \Delta t\{F\}^{t+\Delta t}+[C]\{T\}^{t}$.

The solution for the other techniques can be obtained by writing Eq. (3.60) using the general θ method:

$$\underbrace{([C]+\Delta t\theta[K])}_{[A]}\{T\}^{t+\Delta t} = \underbrace{\Delta t\{F\}^{t}+\big([C]-\Delta t[K](1-\theta)\big)}_{(V)}\{T\}^{t} \tag{3.62}$$

$$\{T\}^{t+\Delta t} = [A]^{-1}(V) \tag{3.60*}$$

When θ is zero the method is forward difference, when θ is one the method employed will be backward difference. When θ is one half and two third the scheme will be Crank -Nicolson, and Galerkin's method respectively.

CHAPTER FOUR

DETERMINATION OF THERMO-PHYSICAL PROPERTIES AND BOUNDARY CONDITIONS

In this chapter, the basic thermo-physical properties and heat transfer coefficients which are used as an input for the simulation are determined analytically.

4.1 Thermo-Physical Property of Injera

Thermo–physical properties of injera are determined from its major components and temperature dependent equations reviewed in chapter two.

4.1.1 Specific Heat Capacity

Specific heat of injera can be obtained from its major components using Eq. (2.7):

$$c_p = \sum_{j=1}^{n} x_j c_{pj} \tag{4.1}$$

Specific heat of the major components of injera batter can be determined using the empirical equations presented in Table 2-2 at the average baking temperature (Table 4-1).

Table 4-1: Determination of specific heat of major components of injera

Components	Composition(%) x_j	Specific heat$(J/kg.K)$ $x_j c_{pj}$
Carbohydrate	0.339	$0.339(1.5488+1.9625\times10^{-3}T-5.9399\times10^{-6}T^2)$
Ash	0.015	$0.015(1.0926+1.8896\times10^{-3}T-3.6817\times10^{-6}T^2)$
Fiber	0.017	$0.0.017(1.8459+1.8306\times10^{-3}T-4.6509\times10^{-6}T^2)$
Fat	0.006	$0.006(1.9842+1.4733\times10^{-3}T-4.8008\times10^{-6}T^2)$
Protein	0.042	$0.042(2.0082+1.2089\times10^{-3}T-1.3129\times10^{-6}T^2)$
Moisture	0.581	$0.581(4.1762-9.0864\times10^{-5}T-5.4731\times10^{-6}T^2)$

The specific heat as a function of temperature becomes:

$$c_p = \sum_{j=1}^{n} x_j c_{pj} = 3.0954 + 7.3158\times10^{-4}T + 9.4806\times10^{-7}T^2 \quad (4.2)$$

The specific heat of injera at the average baking temperature (55^0C) becomes:

$$c_p = 3440.07 J/kg.K$$

4.1.2 Density

The density of injera can be determined from Eq. (2.16), and the density of the major components can also be obtained from the relations presented in Table 2-4 at the average baking temperature.

Table 4-2: Density of major components of injera

Components	Composition(%) x_i	Density(kg/m^3) ρ_i	x_i/ρ_i
Carbohydrate	0.339	1582.025	2.14×10^{-4}
Ash	0.015	2408.365	6.23×10^{-6}
Fiber	0.017	1291.376	1.32×10^{-5}
Fat	0.006	902.624	6.65×10^{-6}
Protein	0.042	1301.388	3.23×10^{-5}
Moisture	0.581	985.987	5.89×10^{-4}
$\sum_{i=1}^{n} x_i/\rho_i = 8.617\times10^{-4}$			

The density of injera at the average baking temperature (55^0C) becomes:

$$\rho = \frac{1}{\sum_{i=1}^{n} x_i/\rho_i} = 1160.55\ kg/m^3 \quad (4.3)$$

4.1.3 Thermal Conductivity

The thermal conductivity of injera varies depending on the moisture content, temperature, and the structural model employed (series or parallel), porosity, shape and distribution.

The volume fraction should be first calculated using Eq. (2.11) to use either of the models:

$$\varepsilon_i = \frac{x_i/\rho_i}{\sum_{i=1}^{n} x_i/\rho_i} \tag{4.4}$$

Table 4-3: Determination of volume fraction of major components of injera

Components	Composition(%) x_i	Density(kg/m^3) ρ_i	x_i/ρ_i	$\varepsilon_i = \frac{x_i/\rho_i}{\sum_{i=1}^{n} x_i/\rho_i}$
Carbohydrate	0.339	1582.025	2.14×10^{-4}	0.248
Ash	0.015	2408.365	6.23×10^{-6}	0.00723
Fiber	0.017	1291.376	1.32×10^{-5}	0.015
Fat	0.006	902.624	6.65×10^{-6}	0.00772
Protein	0.042	1301.388	3.23×10^{-5}	0.03748
Moisture	0.581	985.987	5.89×10^{-4}	0.68353
$\sum_{i=1}^{n} x_i/\rho_i = 8.617\times10^{-4}$				

Using Eq. (2.10) for the parallel model and applying temperature dependent empirical equations (Table 2-3) we can evaluate thermal conductivity of the major components as (Table 4-3).

Table 4-4: Determination of thermal conductivity of major components for the parallel model

Components	ε_i	$\varepsilon_i k_i$
Carbohydrate	0.24800	$0.0499+3.4408\times10^{-4}T-1.0741\times10^{-6}T^2$
Ash	0.00723	$2.3828\times10^{-3}+1.0129\times10^{-5}T-2.1014\times10^{-8}T^2$
Fiber	0.01500	$2.7649\times10^{-3}+1.8746\times10^{-5}T-4.7525\times10^{-8}T^2$
Fat	0.00772	$1.3806\times10^{-3}+2.1302\times10^{-6}T-1.3697\times10^{-9}T^2$
Protein	0.03748	$6.7018\times10^{-3}+4.4819\times10^{-5}T-1.0186\times10^{-7}T^2$
Moisture	0.68353	$0.57109x_w+1.7625\times10^{-3}Tx_w+6.7036\times10^{-6}T^2x_w$
$k=\sum_{i=1}^{n}\varepsilon_i k_i$ $=0.0631+0.57109x_w+4.2999\times10^{-3}T$ $+1.7625\times10^{-3}Tx_w-1.2459\times10^{-6}T^2+6.7036\times10^{-6}T^2x_w$		

The moisture content during injera baking varies linearly from 73% (batter) to 58.1 % (injera) for the baking period ($150s$)[2]. So the thermal conductivity can be determined either at the average baking temperature and average moisture content or at the initial moisture content and initial temperature of the batter. In the later case the thermal conductivity will be updated as a function of temperature and moisture content variation during baking using the MATLAB program.

The thermal conductivity for the parallel model at the average baking temperature (55^0C) becomes:

$$k_{parallel}=0.7501 W/m.K$$

Following the same procedure the thermal conductivity for the series model can be calculated at the average baking temperature (55^0C) as follows (using Eq. (2.9) and Table 2-3):

Table 4-5: Determination of thermal conductivity of major components for the series model

Components	Composition(%) x_i	ε_i	k_i	ε_i/k_i
Carbohydrate	0.339	0.24800	0.38466	0.6447
Ash	0.015	0.00723	0.49789	0.0145
Fiber	0.017	0.01500	0.36346	0.0413
Fat	0.006	0.00772	0.29636	0.026
Protein	0.042	0.03748	0.35358	0.106
Moisture	0.581	0.68353	0.69775	0.9796
$\sum_{i=1}^{n} \varepsilon_i/k_i = 1.8122 W/m.K$				

$$k_{series} = \frac{1}{\sum_{i=1}^{n} \varepsilon_i/k_i} = 0.5518 W/m.K$$

According to the literatures any value between the series and the parallel model can be used as the thermal conductivity of the food. The thermal conductivity of injera used for the simulation is $0.655 W/m.K$.

4.1.4 Moisture Diffusivity

There is no standard method for the determination of moisture diffusion and thermo-gradient coefficient. Therefore, average values obtained from literatures are used in this study. Moisture diffusion coefficient between water vapor and air at a standard pressure and temperature is equal to $D = 0.288 \times 10^{-4} m^2/s$ [20], and latent heat of vaporization of water $h_{fg} = 2256.97$ kj/kg. The thermo-gradient coefficient has less influence on the temperature predictions. The value of the thermal gradient coefficient (δ_t) varies from $0.01/k$ up to $0.02/k$ for food products. There is very little published data concerning the value of the ratio of water evaporation rate to the reduction rate of the moisture content during the baking of foods, therefore the value obtained from the literatures [2, 46,], ε=0.3 is used for injera.

4.2 Thermo-physical property of baking pans

The thermo-physical property of baking pans: thermal conductivity, specific heat, and density are obtained from literatures [2, 13].

- Property of clay baking pan:

$$k = 0.5 W/m.K, \quad c_p = 830 J/kg.K, \quad \rho = 1900\ kg/m^3$$

- Property of ceramic baking pan:

$$k = 0.8 W/m.K, \quad c_p = 960 J/kg.K, \quad \rho = 2400\ kg/m^3$$

4.3 Power Estimation and Distribution in Electric Powered Baking Pans

Electric power is the source of power for conventional electric baking pans. The electric power is converted into heat energy using resistors inserted on grooves at the back side of the pan. The power developed in the resistor can be obtained from Eq. (4.5), and varies depending on the material type and size (diameter and length) of the resistance wire used. For higher power consumption a resistance wire with larger diameter and longer length is required.

$$P = I^2 \times R \tag{4.5}$$

Where:

P = Power developed in the resistor(W),

I = current through the resistor(A), and

R=resistance of the resistor (Ω).

The resistors used in heating applications are almost exclusively metallic. Such materials as platinum, tungsten, and alloy of nickel, iron, and chromium are commonly used. Local electric pan manufacturers use R08, and R09 types of resistors made of nickel-chromium alloys. The existing type of electric baking pan uses $3kW$ power source and has 12 loops of resistors [2].

The power estimated for R07, R08, and R09 resistors for stretched length of 10, 11, and $12m$ is 1.867, 2.2 and 2.5 kW respectively [2].The power consumption in each loop for different power

sources can be calculated as follows. The power supplied for the i^{th} loop is directly proportional to the radius of that loop ($P_i \propto 2\pi r_i$), where, r_i is the radius of thei^{th} loop. The loops in this study are assumed to be circular with constant distance between them, but it is also possible to use spiral loops of resistors with varying distance between them.

The total power supplied is, therefore the sum of the power supplied to each loop:

$$P = \sum_{i=1}^{N} P_i \tag{4.6}$$

The total length of the resistance wire is equal to [2]:

$$1.5\sum_{i=1}^{N} i - 0.25N \tag{4.7}$$

The power supplied becomes:

$$P = 2\pi d(1.5\sum_{i=1}^{N} i - 0.25N) \tag{4.8}$$

Where:

N=12, the total number of loop, and d=distance between consecutive radius (m),

After simplification the power consumed by each loop becomes:

$$P_i = \frac{P\times(1.5i-0.25)}{(1.5\sum_{i=1}^{N} i-0.25N)} \tag{4.9}$$

The power consumption in each loop calculated using Eq. (4.9) for different power sources is presented in Table 4-6 [2].

Table 4-6: Power consumption in each loop of the baking pan for different power sources

Power consumption (W)				
Loop	**Power source**			
	$3kW$	$2.5\ kW$	$2.2\ kW$	$1.867\ kW$
1	32.896	27.412	24.123	20.470
2	72.372	60.310	53.100	45.040
3	111.840	93.200	82.020	69.600
4	151.320	126.100	110.950	94.170
5	190.800	159.000	140.000	118.750
6	230.280	191.900	168.900	143.300
7	269.760	224.800	197.810	167.900
8	309.240	257.700	226.750	192.400
9	348.720	290.600	255.700	217.000
10	388.200	323.500	284.650	241.600
11	427.632	356.400	313.600	266.130
12	467.160	389.300	342.600	290.700

4.4 Determination of Surface Heat Transfer Coefficients

The surface heat transfer coefficient is influenced by the composition of the fluid, the nature and geometry of particle surface, and the hydrodynamics of the fluid moving past the surface. From the boundary conditions the heat transfer coefficient over the baking pan is the combined effect of the heat transfer coefficient due to convection and radiation.

$$h = h_r + h_c \tag{4.10}$$

Where:

h_r=convective heat transfer coefficient$(W/m^2.K)$,

h_c=radiative heat transfer coefficient$(W/m^2.K)$, and

h=surface heat transfer coefficient$(W/m^2.K)$.

The convective heat transfer coefficient over the baking pan can be calculated from:

$$h_c = \frac{Nu\ k}{L} \tag{4.11}$$

Where:

h_c=convection heat transfer coefficient($W/m^2.K$),

Nu=Nusselt number,

k=thermal conductivity of the fluid($W/m.K$), and

L =characteristic length(m).

In the determination of convective heat transfer coefficient a dimensionless functional relationship derived using dimensional analysis between h_c and the relevant physical properties of the flow situation is used.

$$h_c = f(\rho, V, L, \mu, c_p, \Delta T, k, \beta, g) \tag{4.12}$$

Where:

ρ = density of fluid (kg/m^3),

V = average fluid velocity (m/s),

μ = dynamic viscosity ($N.s/m^2$),

c_p = specific heat of the fluid($J/kg.K$),

β = volumetric expansion coefficient($1/K$), and

g = gravitational acceleration (m/s^2).

By performing a dimensional analysis on the above equation, the following equation can be derived:

$$\frac{h_c L}{k} = f\left(\frac{\rho V L}{\mu}, \frac{c_p \mu}{k}, \frac{\rho^2 g \beta L^3 \Delta T}{\mu^2}, \frac{V^2}{c_p \Delta T}\right) \tag{4.13}$$

Where:

$\frac{h_c L}{k}$ = Nusselt number (Nu),

$\frac{\rho V L}{\mu}$ = Reynolds number (Re),

$\frac{c_p \mu}{k}$ = Prandtle number (Pr),

$\frac{\rho^2 g \beta L^3 \Delta T}{\mu^2}$= Grashof number ($Gr$), and

$\frac{V^2}{c_p \Delta T}$ = Eckert number.

In natural convection, many correlations contain the product of the grashof number and the prandtle number; the product of the two is defined as the Rayleigh number:

$$Ra = Gr \times Pr \tag{4.14}$$

As the motion of fluid in free convection is caused by buoyancy force, for horizontal plates either from the plate or toward the plate, two situations should be distinguished.

1. Heat transfer occurs in the direction of gravitational force (lower surface heated upper surface cooled), and
2. Heat transfer against the direction of gravitational force (Upper surface heated lower surface cooled).

A general correlation between the Nusselt number and Rayleigh number is developed based on the above two cases as:

$$Nu = C(Gr \times Pr)^m \tag{4.15}$$

Where, (m) and (C) are constants .The value of the constants depends on geometry.
Since heat transfer during injera baking is against the direction of gravitational force, only the second case is used for this study.

Fuji and imura (1972) proposed the following correlation for heat transfer to or from the horizontal plate with constant heat flux [19, 41, 42, and 48]:

$$\left.\begin{array}{l} Nu=0.13(Gr\times Pr)^{1/3}, \text{ for } Gr\times Pr<2\times 10^{8} \\ Nu=0.16(Gr\times Pr)^{1/3}, \text{ for } 2\times 10^{8}< Gr\times Pr<10^{11} \end{array}\right\} \quad (4.16)$$

In these equations β is evaluated at T_∞+0.25(($T_s - T_\infty$), and all other properties at T_s-0.25($T_s - T_\infty$), T_s is the average wall temperature.

Correlations are also presented for flat surfaces without constant heat flux as [19, 41, 42, and 48]:

$$\left.\begin{array}{l} Nu=0.54(Gr\times Pr)^{1/4}, \text{ for } 10^{4}< Gr\times Pr<10^{7} \\ Nu=0.15(Gr\times Pr)^{1/3}, \text{ for } 10^{7}< Gr\times Pr<10^{11} \end{array}\right\} \quad (4.17)$$

4.4.1 Heat Transfer Coefficient at the Surface of the Baking Pan

To determine the convective heat transfer coefficient first evaluate the property of air at the average film temperature.

$$T_s = \frac{T_s+T_\infty}{2} = \frac{20+200}{2} = 110\ ^0\text{C} \quad (4.18)$$

The film temperature to evaluate the properties becomes $T_w = T_s$-0.25($T_s - T_\infty$) =110-0.25(110−20) =87.5^{0}C.

Properties at the average film temperature:

ρ =0.996kg/m^3, c_p=1010$J/kg.K$, k=30.5275×10^{-3} $W/m.K$,

β=2.7739 ×10^{-3}/K, μ=2.1193×10^{-5} $kg/m.s$, v=2.216×10^{-5} m^2/s,

$\propto$=3.131×10^{-5} m^2/s, Pr=0.71, g =9.81m/s^2,

The characteristics length for circular disk is experimentally approximated as L=0.9D [19, 42], where D is the diameter of the pan.

The dimensionless Grashof and Rayleigh numbers become:

$$Gr = \frac{g\beta L^3 \Delta T}{v^2} = \frac{9.81\times 2.7739\times 10^{-3}\times (0.9\times 0.6)^3 (110\text{-}20)}{\left(2.216\times 10^{-5}\right)^2} = 7.85\times 10^{8}$$

$$Ra = Gr\times Pr = 5.57\times 10^{8}$$

Using Eq. (4.16):

$$Nu = 0.16(Gr \times Pr)^{1/3} = 131.69$$

The convective heat transfer coefficient becomes:

$$h_c = \frac{Nu.k}{L} = \frac{131.69 \times 30.5275 \times 10^{-3}\ W/m.K}{0.9 \times 0.6m} = 7.45 W/m^2.K$$

The radiative heat transfer coefficient at the surface of the baking pan is given by:

$$h_r = \delta \times \varepsilon \left(\frac{T_s^4 - T_\infty^4}{T_s - T_\infty}\right) \tag{4.19}$$

$$= \delta \times \varepsilon (T_s^2 + T_\infty^2) \times (T_s - T_\infty)$$

Where δ is the Stefan Boltzmann constant ($5.67 \times 10^{-8}\ W/m^2.K^4$) , and ε is the emissivity of the surface (0.95).

Substituting the values into Eq. (4.20):

$$h_r = 8.47 W/m^2.K$$

The surface heat transfer coefficient on the top surface of the baking pan will be:

$$h = h_c + h_r = 15.92 W/m^2.K$$

4.4.2 Convective Heat Transfer Coefficient of Heated Oil Used as Heat Transfer Fluid

The heat transfer fluid used in oil baking pans is shell themia oil B. The oil heated by solar energy is circulated heating the bottom of the baking pan. The shell thermia oil B is chosen for its ability to provide superior performance in indirect closed fluid heat transfer systems operating at higher temperature. According to shell safety data sheet Shell thermia oil B has exceptionally good thermal stability at bulk temperatures up to 320*ºC*, and film temperature up to 340*ºC*. Typical design data for thermia oil B is obtained from shell data sheet shown in appendix A.

The convective heat transfer coefficient of heated oil in a cylindrical container is calculated from Eq. (4.11), but in this case the characteristic length is the diameter of the cylinder. The Nusselt number correlation for free convection in a cylinder is expressed as [43, 45]:

$$Nu = \left[0.6 + \frac{0.387(Gr \times Pr)^{1/6}}{\left(1 + (0.559/Pr)^{9/16}\right)^{8/27}}\right]^2,\ 10^{-4} \leq Gr \times Pr \leq 10^{12} \tag{4.20}$$

The thermal property is evaluated at the film temperature from Table A-1 (Appendix A):

$$T = \frac{20+300}{2} = 160\ ^oC$$

$C_p = 2400 J/kg.K$, $k = 0.123\ W/m.K$, $Pr = 29$,

$\beta = 0.0008/K$, $v = 2.85 \times 10^{-6}\ m^2/s$, $g = 9.81 m/s^2$.

The dimensionless numbers are:

$$Gr = \frac{g\beta L^3 \Delta T}{v^2} = \frac{9.81 \times 0.0008 \times (0.6)^3 \times (300\text{-}20)}{\left(2.85 \times 10^{-6}\right)^2} = 5.844 \times 10^{10}$$

$$Ra = Gr \times Pr = 5.844 \times 10^{10} \times 29 = 1.695 \times 10^{12}$$

Substituting into Eq. (4.20):

$$Nu = \left[0.6 + \frac{0.387\left(1.695 \times 10^{12}\right)^{1/6}}{\left(1+(0.559/29)^{9/16}\right)^{8/27}}\right]^2 = 1729.42$$

The convective heat transfer coefficient becomes:

$$h_o = \frac{Nu.k}{L} = \frac{1729.42 \times 0.123}{0.6} = 354.5 W/m^2.K$$

4.5 Experimental test

The first experimental test done in this study was the measurement of heat up time of conventional clay baking pan. Clay baking pan, data logger with thermocouples, and PC loaded with lab view shown in figure 4-1 was used for the test. The heat up time obtained from the experiment is compared with the simulation result in figure 5-4, and presented in table form in table B-2 (appendix).

Figure 4-1: Experimental set up to measure heat up time.

The other experimental test was the measurement of mass of batter and injera before and after baking using digital mass balance. This experiment was done during baking using ceramic and clay baking pans. The result obtained is summarized in tables 6-1, and 6-2.

Figure 4-2: Digital mass balance with batter and injera

CHAPTER FIVE

NUMERICAL SIMULATION

A MATLAB code was written based on the formulated finite element equations to study the temperature distribution during heat up and cyclic baking founded on the previous work by Assefa [2]. The program written for the simulation of heat up time is similar with the previous work, but the program written for cyclic baking is different. In the previous work simulation was done by simply imposing boiling heat transfer coefficient on the surface of the baking pan without considering the thickness of injera, which in turn results the same type of injera for all baking pan types and power sources. The current program includes simulation of both injera and baking pan together for the baking period. This helps to study the temperature profile of injera for different baking pan types and energy sources during the baking period.

Results obtained during heat up time, and cyclic baking for different types of baking pans(clay and ceramic) with different power sources(electric and indirect solar power) are presented in this chapter. Simulation of heat up time and cyclic baking was done for four different thicknesses of clay baking pans (0.0075, 0.01, 0.015, and 0.02m), and for two ceramic baking pan thicknesses (0.01, and 0.008m). Graphs representing temperature profiles during heat up, baking, and idle periods are plotted as a function of time for selected pan thicknesses, In addition to that heat up and idle periods for different baking pan thicknesses and power sources are summarized in table form.

The computer algorithm (flow chart) for a two dimensional axisymmetric transient finite element problem, and the various parameters used as an input for the simulation are presented in Figure 5-1 and Table 5-1 respectively. The finite element discretization of the baking pan for heat up time simulation, and discretization of baking pan and injera for cyclic baking simulation are shown in figure 5-2, and figure 5-8 respectively.

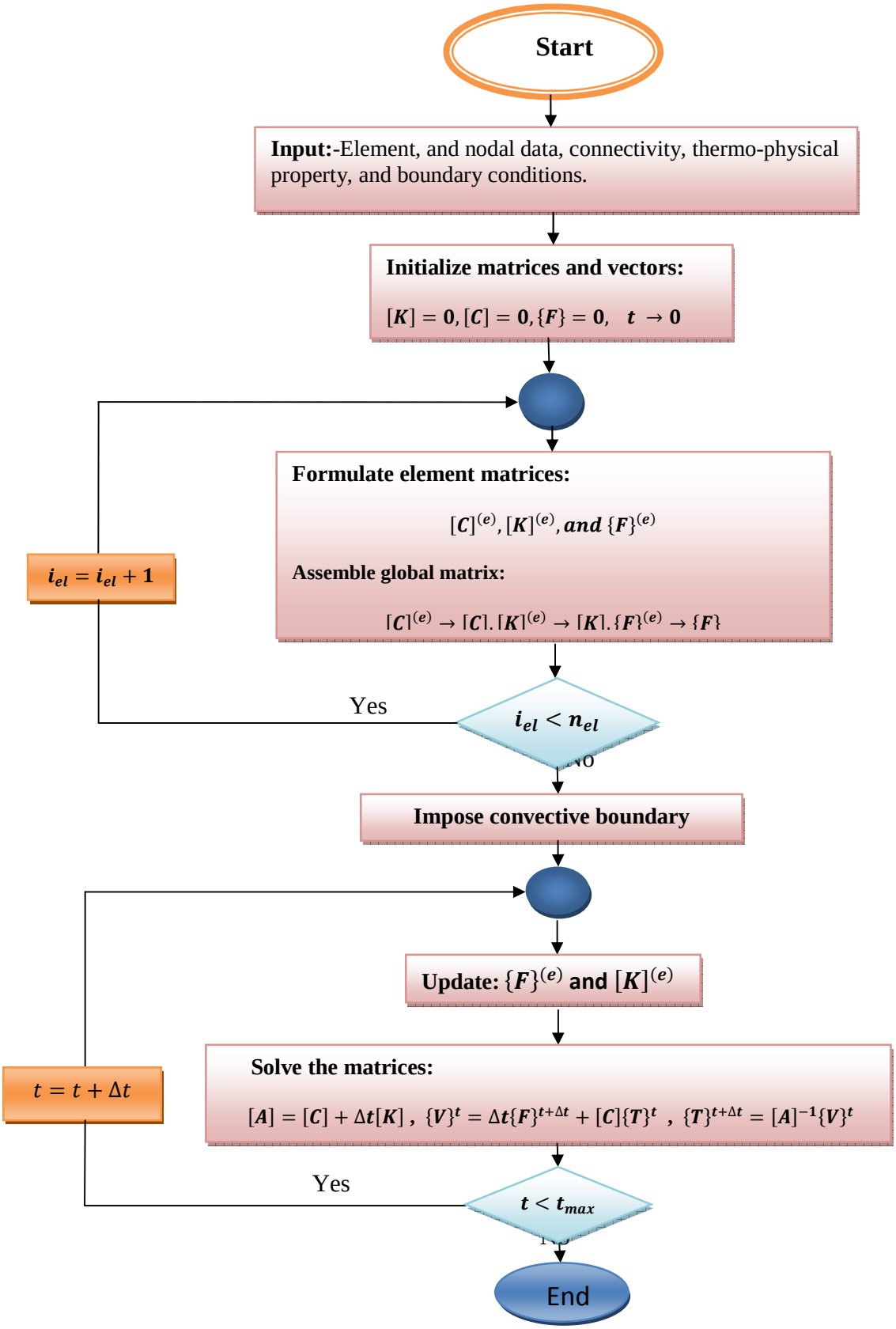

Figure 5-1: Flow chart for the MATLAB program

Table 5-1: Parameters used for the simulation

Parameters	Value
Baking time(t)	120-180s
Boiling heat transfer coefficient	2000$W/m^2.K$
Convective heat transfer coefficient of oil (h_o)	354.53$W/m^2.K$
Density of clay	1900kg/m^3
Density of injera	1160.55kg/m^3
Density of ceramic	2400kg/m^3
Diameter of clay pan	0.6m
Diameter of injera	0.6m
Diameter of ceramic pan	0.6m
Free convective heat transfer coefficient over the baking pan(h_c)	7.45$W/m^2.K$
Initial temperature of baking pan	20-25^oC
Initial temperature of injera batter	20-25^oC
Input electric power	1.867, 2.2, 2.5, and 3kW
Input heated oil temperature	250, 275, 300, and 325^oC
Latent heat of evaporation of water	2256.97 kJ/kg
Radiative heat transfer coefficient over the baking pan (h_r)	8.47$W/m^2.K$
Specific heat of clay	830$J/kg.K$
Specific heat of ceramic	960$J/kg.K$
The average specific heat of injera	3440.07$J/kg.K$
Thermal conductivity of clay pan	0.5$W/m.K$
Thermal conductivity of injera batter	0.655 $W/m.K$
Thermal conductivity of ceramic	0.8 $W/m.K$
Thermo gradient coefficient	0.01-0.02$/K$
Thickness of ceramic pan	0.008, and 0.01m
Thickness of clay pan	0.02,0.015,0.01,and0.0075m
Thickness of injera(average)	0.003m

5.1 Simulation of Baking Pans for Heat up Time

The heat up time of a baking pan is the amount of time required to increase the surface temperature of the pan from its initial temperature (20-25^{o}C) to the temperature required for the baking of injera (180-220^{o}C). The heat up time depends on the input power, thickness, and thermal property of the baking pan.

The finite element discretizations of the conventional baking pan into a finite number of triangular elements with the boundary conditions is shown below.

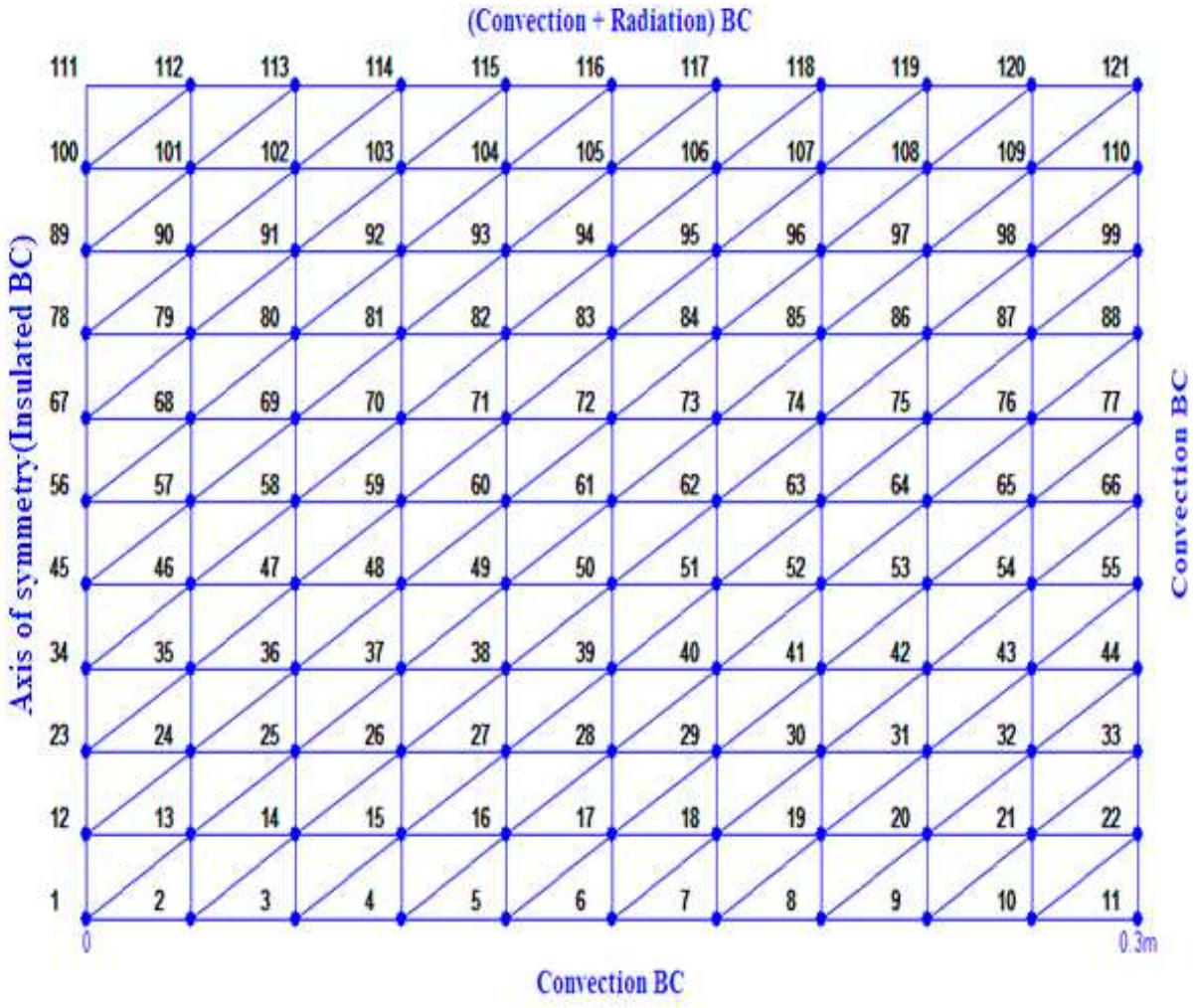

Figure 5-2: Finite element discretization of baking pan

5.1.1 Heat up Time of Clay Baking Pans

Figure 5-3 shows the surface node (node 118) temperature profile of 0.02 *m* electric clay baking pan as a function of heat up time for different electric power input. The heat up time for other pan thicknesses as a function of power source is summarized in Table 5-2. As it is shown in the graph the heat up time increases as the power source decreases for a given pan thickness.

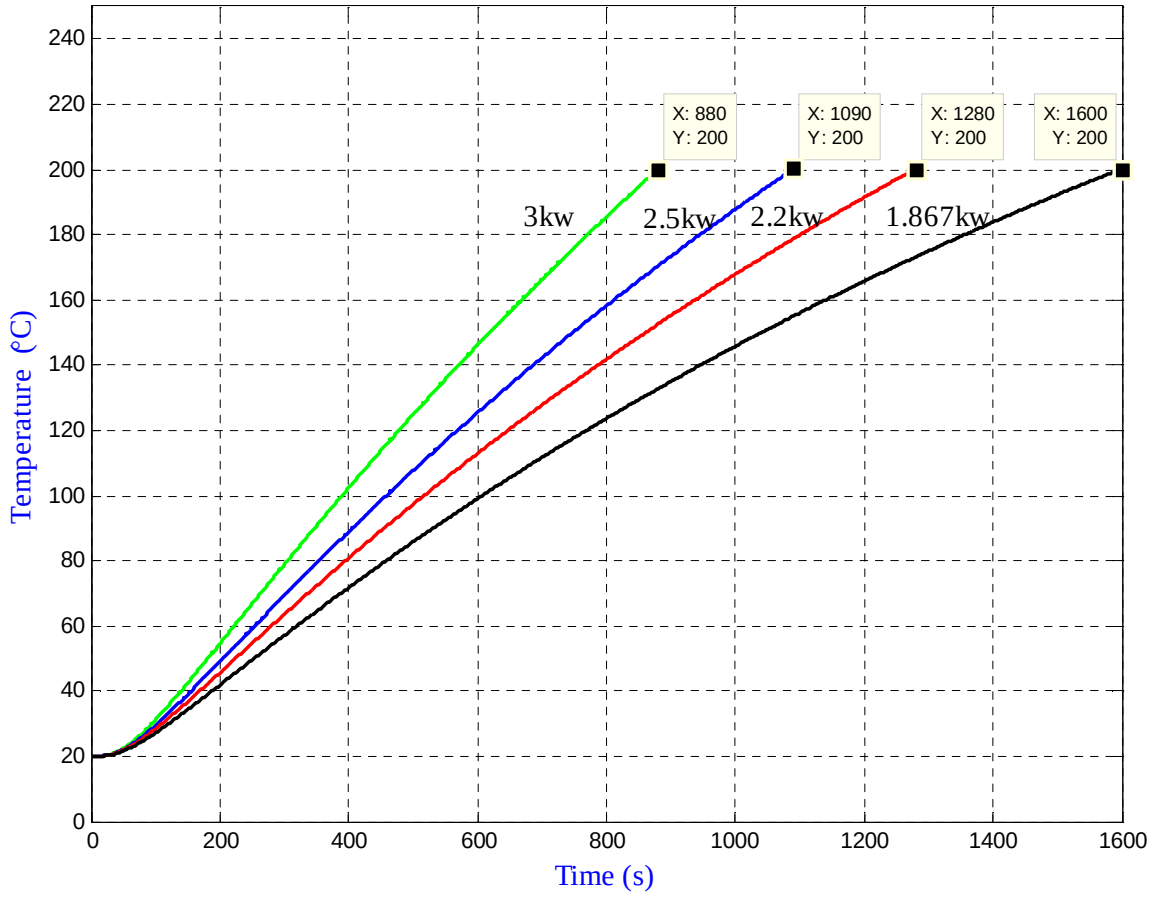

Figure 5-3: Heat up time of 0.02*m* electric clay baking pan with different power input

Figure 5-4 shows the comparison of heat up time obtained from experiment with the one obtained from finite element simulation. The comparison was done for 3*kw* electric power source and 0.02*m* conventional clay baking pan thickness.

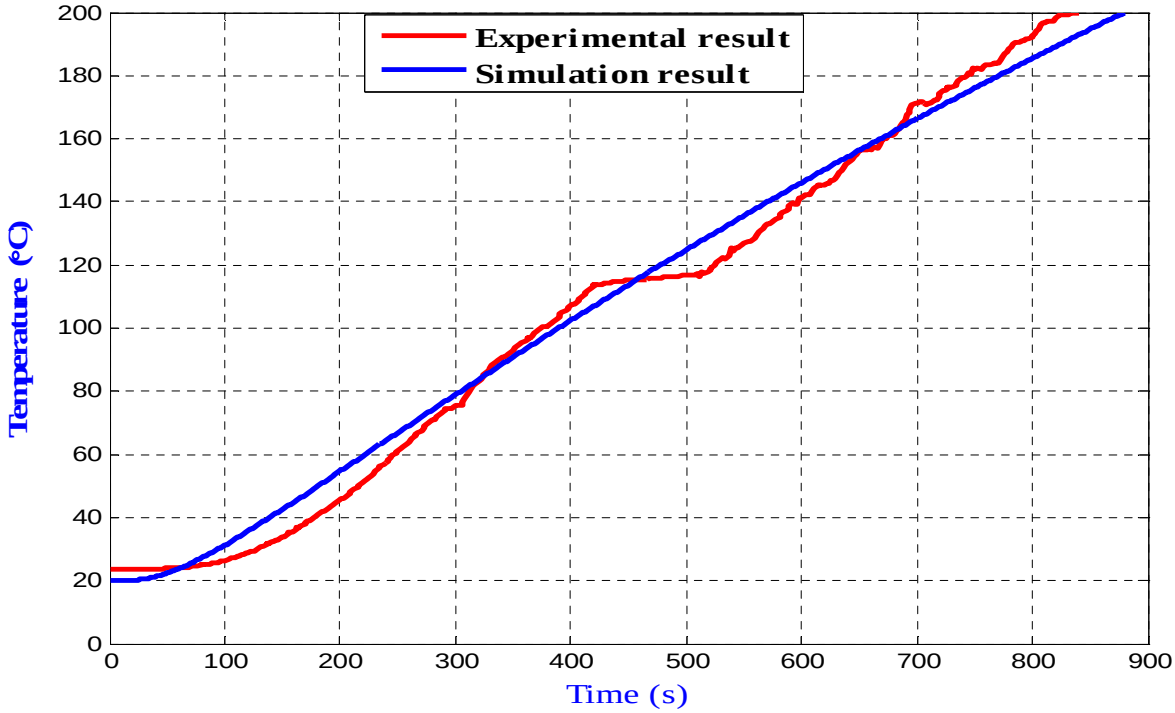

Figure 5-4: Comparison of heat up time obtained from experiment and FEM for electric clay pan

Figure 5-5 shows the surface node (node 118) temperature profile of different clay pan thicknesses with different heated oil temperatures as a function of heat up time.

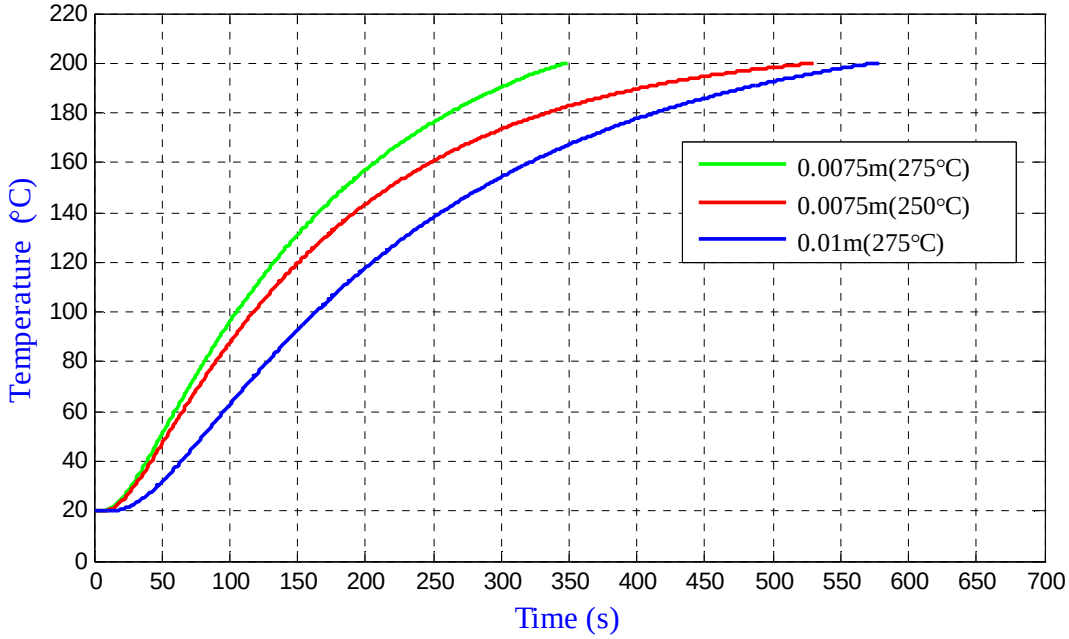

Figure 5-5: Heat up time for clay pan with different thicknesses and heated oil temperatures

Table 5-2 shows the heat up time of different thickness clay baking pans as a function of power source. Simulation was not done for 0.0075 m electric clay baking pan thickness. The heat up time is represented in hyphen when the baking pan does not reach the heat up temperature for the given power input.

Table 5-2: Summery of heat up time for different clay pan thicknesses and power sources

Heat up time(s)								
Baking pan thickness (m)	Power source							
	Electric power (kW)				Heated oil(^oC)			
	3 kW	2.5 kW	2.2 kW	1.867 kW	325^oC	300^oC	275^oC	250^oC
0.0075	-	-	-	-	235	277	350	531
0.01	420	517	603	744	365	440	580	-
0.015	635	785	918	1139	760	970	1800	-
0.02	880	1100	1280	1600	1436	2300	-	-

5.1.2 Heat up Time of Ceramic Baking Pans

Figure 5-5 shows the surface node (node 118) temperature profile of 0.008 *m* electric ceramic baking pan as a function of heat up time for different input power. The heat up time for other electric ceramic pan thicknesses as a function of power source is shown in Table 5-3. Similar to the case of clay baking pans the heat up time increases as the power source decreases for a given pan thickness.

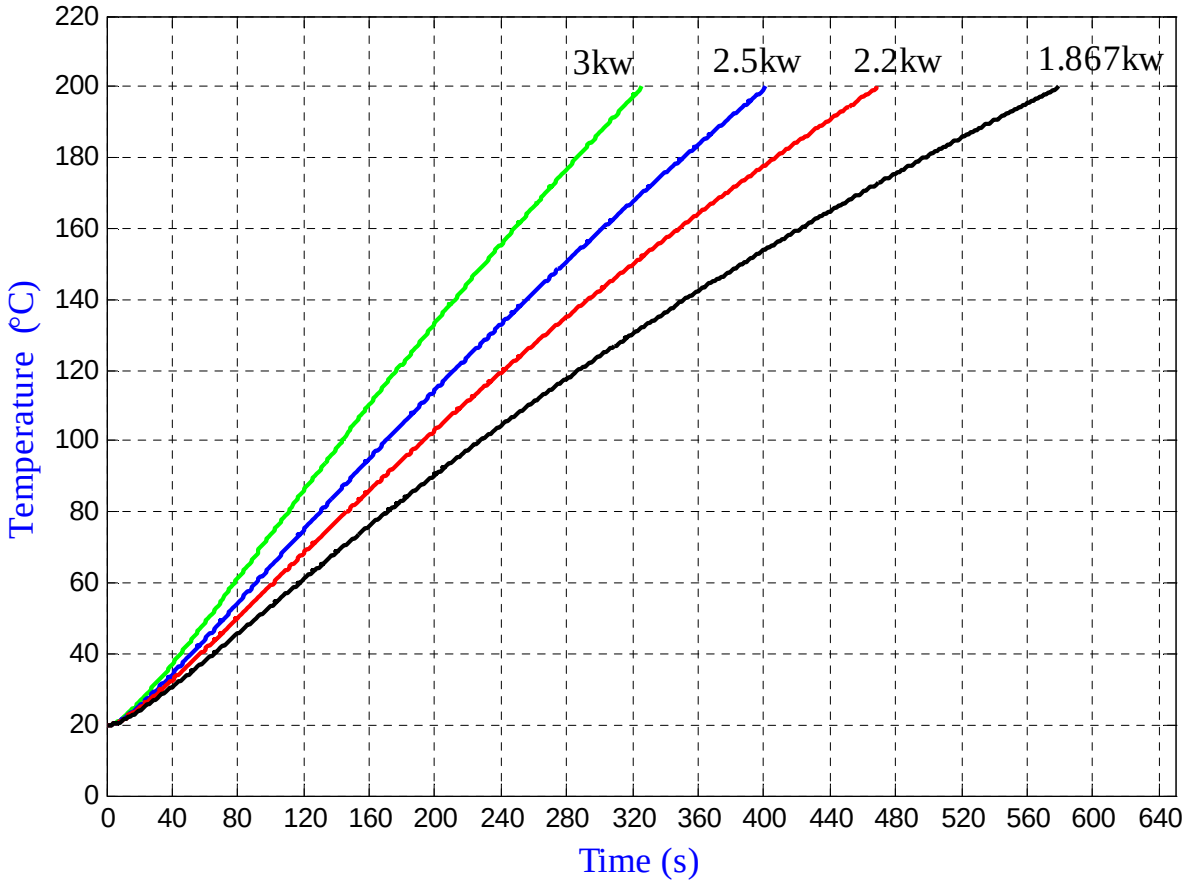

Figure 5-6: Heat up time of electric ceramic pan with a thickness of 0.008*m* and different power input.

Figure 5-7 shows the surface node (node 118) temperature profile of 0.008 *m* heated oil ceramic baking pan as a function of heat up time for different heated oil input temperatures. The heat up time for other heated oil ceramic pan thicknesses as a function of power source is shown in Table 5-3.

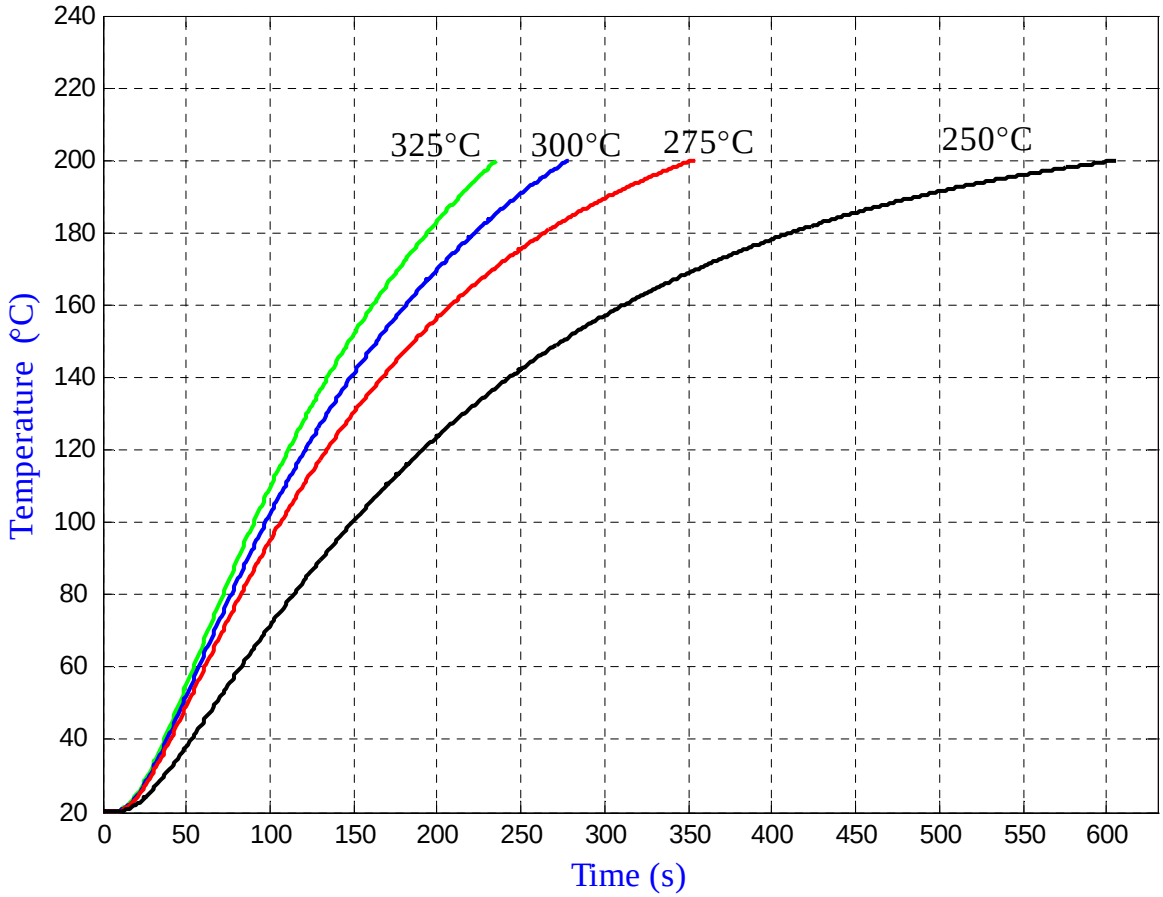

Figure 5-7: Heat up time of 0.008m ceramic pan with different heated oil temperatures

Table-5.3: Summery of heat up time for different ceramic pan thicknesses and power sources

Heat up time (s)								
Baking pan thickness (m)	Power source							
	Electric power (kW)				Heated oil(^oC)			
	3 kW	2.5 kW	2.2 kW	1.867 kW	325^oC	300^oC	275^oC	250^oC
0.008	326	402	470	580	236	280	355	510
0.01	400	495	580	716	335	400	525	-

5.2 Simulation of Injera and Baking Pans for Cyclic Baking

Once the heat up time is obtained, simulation of baking pans and injera for successive baking cycles was done in this section. A single baking cycle includes the baking period and the idle period (see figure 5-9). The baking period for all cyclic baking simulation is taken to be $150s$. The idle period varies depending on the baking pan thermal property, thickness and power input.

Finite element discretization of injera and baking pan for cyclic baking simulation is shown below.

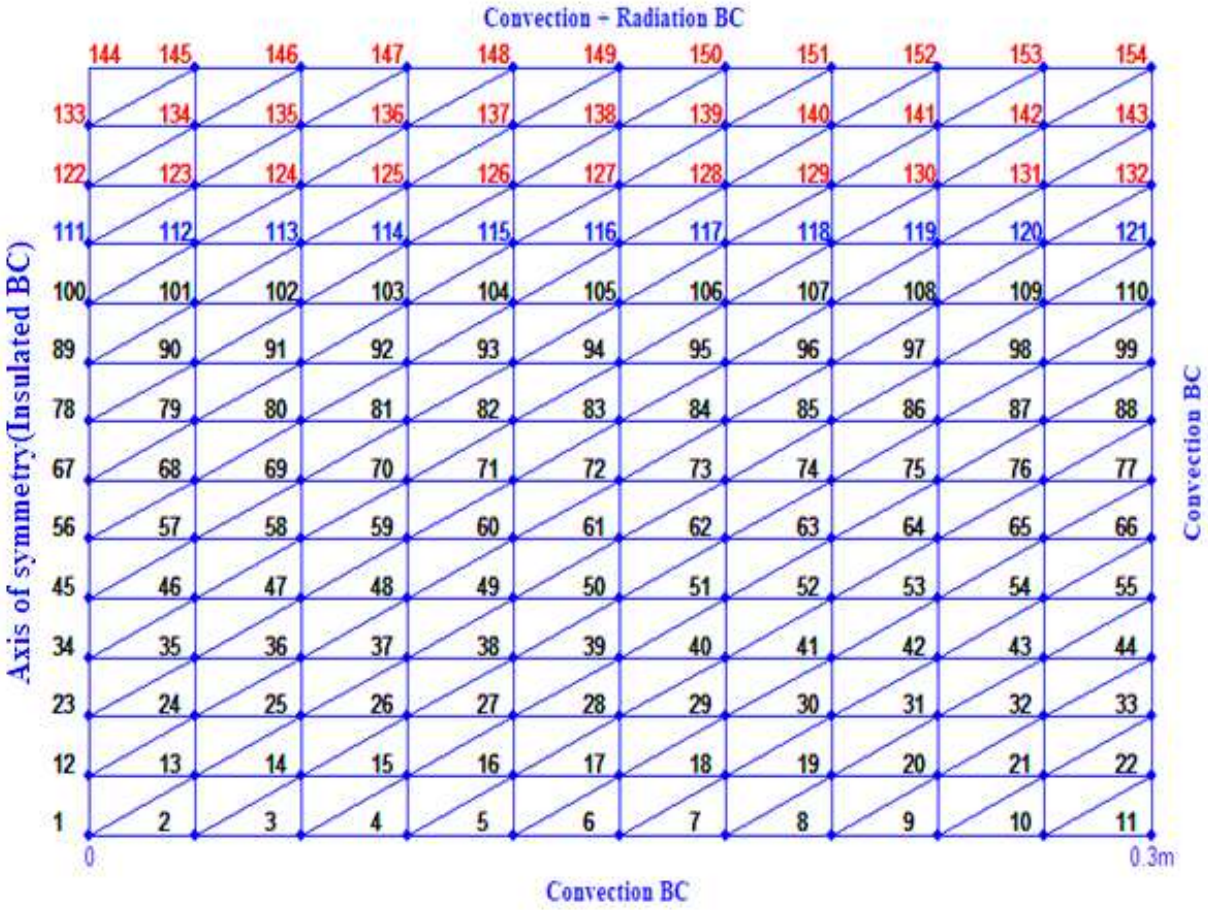

Figure 5-8: Finite element discretization of injera and baking pan

The nodes in figure 5-8 labeled in black are nodes of baking pan, nodes written in red represent nodes of injera, and nodes in blue are interface nodes.

5.2.1 Cyclic Baking Simulation of Electric Clay Baking Pans

Figure 5-9 shows temperature profiles of selected nodes of injera and baking pan for pan thickness 0.02m and power source 3 kW**.** Simulation was done for six baking cycles, and the idle period was 100s. Node 149 represents the surface temperature of six injeras (inj-1, inj-2…inj-6) during baking, and node 118 represents the surface temperature of the baking pan during heat up, baking, and idle periods.

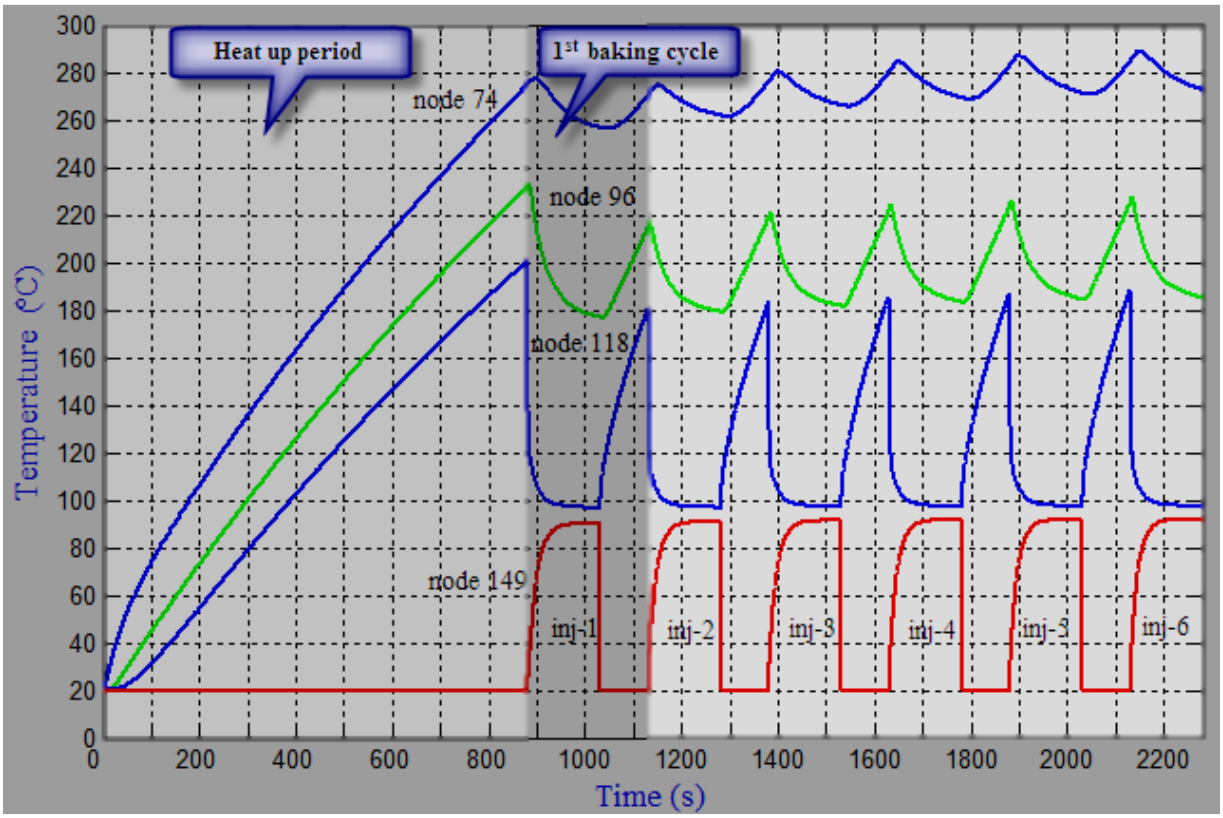

Figure 5-9: Temperature profile of nodes for pan thickness of 0.02m and power source of 3 kW

Figure 5-10 shows temperature profiles of selected nodes of injera and baking pan for pan thickness 0.02m and power source 2.5 kW**.** Simulation was done for six baking cycles, and the idle period was 120s. Node 149 represents the surface temperature of six injeras (inj-1, inj-2…inj-6) during baking, and node 118 represents the surface temperature of the baking pan during heat up, baking, and idle periods.

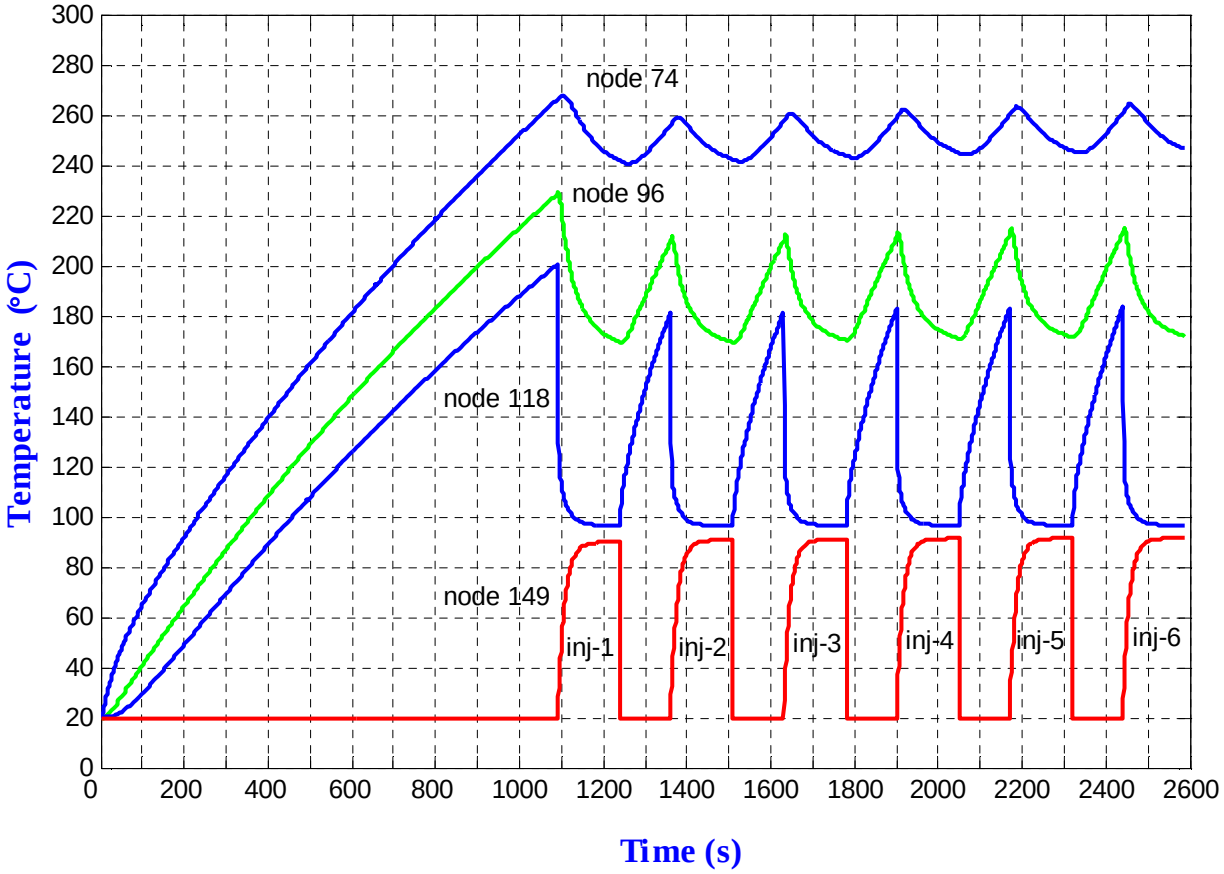

Figure 5-10: Temperature profile of nodes for pan thickness 0.02m and power source 2.5 kW

Figure 5-11 shows temperature profiles of selected nodes of injera and baking pan for pan thickness 0.02m and power source 2.2 kW**.** Simulation was done for six baking cycles, and the idle period was 145s. Node 149 represents the surface temperature of six injeras (inj-1, inj-2…inj-6) during baking, and node 118 represents the surface temperature of the baking pan during heat up, baking, and idle periods.

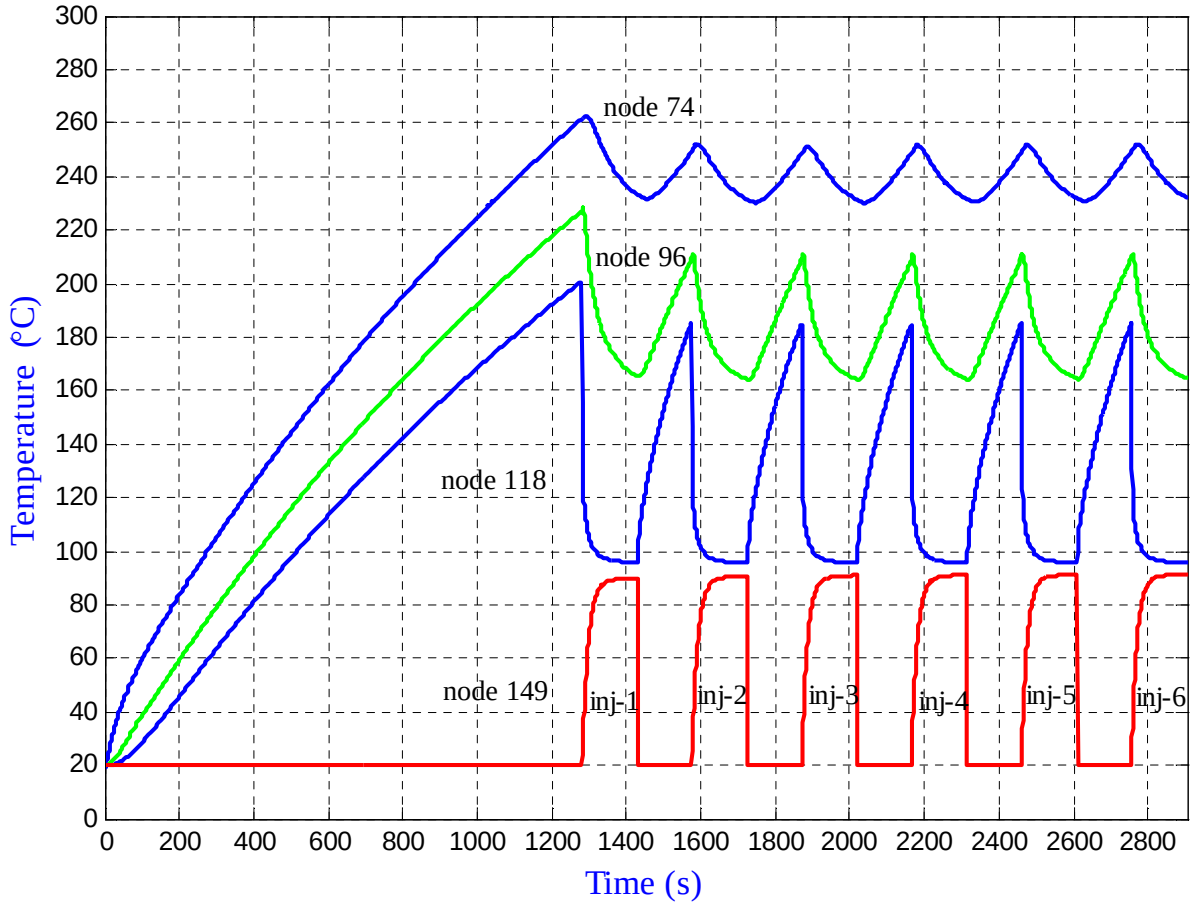

Figure 5-11: Temperature profile of nodes for pan thickness 0.02m and power source 2.2kW

Figure 5-12 shows temperature profiles of selected nodes of injera and baking pan for pan thickness 0.02m and power source 1.867 kW**.** Simulation was done for six baking cycles, and the idle period was 175s. Node 149 represents the surface temperature of six injeras (inj-1, inj-2…inj-6) during baking, and node 118 represents the surface temperature of the baking pan during heat up, baking, and idle periods.

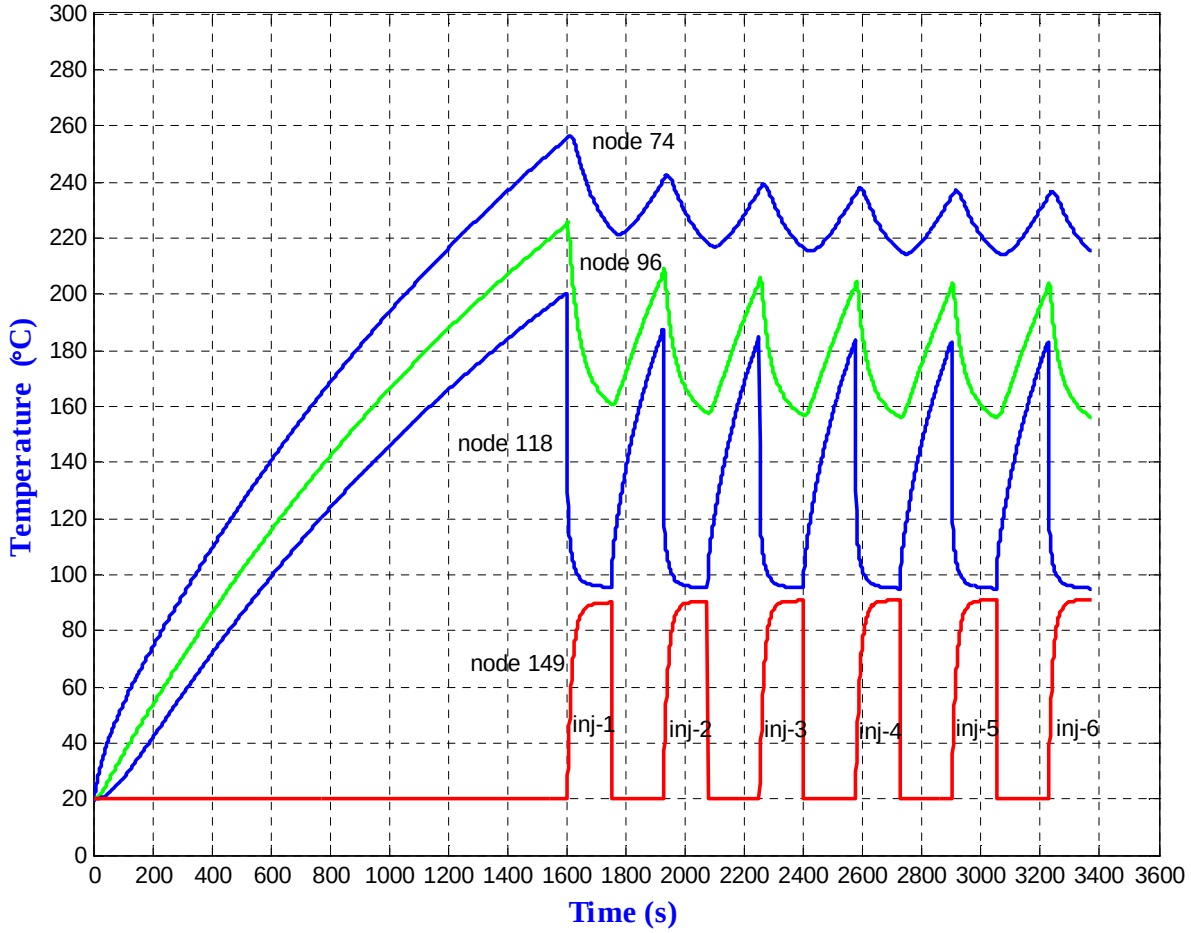

Figure 5-12: Temperature profile of nodes for pan thickness 0.02m and power source 1.867 kW

The idle time for other electric clay pan thicknesses with different power source is summarized in table 5-4.

5.2.2 Cyclic Baking Simulation of Clay Baking Pans with heated oil as power source

Figures 5-13, 5-14, and 5-15 represents temperature profiles of selected nodes of injera and baking pan for pan thickness of 0.0075 *m*, with heated oil temperatures of 250, 275 *ºC*, and 0.01 *m* with heated oil temperature 275*ºC*. Simulation was done for five baking cycles. The idle periods were 155, 115, and 160 *s* respectively. Node 149 represents the surface temperature profile of five injeras (inj-1, inj-2…inj-5) during baking, and node 118 represents the surface temperature of the baking pan during heat up, baking, and idle periods.

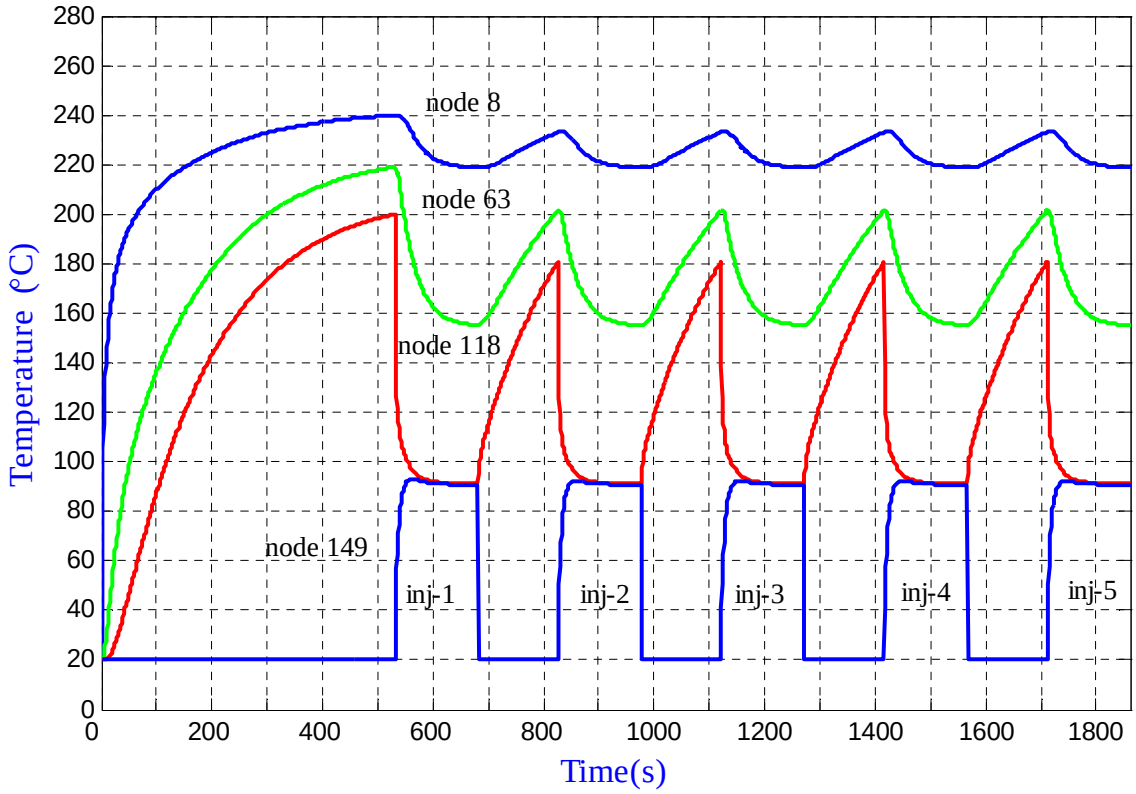

Figure 5-13: Temperature profile of nodes for pan thickness 0.0075*m* and oil temperature 250*ºC*

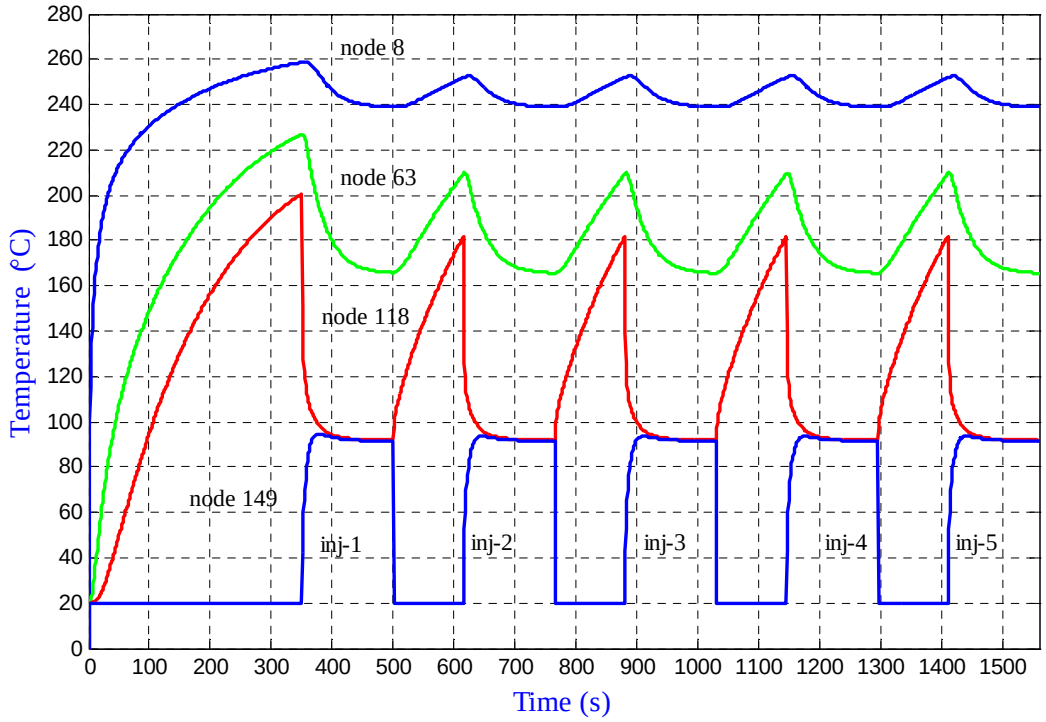

Figure 5-14: Temperature profile of nodes for pan thickness 0.0075*m* and oil temperature 275*ºC*

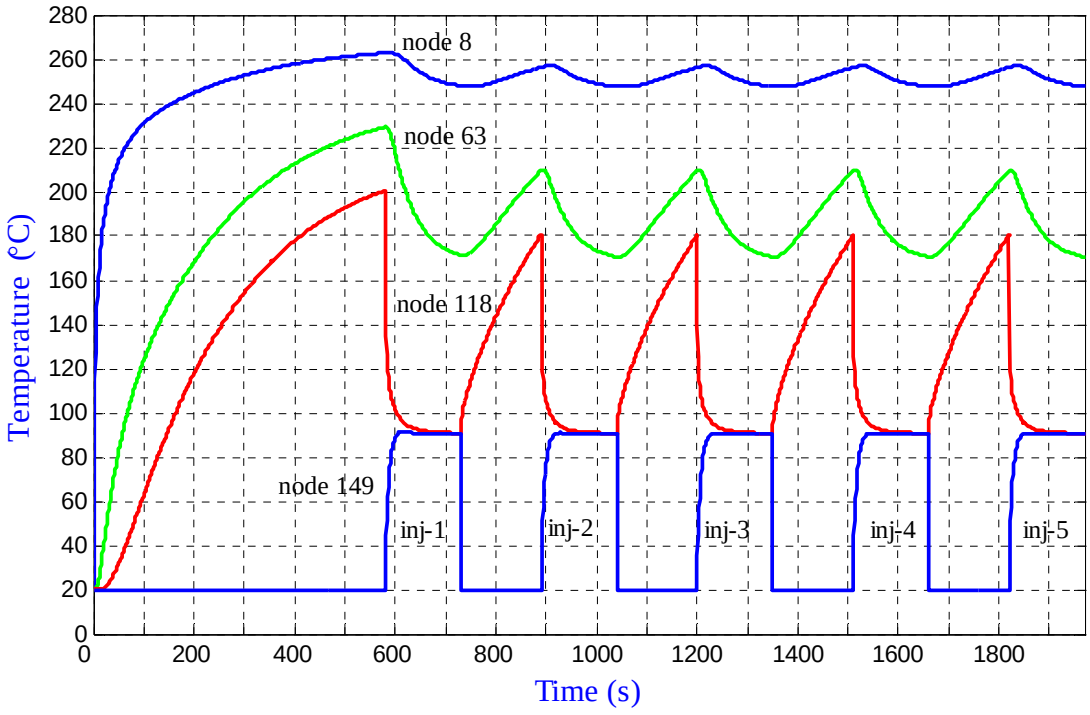

Figure 5-15: Temperature profile of nodes for pan thickness 0.01*m* and oil temperature 275*ºC*

Figure 5-16 shows a magnified view of the temperature profile of the surface of injera and baking pan for the first baking cycle of figure 5-15.

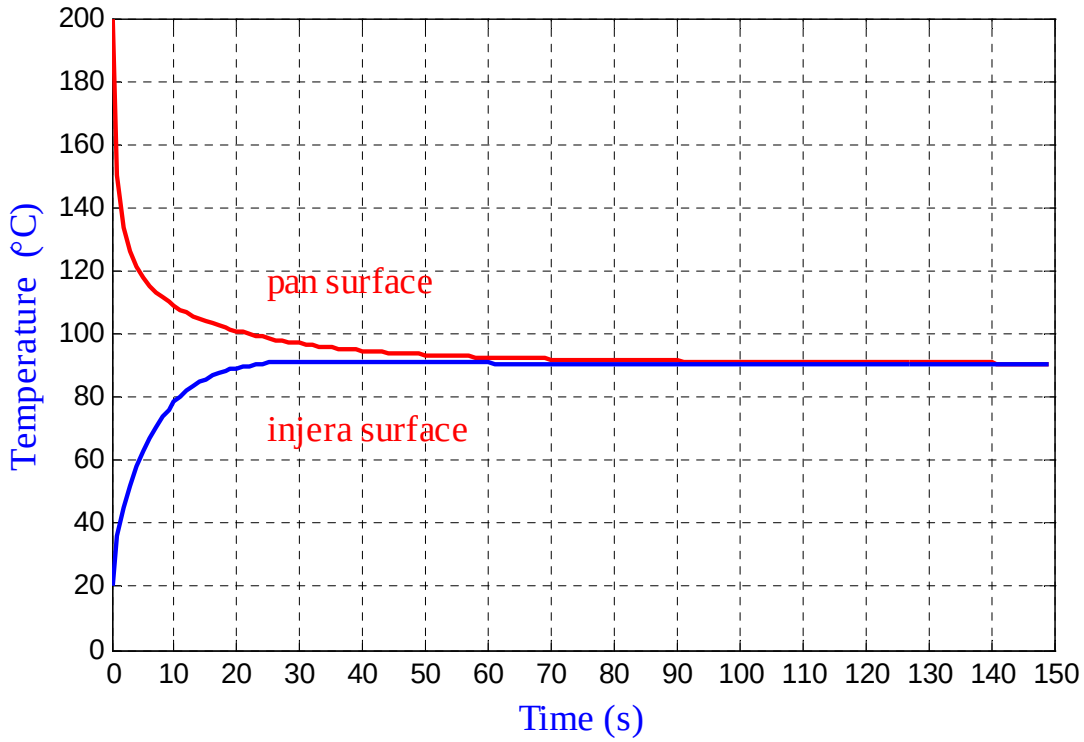

Figure 5-16: Temperature profile of injera and pan for the first baking cycle of figure 5-15

Table 5-4 shows idle periods for different clay pan thicknesses with different power sources. Simulation was not done for 0.0075 *m* electric clay pan thickness.

Table 5-4: Summery of idle period for clay baking pans with different power sources

Idle time (s)								
Baking pan thickness (m)	Power source							
	Electric power (kW)				Heated oil(^oC)			
	3 kW	2.5 kW	2.2 kW	1.867 kW	325^oC	300^oC	275^oC	250^oC
0.0075	-	-	-	-	75	90	115	155
0.01	70	85	110	135	105	125	160	-
0.015	80	100	120	150	165	200	235	-
0.02	100	120	145	175	220	270	-	-

5.2.3 Cyclic Baking Simulation of Electric Ceramic Baking Pan

Figure 5-17 shows temperature profiles of selected nodes of injera and baking pan for pan thickness 0.008m and power source 3 kW**.** Simulation was done for six baking cycles, and the idle period was 65s. Node 149 represents the surface temperature of six injeras (inj-1, inj-2…inj-6) during baking, and node 118 represents the surface temperature of the baking pan during heat up, baking and idle periods.

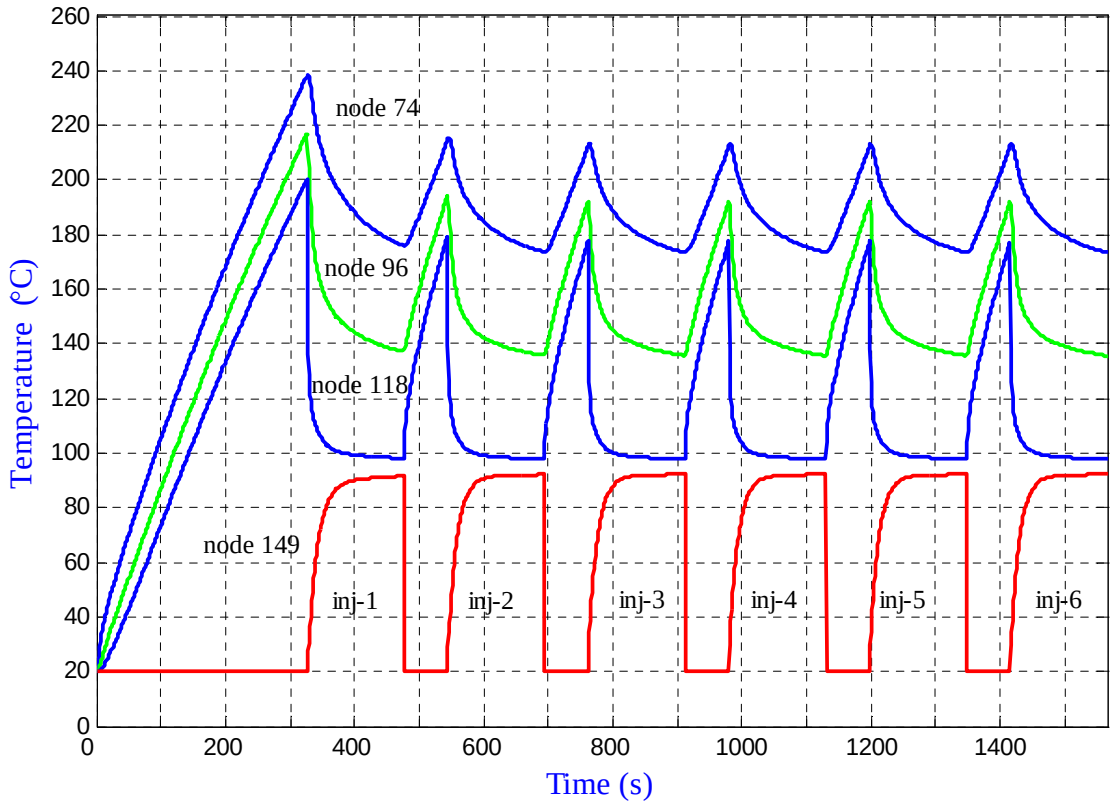

Figure 5-17: Temperature profile of nodes for pan thickness 0.008m and power source 3kW

Figure 5-18 shows temperature profiles of selected nodes of injera and baking pan for pan thickness 0.008m and power source 2.5 kW**.** Simulation was done for six baking cycles, and the idle period was 85s. Node 149 represents the surface temperature of six injeras (inj-1, inj-2…inj-6) during baking, and node 118 represents the surface temperature of the baking pan during heat up baking, and idle periods.

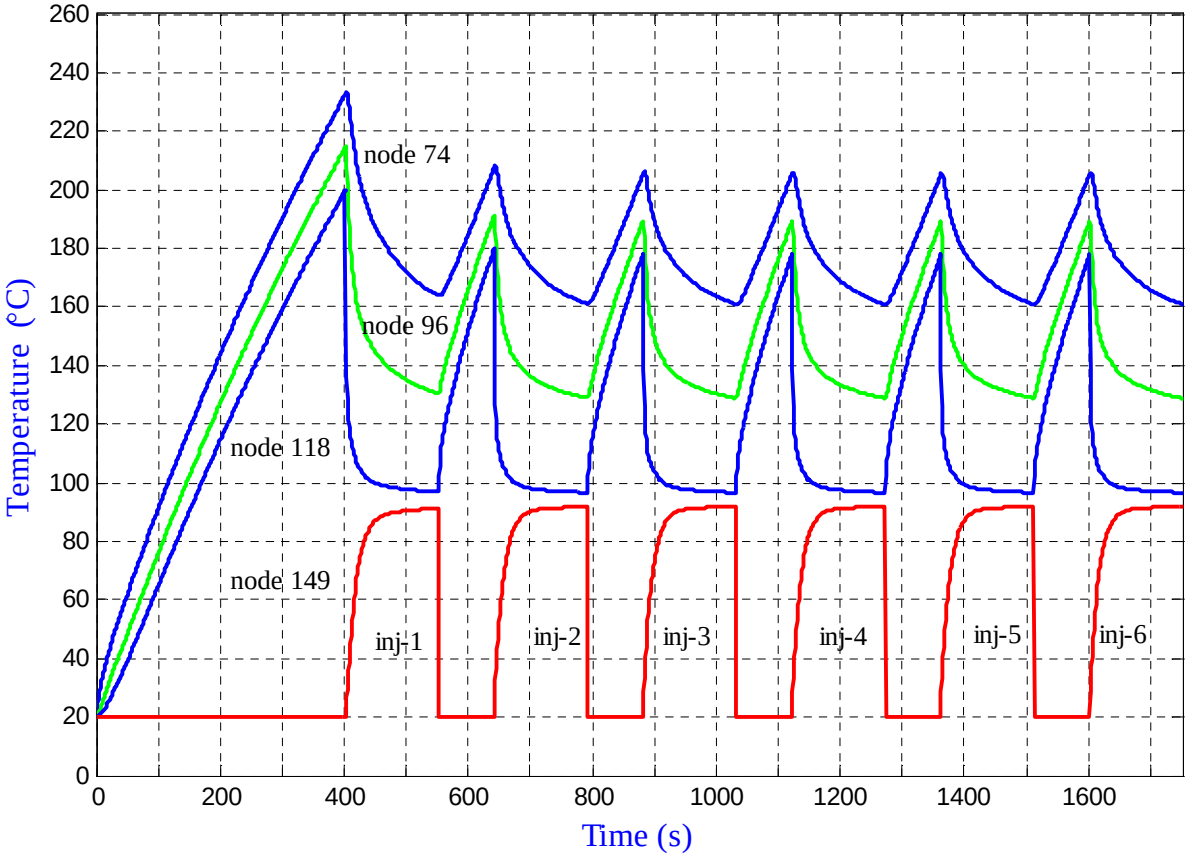

Figure 5-18: Temperature profile of nodes for pan thickness 0.008m and power source 2.5 kW

Figure 5-19 shows temperature profiles of selected nodes of injera and baking pan for pan thickness 0.008m and power source 2.2 kW**.** Simulation was done for six baking cycles, and the idle period was 105s. Node 149 represents the surface temperature of six injeras (inj-1, inj-2…inj-6) during baking, and node 118 represents the surface temperature of the baking pan during heat up, baking, and idle periods.

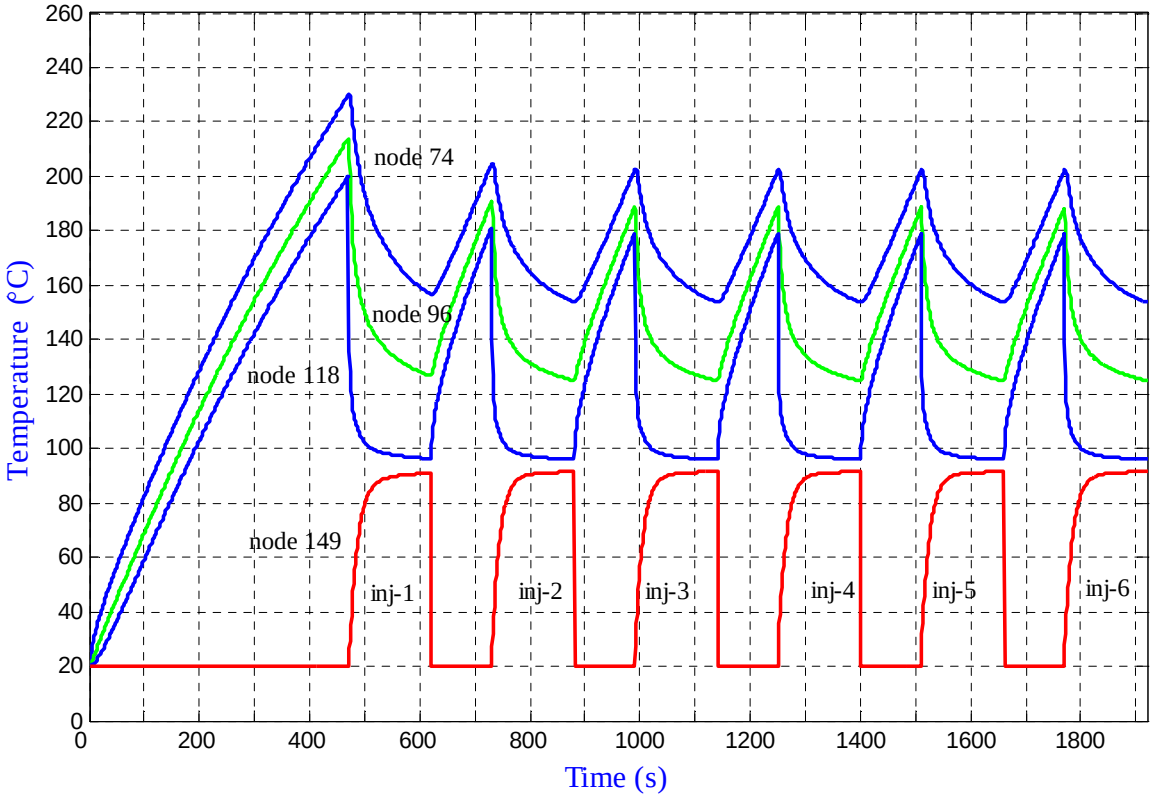

Figure 5-19: Temperature profile of nodes for pan thickness 0.008m and Power source 2.2kW

Figure 5-20 shows temperature profiles of selected nodes of injera and baking pan for pan thickness 0.008m and power source 1.867 kW**.** Simulation was done for six baking cycles, and the idle period was 125s. Node 149 represents the surface temperature of six injeras (inj-1, inj-2…inj-6) during baking, and node 118 represents the surface temperature of the baking pan during heat up, baking, and idle periods.

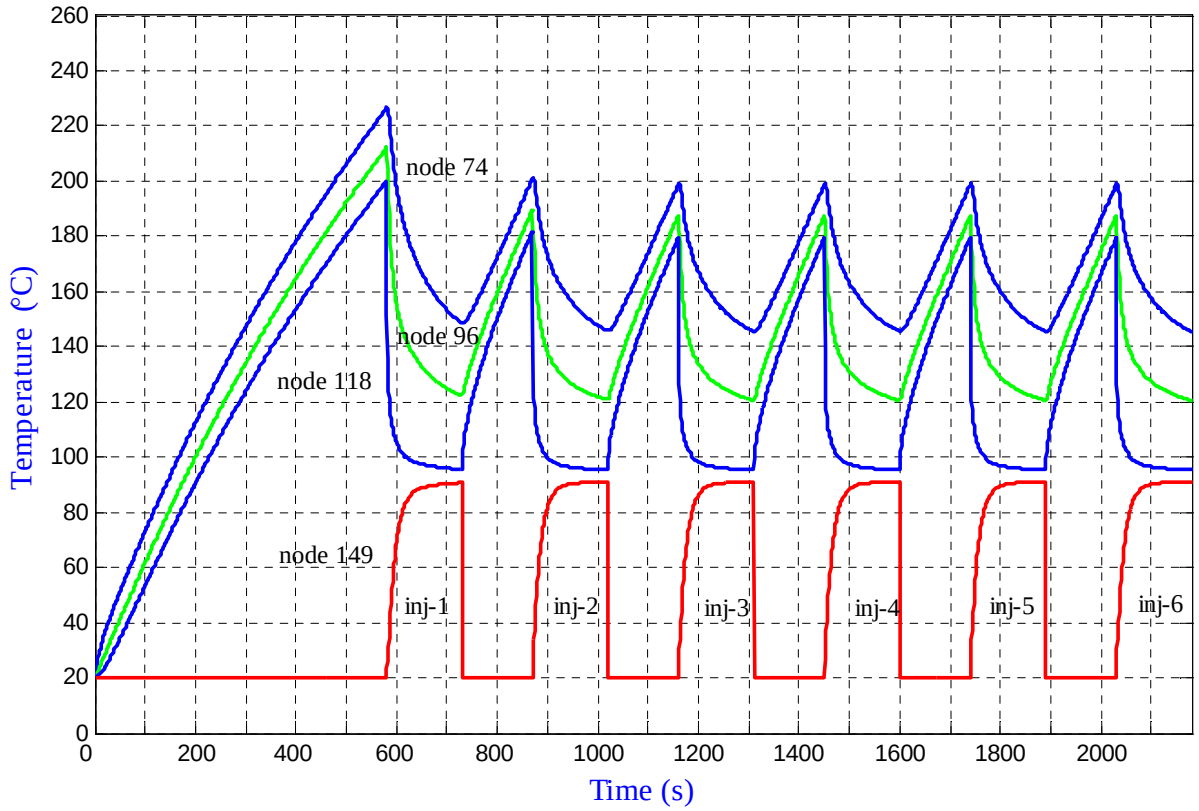

Figure 5-20: Temperature profile of nodes for pan thickness 0.008m and power source 1.876 kW

The idle period for other ceramic baking pan thicknesses with different power source is summarized in Table 5-5.

5.2.4 Cyclic Baking Simulation of ceramic baking pans with heated oil as power source

Figures 5-21, 5-22, and 5-23 represents temperature profiles of selected nodes of injera and baking pan for pan thicknesses 0.008 *m*, with heated oil temperatures 250, 275 *ºC*, and 0.01 *m* with heated oil temperature 275*ºC*. Simulation was done for five baking cycles. The idle periods were 165, 120, and 145 *s* respectively. The idle time for other pan thicknesses with different heated oil temperature sources are summarized in table 5-5. Node 149 represents the surface temperature of five injeras (inj-1, inj-2…inj-5) during baking, and node 118 represents the surface temperature of the baking pan during heat up, baking, and idle periods.

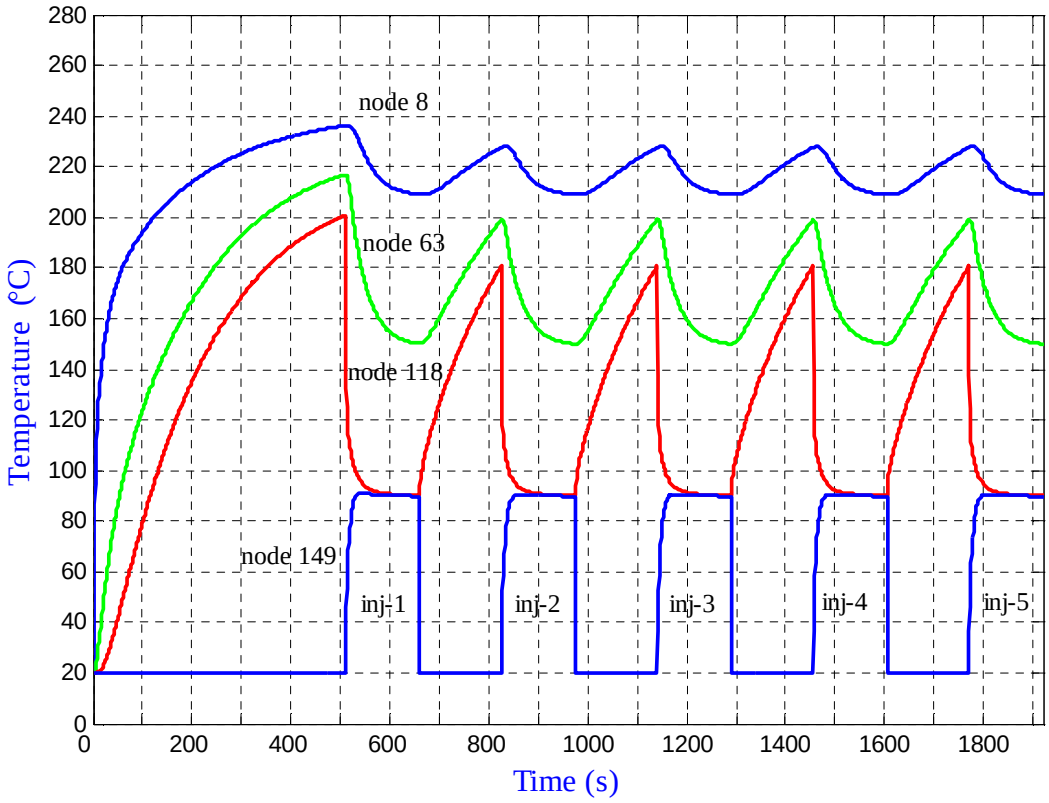

Figure 5-21: Temperature profile of nodes for pan thickness 0.008*m* and oil temperature 250*ºC*

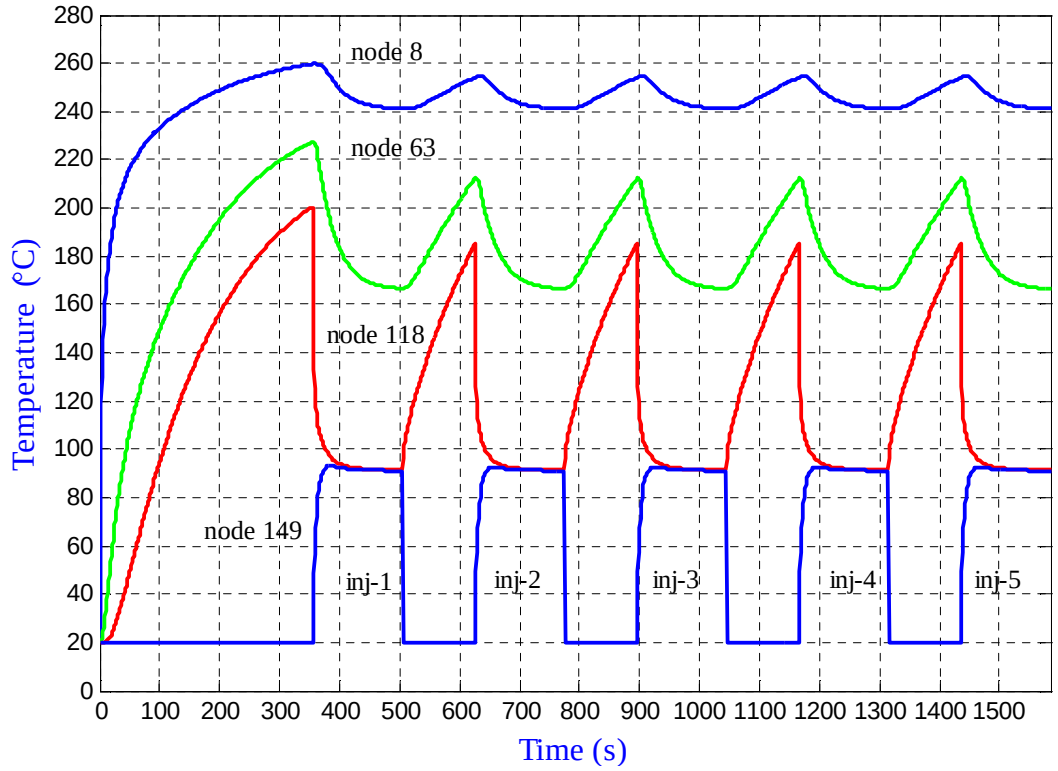

Figure 5-22: Temperature profile of nodes for pan thickness 0.008*m* and oil temperature 275*°C*

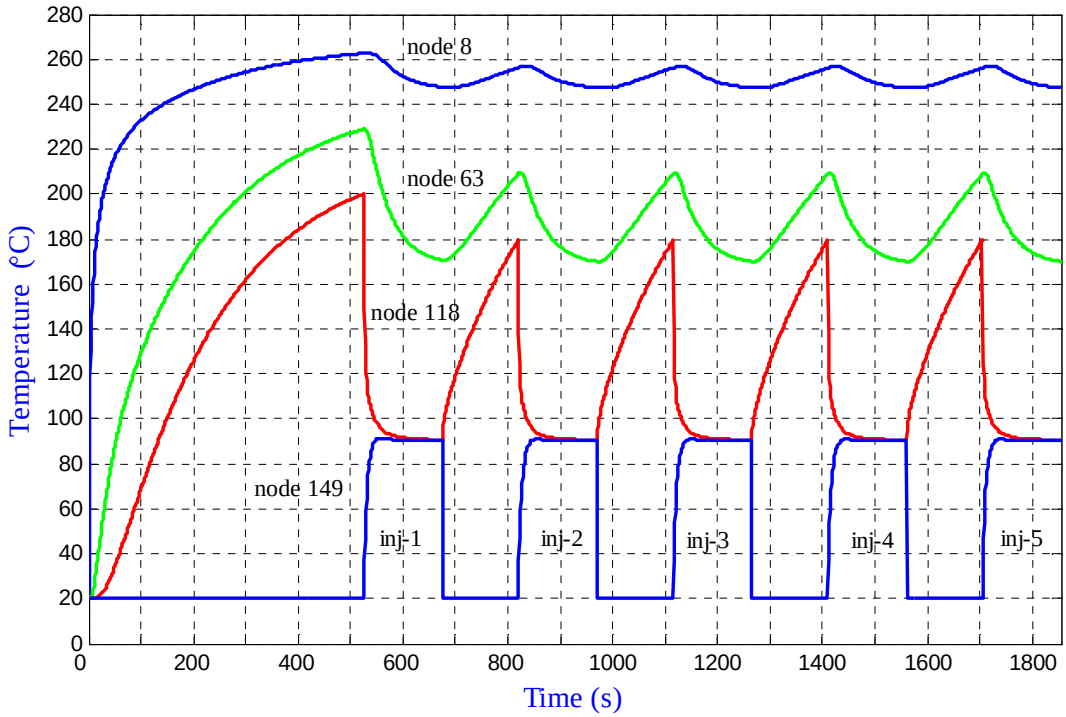

Figure 5-23: Temperature profile of nodes for pan thickness 0.01*m* and oil temperature 275*°C*

Figure 5-24 shows simulation results of injeras baked with electric ceramic baking pan (with power input 2.5 kW and thickness 0.008m), and heated oil ceramic baking pan (with power input 275^oC and thickness 0.008m). As it is shown in the graph, the surface temperature of injera baked using heated oil reaches to the baking temperature (boiling temperature of water around that area, 90-94 ^oC) faster than the one baked with electric ceramic baking pan.

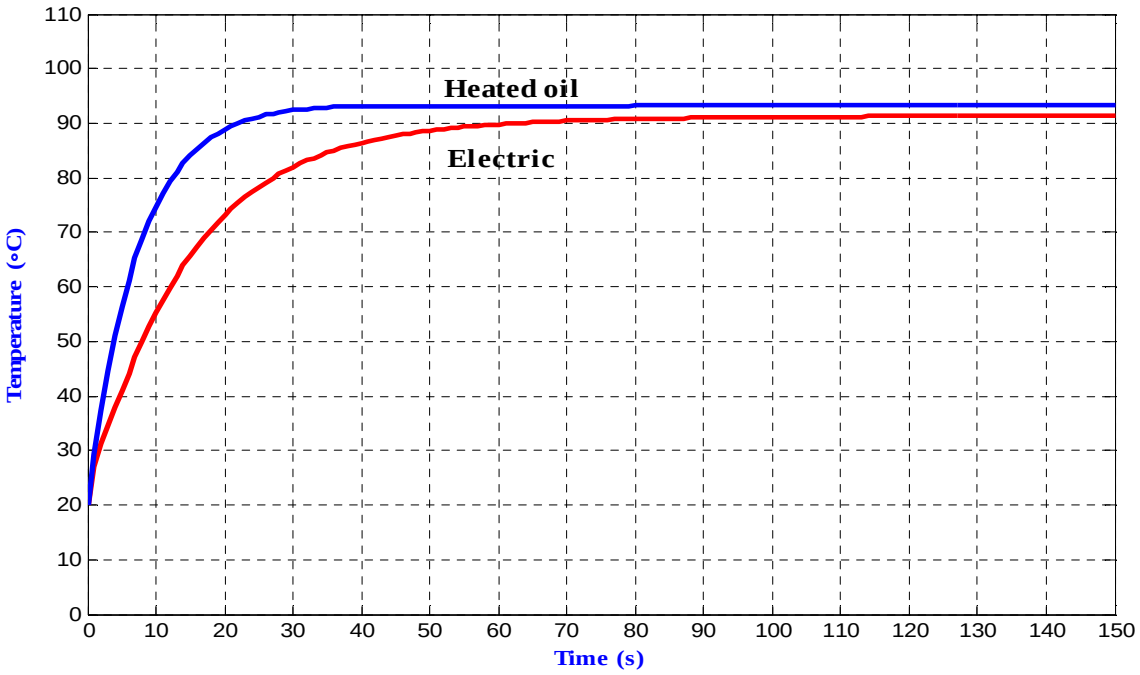

Figure 5-24: Temperature profile of injeras baked with electric and heated oil ceramic pan

Table 5-5 shows idle periods for different ceramic pan thicknesses with different power sources. The idle period of a baking pan increases when the power input decreases for a given pan thickness.

Table 5-5: Summery of idle time for ceramic baking pans with different power source

Idle time (s)								
Baking pan thickness (m)	Power source							
	Electric power (kW)				Heated oil(^oC)			
	3 kW	2.5 kW	2.2 kW	1.867 kW	325^oC	300^oC	275^oC	250^oC
0.008	65	85	105	125	75	95	120	165
0.01	70	90	110	130	100	120	145	-

CHAPTER SIX

ENERGY UTILIZATION AND EFFICIENCY OF BAKING PANS

There are three quantities to be noted with regard to the energy use of baking pans: the total energy, the utilized energy, and efficiency of baking pans [14]. These quantities are used in the study of the performance of electric clay and ceramic baking pans.

6.1 Energy Utilization

The total energy is the amount of energy used to cook a certain amount of injera. It includes both the energy actually utilized in cooking the injera and the energy lost during baking. The utilized energy is the amount of energy which is actually used in cooking injera, not including any of the losses during the process of baking. The utilized energy during injera baking includes the energy required to raise the temperature of the batter to the boiling point of water, plus the energy required to vaporize a portion of the water in the batter. The following assumptions are made in order to calculate the amount of utilized energy by a baking pan [14]:

- The average mass of injera and moisture loss for every single injera is constant.
- The heat capacity of the batter is nearly equal to the heat capacity of water.
- The difference in weight between the baked injera and the initial batter is equal to the weight of moisture loss during baking.

Applying the above assumptions, the utilized energy can be obtained from the following equation [14]:

$$E_{utilized} = m_{batter} c_p \left(T_{boiling} - T_o\right) + h_{fg}\left(m_{batter} - m_{injera}\right) \quad (6.1)$$

Where:

$E_{utilized}$= energy utilized(J),

m_{batter}= mass of batter(kg),

m_{injera}= mass of baked injera(kg),

c_p= heat capacity of water$(J/kg.K)$,

$T_{boiling}$ = boiling temperature of water in that area (^oC),

T_o= room temperature (^oC), and

h_{fg}= heat of vaporization of water at the boiling temperature in that area (J/kg).

The average mass of injera and batter during baking using clay and ceramic baking pans is obtained experimentally using mass balance by taking four different samples(see Tables 6-1, and 6-2 below).

Table 6-1: Mass balance of injera and batter during baking using clay baking pan

Sample	Mass of batter (kg)	Mass of injera(kg)	Mass loss (kg)
1	0.6930	0.5025	0.1905
2	0.6125	0.4355	0.1770
3	0.6295	0.4345	0.1950
4	0.6460	0.4425	0.2035
Average	0.6453	0.4538	**0.1915**

Table 6-2: Mass balance of injera and batter during baking using ceramic baking pan

Sample	Mass of batter (kg)	Mass of injera(kg)	Mass loss (kg)
1	0.6240	0.4560	0.1680
2	0.6040	0.4445	0.1595
3	0.6665	0.4785	0.1880
4	0.6230	0.4540	0.1690
Average	0.6294	0.4583	**0.1711**

6.2 Efficiency of Baking Pans

The efficiency of a baking pan is simply the utilized energy divided by the total energy input (or the energy utilized during a baking session divided by total energy consumed by the baking pan).

$$efficiency = \frac{Energy\ utilized}{Energy\ input} \times 100\%$$

$$\eta_{th} = \frac{E_{utilized}}{E_{input}} = \frac{m_{batter} c_p (T_{boiling} - T_o) + h_{fg}(m_{batter} - m_{injera})}{\dot{Q}_v \times t} \times 100\% \quad (6.2)$$

Where:

E_{input}= energy input (J),

$\dot{Q}_v$= rate of energy input (W), and

t= total time taken during the baking session (s).

The total time taken for a baking session is the sum of, the heat up time, the total baking time, and the total idle time [2].

$$t = t_{heat\ up} + n \times t_{baking} + (n-1) \times t_{idle} \quad (6.3)$$

Where:

t= total time for the baking session(s),

$t_{heat\ up}$= heat up time(s),

t_{baking}= baking time for a single injera(s),

t_{idle}= idle time(s), and

n=number of baking cycle.

6.2.1 Efficiency of Electric Clay Baking Pans

Table 6-3 shows the utilized energy and efficiency of clay baking pans for 10 baking cycles. Table 6-4 shows the efficiency of clay baking pans for 20, 30, 40, and 50 baking cycles. The utilized energy for the calculation of efficiency is obtained from Eq. (6.1), and the total time is obtained from Eq. (6.3) with the help of Tables 5-2, and 5-4.

Table 6-3: Utilized energy and efficiency of different clay baking pans for 10 baking cycles

Power source(kW)	Pan thickness (m)	Total time(s)	Energy input(J)	Energy utilized(J)	Efficiency(%)
1.867	0.010	4224	7886208	5225575	66.26
	0.015	4709	8791703		59.44
	0.020	5350	9988450		52.32
2.2	0.010	3228	7101600		73.58
	0.015	3633	7992600		65.38
	0.020	4085	8987000		58.15
2.5	0.010	2782	6955000		**75.13**
	0.015	3185	7962500		65.63
	0.020	3680	9200000		56.80
3	0.010	2550	7650000		68.31
	0.015	2855	8565000		61.01
	0.020	**3280**	**9840000**		**53.11**

Table 6- 4: Efficiency of clay baking pans for different baking cycles

Efficiency(%)					
Power source(kW)	Pan thickness (m)	Baking cycle			
		20	30	40	50
1.867	0.010	70.64	72.24	73.06	73.56
	0.015	65.79	68.22	69.50	70.29
	0.020	59.87	62.90	64.53	65.55
2.2	0.010	79.47	81.64	82.78	83.47
	0.015	73.28	76.35	77.99	79.00
	0.020	67.53	71.36	73.45	74.76
2.5	**0.010**	**81.46**	**83.81**	**85.04**	**85.79**
	0.015	73.53	76.61	78.25	79.27
	0.020	65.52	69.06	70.98	72.18
3	0.010	73.34	75.19	76.15	76.73
	0.015	67.58	70.09	71.42	72.25
	0.020	60.27	63.11	64.63	**65.58**

Figure 6-1 shows the efficiency of clay baking pans with different thickness as a function of power input for 20 baking cycles.

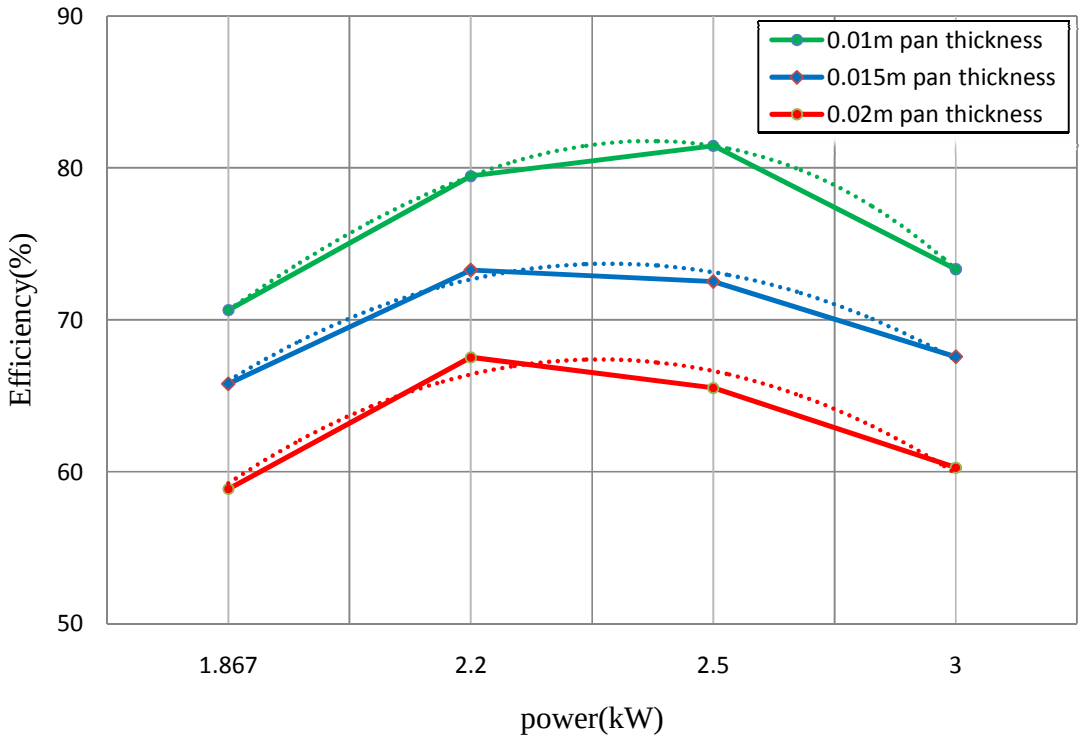

Figure 6-1: Efficiency of clay baking pans as a function of power input

In order to find efficiency using Eq. (6.2), the weight loss of injera for clay baking pan thicknesses other than the conventional baking pan was based on the assumption that the weight loss was the same as the experimentally found weight loss of the conventional clay baking pan. Because of this assumption the utilized energy of all clay baking pans is the same for a given baking cycle.

The efficiency of clay baking pan with a thickness of 0.02 and power input of 3 (conventional baking pan) for 10 baking cycle is 53.11 %(Table 6-3), this efficiency is improved to 65.58% (Table 6-4) by increasing the baking cycle to 50. The main reason for the improvement in efficiency as the baking cycle increase was the increase in utilized energy. The efficiency of the conventional baking pan further increased to 85.79%, for 50 baking cycle, by reducing the thickness of the baking pan to 0.01 , and the power source to 2.5 .

6.2.2 Efficiency of Electric Ceramic Baking Pans

Table 6-5 shows the utilized energy and efficiency of electric ceramic baking pans for 10 baking cycles. Table 6-6 shows the efficiency of ceramic baking pans for 20, 30, 40, and 50 baking cycles. The utilized energy for the calculation of efficiency is obtained from Eq. (6.1), and the total time is obtained from Eq. (6.3) with the help of Tables 5-3, and 5-5.

Table 6-5: Utilized energy and efficiency of ceramic baking pans for 10 baking cycles

Power source(kW)	Pan thickness (m)	Total time(s)	Energy input(J)	Energy utilized(J)	Efficiency(%)
1.867	0.010	4151	7749917	4742887	61.20
	0.008	3925	7327975		64.72
2.2	0.010	3295	7249000		65.43
	0.008	3095	6809000		69.66
2.5	0.010	2805	7012500		67.63
	0.008	2667	6667500		**71.13**
3	0.010	2530	7590000		62.49
	0.008	2411	7233000		**65.57**

Table 6-6: Efficiency of ceramic baking pans for different baking cycles

Efficiency(%)					
Power source(kW)	Pan thickness (m)	Baking cycle			
		20	30	40	50
1.867	0.010	65.13	66.55	67.29	67.74
	0.008	67.97	69.13	69.72	70.08
2.2	0.010	70.17	71.90	72.80	73.35
	0.008	73.77	75.25	76.01	76.48
2.5	0.010	72.90	74.84	75.85	76.47
	0.008	**75.63**	**77.26**	**78.10**	**78.61**
3	0.010	66.85	68.44	69.26	69.77
	0.008	69.33	70.67	71.37	**71.79**

Figure 6-2 shows the efficiency of ceramic baking pans with different thickness as a function of power input for 20 baking cycles.

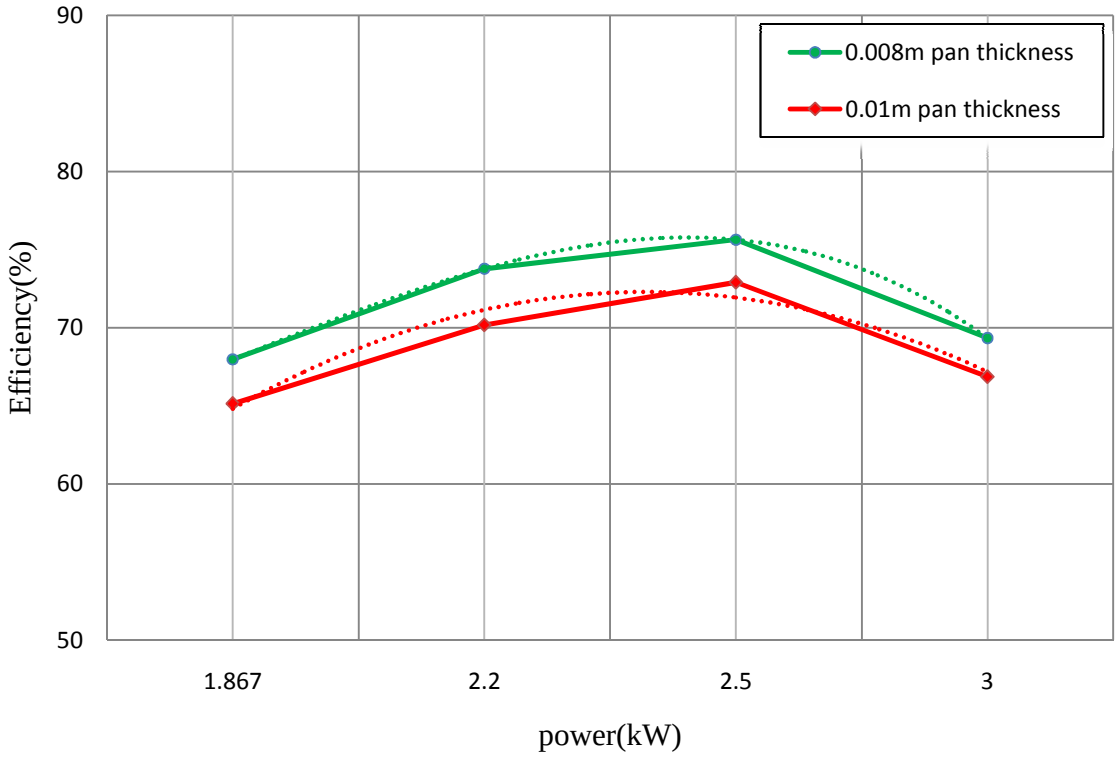

Figure 6-2: Efficiency of ceramic baking pans as a function of power input

The utilized energy of 0.01 ceramic baking pan was calculated based on the assumption that the weight loss of injera was the same as the experimentally found weight loss of 0.08 ceramic baking pan. The efficiency of 0.08 ceramic baking pan for 10 baking cycle is 65.57 %(Table 6-5), this efficiency is improved to 71.79% (Table 6-5) by increasing the baking cycle to 50. The maximum efficiency of ceramic baking pans (78.61%) was obtained for a baking pan thickness of 0.08m, and a power source of 2.5 .

The overall improvement in efficiency of ceramic baking pans is smaller than clay baking pans; this is because of the fact that the energy utilized by ceramic baking pans was smaller than clay baking pans as a result of the decrease in weight loss of injeras baked with ceramic baking pans (Table 6-2).

CHAPTER SEVEN

CONCLUSIONS AND RECOMMENDATIONS

The general objective of this thesis was to study the transient heat transfer analysis during injera baking process. In doing this, a mathematical model for simultaneous heat and mass transfer during baking of injera was developed. A finite element scheme was used to implement this mathematical model for baking and an efficient code was written in MATLAB to simulate the model numerically. The process was simulated in terms of temperature profiles at certain baking pan and injera positions. The profile for temperature distribution during heat up and cyclic baking are plotted. Thermo-physical properties and moisture transport parameters of injera were predicted analytically and were used for the temperature profile prediction using the numerical model.

The results from this research lead to the following conclusions:

- Given the same thermal property(thermal conductivity, specific heat, and density) and power input, decreasing the thickness of a baking pan results a decrease in heat up time and idle time of the baking pan. Given the same thermal property and same pan thickness, decreasing power input results an increase in heat up time and idle time.

- Simulation results shows that, heat up and idle time of a baking pan decreases as thermal conductivity increases, so a major improvement in efficiency will be obtained if baking pan thermal conductivity is improved. On the other hand, increase in specific heat capacity and density of baking pans increases the heat up time and idle time.

- Simulation of baking pans for heat up time with thicknesses greater than or equal to $0.01m$ shows that, it is difficult to achieve surface baking temperature (200℃) using heated oil temperature of 250℃. For the conventional baking pan heated oil temperatures of 300℃ and above are required to achieve surface baking temperature.

- From the temperature of injeras baked with different power sources, we can conclude that, the formation of proper injera requires a specific rate of initial power delivery. Too little power delivery will not properly boil the water in the batter, while too much power will create uneven boiling which may result in an improper moisture content of injera.

- The temperature profile of injera increases rapidly toward the boiling point of water at the associated pressure when heated oil was used as a power source instead of electric power, (see figure 5-24).

- There was a slight increase in surface temperature of injera when the baking pan thickness becomes smaller for the same power source. Therefore, further decrease in baking pan thickness with higher thermal conductivity may result in a lower quality of injera.

- Experimental test on the mass balance of batter and injera shows that injera baked with $0.02m$ conventional clay baking pan has more loss of weight than injera baked with $0.008m$ ceramic baking pan. This shows that the utilized energy by the ceramic baking pan is smaller than the conventional clay baking pan(see Tables 6-1, and 6-2).

- From the efficiency calculation, efficiency of electric baking pans of all types increases as the number of baking cycle (baking session) increases, because of the increase in utilized energy. Clay and ceramic electric baking pans with thicknesses $0.01m$ and $0.008m$ respectively, and with a power input of $2.5kW$ are more efficient in comparison with other baking pan thicknesses and power sources. The $0.008\ m$ ceramic baking pan is currently under experimental investigation, while the $0.01\ m$ clay baking pan is not yet realized.

Recommendations for future work:

- Experimental study of thermo-physical property of injera and baking pan.
- Energy auditing during the process of injera baking to exactly identify the losses.
- Experimental investigation of modified clay baking pans with better thermal property.

REFERENCES

1. Adefemi Farinu, “Heat and Mass Transfer Analogy under Turbulent Conditions of Frying”, Unpublished thesis, University of Saskatchewan, Canada, 2006.
2. Assefa Abate, “Transient heat transfer analysis of injera baking pan (“mittad”) by finite element method”, Unpublished thesis, Addis Ababa University, 2010.
3. Banooni S., Hosseinalipour S. M., Mujumdar A. S., Taheran E., Bahiraei M.,and Taherkhani P., “Baking of Flat Bread in an Impingement Oven: An Experimental Study of Heat Transfer and Quality Aspects”, Drying Technology, 26: 902–909, 2008.
4. Banooni S., Hosseinalipour S. M., Mujumdar A. S., Taheran E., Bahiraei M., and Taherkhani P. , “Baking of Flat Bread in an Impingement oven: Modeling and Optimization”, Drying Technology , 27(1)1,103:112, 2008.
5. Banooni S., Hosseinalipour S. M., Mujumdar A. S., Taheran E., Bahiraei M., and Taherkhani P., “Impingement Heat Transfer Effects on Baking of Flat Bread”, Drying technology 26(7), 910-919, 2008.
6. Barbosa-Cánovas G.V., Juliano P. and Peleg M. Engineering Properties of Foods, Washington State University, USA, 2006.
7. Boukouvalas Ch. J., Krokida M.K., Maroulis Z.B. and Marinos-Kouris D., “Density and Porosity: Literature Data Compilation for Food Stuffs”, International Journal of Food Properties, 9(4), 715 — 746, 2006.
8. Choi Y. and M. R. Okas, “Effect of Temperature and Composition on Thermal Properties of Foods”, Food Engineering and Process Applications, Volume1, 93, London, UK: Elsevier, 1986.
9. Comini G. and Lewis R. W., “A Numerical Solution of Two-Dimensional Problems Involving Heat and Mass Transfer”, International Journal of Heat and Mass Transfer, 19, 1387-1392, 1975.
10. Francisco Javier Sayas, A Gentle Introduction to the Finite Element Method, 2008.
11. David V. Hutton, Fundamentals of Finite Element Analysis, McGraw-Hill, 2004.
12. Emmanuel P., Viviana O., “Bread Baking as a Moving Boundary Problem Part 1: Mathematical Modeling”, Journal of Food Engineering, volume 91, pages 428–433, 2009.
13. Ezana Negusse and Robert Van Buskirk, “Electric Enjera Cooker (Mogogo) Efficiency. Research Report: October, Asmara, Eritrea, 1996.

14. Ezana Negusse, Robert Van Buskirk, and Haile Teclai,"The Effect of Clay and Iron Cooking Plates on Mogogo Efficiency and Energy use: Experimental Results", Energy Research and Training Center, P.O. Box 5285, Asmara, ERITREA.
15. Gebrehiwot and Gebrekidan," Fermented Cereals. A Global Perspective," FAO report, 1982, http://www.fao.org/docrep.
16. Gibin G. Powathil," A Heat and Mass Transfer Model for Bread Baking: An Investigation using Numerical Schemes", Unpublished thesis, Department of Mathematics, National University of Singapore, 2004.
17. Gonul Kaletunc, "Prediction of Specific Heat of Cereal Flours: A Quantitative Empirical Correlation", Journal of Food Engineering, 82,589–594, 2007.
18. Gupta T.R,"Individual heat transfer modes during contact baking of Indian unleavened flat bread (chapatti) in continuous oven, Journal of Food Engineering, 43-313-319, 2001.
19. Hans Dieter Baehr and Karl Stephan, Heat and mass transfer, Springler, second revised edition, Germany, 2006.
20. Holman, J. P., Heat Transfer, third Edition, McGraw-Hill, New York, 1972.
21. Huang H., P. Lin and W. Zhou, "Moisture Transport and Diffusive Instability during Bread Baking, Unpublished M.Sc thesis, York University, June 9, 2006.
22. John H.Lienhard IV and John H.Lienhard V, A Heat Transfer Text Book, third edition. Phlogiston press, Cambridge Massachusetts, 2004.
23. Joseph Irudyaraj, Food Processing Operations Modeling Design and Analysis, Marcel Dekker, Inc., New York, 2002.
24. Karin Thorvaldsen, Hans Janestad, "A Model for Simultaneous Heat, Water and Vapor Diffusion", Journal of Food Engineering, 40, 167-172, 1999.
25. Kenneth J. Valentas, Enrique Rothstein, and R. Paul Singh; Hand Book of Food Engineering Practice, CRC press, Newyork , 1997 ,
26. Krokida M. K., Michailidis P. A., Maroulis Z. M., and Saravacos G. D, "Literature Data of Thermal Conductivity of Food Stuffs", International Journal of Food Properties, 5(1), 63-111, 2002.
27. Krokida M. K., Zogzas N. P., and Maroulis Z. B., "Mass Transfer Coefficient in Food Processing: Compilation of Literature Data, International Journal of Food Properties, 4(3), 373-382, 2001.

28. Krokida M. K., Michailidis P. A, Maroulis Z. M, and Saravacos G. D, “Thermal Conductivity: Literature Data Compilation for Food Stuffs”, International Journal of Food Properties, 4: 1,111- 137, 2001.
29. Lewis R.W., K. Morgan, H.R. Thomas, and K.N. Seetharamu, The Finite Element Method in Heat Transfer Analysis , John Wiley and Sons, Inc., 1996.
30. Luikov A.V.,” Systems of Differential Equations of Heat and Mass Transfer in Capillary Porous Bodies (Review)”, ht.J, Heat Mass Transfer, vol.18, pp. 1-14, 1973.
31. Melike Sakin, Figen Kaymak-Ertekin, Coskan Ilicali, “Simultaneous Heat and Mass Simulation Applied to Convective Oven Cup Cake Baking”, Journal of Food Engineering, 83, 463–474, 2007.
32. Melike Sakin, Figen Kaymak-Ertekin, Coskan Ilicali, “Convection and Radiation Combined Surface Heat Transfer Coefficient in Baking Ovens’, Journal of Food Engineering, 94 344–349, 2009.
33. Michel Favre-Marinet and Sedat Tardu, Convective Heat Transfer. John Wiley & Sons, Inc., 2009.
34. Nalaini D. Sabapathy,” Heat and Mass Transfer during Cooking of Chickpea Measurements and Computational Simulation”, Unpublished thesis, University of Saskatchewan, 2005.
35. Nantawan Therdthai, Weibiao Zhou, Thomas Adamczak, “Optimization of the Temperature Profile in Bread Baking”, Journal of Food Engineering, volume 55, pages 41–48. 2002.
36. Puri V. M. & Anantheswaranb R. C.,"The Finite-Element Method in Food Processing: A Review”, Journal of Food Engineering, volume 19, pages 247-274, 1993.
37. Rao S. S, The Finite Element Method in Engineering, Fourth Edition, Elsevier Science & Technology Books, USA, December 2004.
38. Ressing H., M. Ressing, T. Durance, "Modeling the Mechanisms of Dough Puffing During Vacuum Microwave Drying Using the Finite Element Method”, Journal of Food Engineering, volume 82, page 498–508, 2007.
39. Rita M. Abalone, Analía G. Gastón1, and Miguel A. Lara,” Effect of Phase Change Criterion on the Prediction of Temperature Evolution During Food Drying”, Mecanica Computacional vol XXIV, 1135- 1147, Buenos Aires, Argentina, 2005.

40. Sablani S. S., Marcotte M., Baik O. D., and Castaigne F., Review Article: “Modeling of Simultaneous Heat and Water Transport in the Baking Process”, Lebensm.-Wiss. U. - Technol., 31, 201–209, 1998.
41. Sadik Kakac and Yaman Yener, Convective Heat Transfer, Second Edition, CRC Press, 1995, Tokyo.
42. Shaifur Rahman, Food Properties Handbook, second edition. CRC press, Washington, D.C, 1995.
43. Shahin Rafiee, Alireza Keyhani and Ali Mohammadi, “Soybean Seeds Mass Transfer Simulation during Drying Using Finite Element Method”, World Applied Sciences Journal 4 (2): 284-288, 2008.
44. Sharanjeet Dhawan and Sheo Kumar, “A Comparative Study of Numerical Techniques for 2D Transient Heat Conduction Equation using Finite Element Method”, International Journal of Research and Reviews in Applied Sciences, Volume 1, Issue 1(October 2009).
45. Tong C.H., and Lund, D.B., “Microwave Heating of Baked Dough Products with Simultaneous Heat and Moisture Transfer”, Journal of Food Engineering, 19,319-339, 1993.
46. Wu Y., Irudyaraj J., “Analysis of Heat, Mass and Pressure Transfer in Starch Based Food Systems”, Journal of Food Engineering, 29, 399-414, 1996.
47. Young W. Kwon, The Finite Element Method Using Matlab, Second Edition, CRC press, 1997.
48. Yunus, A. Cengal, Heat Transfer: A practical Approach, McGraw-Hill series in Mechanical Engineering, USA, 1998.
49. Zanoni B., Peri C. and S. Pierucci, “A Study of the Bread-Baking Process I: A Phenomenological Model”, Journal of Food Engineering, 19, No. 4, 389-398, 1993.
50. Zanoni B., Pierucci S., Peri C., “Study of the Bread Baking Process-II. Mathematical Modeling”, Journal of Food Engineering, 23, 321-336, 1994.
51. Zhang J., Datta, A.K. "Mathematical Modeling of Bread Baking Process”, Journal of Food Engineering, volume 75, pages 78–89, 2006.
52. Zheleva Ivanka and Kambourov Vesselka, “Identification of Heat and Mass Transfer Processes in Bread during Baking”, Thermal Science: Vol. 9, No. 2, pp. 73-86, 2005.

Appendix A

Property Table

Table A-1: Property design data for thermia oil B

Temperature (^oC)	Density (kg/m^3)	Specific heat ($kJ/kg.K$)	Thermal conductivity ($W/m.K$)	Kinematic viscosity ($10^{-6}\times m^2/s$)	Prandtle number
0	876	1.809	0.136	230	3375
20	863	1.882	0.134	-	919
40	850	1.954	0.133	25	375
60	837	2.027	0.131	18.2	273
80	824	2.100	0.129	11.5	171
100	811	2.173	0.128	4.7	69
120	797.8	2.246	0.127	-	54
150	778	2.355	0.125	-	32
200	746	2.538	0.121	1.2	20
250	713	2.720	0.118	-	14
300	681	2.902	0.114	0.5	11
320	668	2.975	0.113	-	10
340	655	3.048	0.111	-	9

APPENDIX B

Experimental and simulation results

Table B-1: Heat up time results for $3kw$ and $0.02m$ electric clay baking pan obtained from Matlab

Time (s)	Temp. (^oC)	Time (s)	Temp. (^oC)	Time (s)	Temp. (^oC)	Time (s)	Temp. (^oC)	Time (s)	Temp. (^oC)
0	20	200	54.57	400	102.34	600	146.05	800	185.40
5	20.08	205	55.79	405	103.49	605	147.09	805	186.33
10	20.12	210	57.01	410	104.63	610	148.12	810	187.26
15	20.15	215	58.23	415	105.77	615	149.15	815	188.19
20	20.20	220	59.45	420	106.91	620	150.18	820	189.11
25	20.33	225	60.67	425	108.05	625	151.20	825	190.03
30	20.55	230	61.89	430	109.18	630	152.22	830	190.95
35	20.87	235	63.11	435	110.31	635	153.24	835	191.87
40	21.28	240	64.33	440	111.44	640	154.26	840	192.78
45	21.78	245	65.55	445	112.57	645	155.27	845	193.70
50	22.36	250	66.76	450	113.69	650	156.28	850	194.61
55	23.01	255	67.98	455	114.81	655	157.29	855	195.51
60	23.73	260	69.19	460	115.93	660	158.30	860	196.42
65	24.50	265	70.41	465	117.04	665	159.30	865	197.32
70	25.33	270	71.62	470	118.15	670	160.30	870	198.22
75	26.20	275	72.83	475	119.26	675	161.30	875	199.12
80	27.12	280	74.03	480	120.36	680	162.29	880	200.00
85	28.07	285	75.24	485	121.47	685	163.29		
90	29.06	290	76.44	490	122.57	690	164.27		
95	30.06	295	77.64	495	123.66	695	165.26		
100	31.12	300	78.84	500	124.76	700	166.25		
105	32.19	305	80.04	505	125.85	705	167.23		
110	33.27	310	81.24	510	126.94	710	168.21		
115	34.38	315	82.43	515	128.02	715	169.18		
120	35.50	320	83.62	520	129.11	720	170.16		
125	36.64	325	84.81	525	130.19	725	171.13		
130	37.78	330	85.99	530	131.26	730	172.10		
135	38.94	335	87.18	535	132.34	735	173.07		
140	40.11	340	88.36	540	133.41	740	174.03		
145	41.29	345	89.54	545	134.48	745	174.99		
150	42.48	350	90.72	550	135.54	750	175.95		
155	43.67	355	91.89	555	136.61	755	176.91		
160	44.87	360	93.06	560	137.67	760	177.86		
165	46.07	365	94.23	565	138.73	765	178.81		
170	47.27	370	95.39	570	139.78	770	179.76		
175	48.48	375	96.56	575	140.83	775	180.71		
180	49.69	380	97.72	580	141.88	780	181.65		
185	50.91	385	98.88	585	142.93	785	182.59		
190	52.13	390	100.04	590	143.97	790	183.53		
195	53.35	395	101.19	595	145.01	795	184.47		

Table B-2: Heat up time results for a $3kw$ and $0.02m$ electric clay baking pan obtained from experiment

Time (s)	Temp. (^oC)	Time (s)	Temp. (^oC)	Time (s)	Temp. (^oC)	Time (s)	Temp. (^oC)	Time (s)	Temp. (^oC)	Time (s)	Temp. (^oC)
0	23.77	70	24.45	139	31.94	209	48.27	279	70.34	348	92.28
2	23.79	72	24.56	141	32.20	211	48.81	280	70.76	349	92.83
4	23.71	73	24.60	143	32.54	213	49.28	282	71.24	351	93.78
6	23.76	75	24.70	144	32.78	215	49.81	284	71.93	353	94.15
7	23.79	77	24.77	146	33.07	216	50.23	286	72.37	355	94.56
9	23.76	79	24.85	148	33.38	218	50.76	287	73.01	356	94.88
11	23.76	80	24.99	149	33.69	220	51.20	289	73.63	358	95.44
13	23.76	82	25.04	151	34.00	222	51.71	291	73.96	360	96.03
14	23.77	84	25.18	153	34.35	223	52.15	292	74.42	362	96.49
16	23.73	85	25.27	155	34.77	225	52.74	294	74.52	363	96.74
18	23.79	87	25.38	156	35.13	227	53.26	296	74.65	365	97.10
19	23.79	89	25.51	158	35.52	228	53.86	298	74.89	367	97.57
21	23.75	91	25.61	160	35.96	230	54.52	299	75.03	368	98.39
23	23.76	92	25.75	162	36.31	232	55.14	301	75.46	370	98.94
25	23.77	94	25.89	163	36.72	234	55.69	303	73.50	372	99.50
26	23.80	96	26.05	165	37.11	235	56.17	305	75.81	374	100.19
28	23.79	98	26.17	167	37.50	237	56.65	306	76.56	375	100.52
30	23.79	99	26.32	169	37.90	239	57.14	308	77.70	379	100.66
32	23.80	101	26.44	170	38.34	241	57.74	310	78.71	381	101.07
33	23.80	103	26.66	172	38.71	242	58.28	311	79.78	383	101.63
35	23.82	104	26.86	174	39.15	244	59.03	313	80.61	384	101.90
37	23.83	106	27.01	176	39.68	246	59.59	315	81.50	386	102.45
39	23.84	108	27.22	177	40.13	248	60.18	317	82.26	388	102.96
40	23.86	110	27.38	179	40.58	249	60.75	318	82.79	390	103.76
42	23.87	111	27.68	181	40.96	251	61.34	320	83.22	391	104.37
44	23.88	113	27.87	183	41.34	253	62.03	322	83.91	393	105.12
46	23.89	115	28.11	185	41.83	254	62.53	324	84.63	395	105.53
47	23.90	117	28.35	187	42.22	256	63.03	325	85.48	397	105.92
49	23.96	118	28.57	189	42.72	258	63.51	327	86.13	398	106.55
51	23.94	120	28.77	190	43.14	260	64.10	329	86.84	400	107.17
52	23.97	122	29.03	192	43.60	261	64.77	330	87.45	402	107.39
54	24.04	124	29.29	194	43.98	263	65.28	332	88.10	403	107.80
56	24.06	125	29.48	196	44.42	265	65.83	334	88.56	405	108.20
58	24.11	127	29.73	197	44.90	266	66.39	336	89.22	406	108.67
59	24.15	129	30.03	199	45.44	268	67.00	337	89.68	407	109.06
61	24.16	130	30.37	201	45.83	270	67.67	339	90.25	408	109.49
63	24.21	132	30.59	203	46.28	272	68.44	341	90.77	410	110.15
65	24.33	134	30.90	204	46.81	273	68.84	343	90.98	412	110.73
66	24.33	136	31.28	206	47.29	275	69.24	344	91.36	413	111.25
68	24.40	137	31.57	208	47.77	277	69.87	346	91.80	415	111.95

...experimental result continued

Time (s)	Temp. (ºC)	Time (s)	Temp. (ºC)	Time (s)	Temp. (ºC)	Time (s)	Temp. (ºC)	Time (s)	Temp. (ºC)	Time (s)	Temp (ºC)
417	112.51	487	116.29	558	128.06	631	148.22	703	171.58	774	186.10
419	113.03	489	116.35	560	128.65	633	149.55	705	171.52	776	186.99
420	113.58	490	116.41	561	129.61	635	149.67	707	171.12	778	187.42
422	113.65	492	116.47	563	130.56	637	150.78	708	170.69	779	188.61
424	113.80	494	116.53	565	130.86	639	151.76	710	171.04	781	188.92
426	113.87	496	116.59	566	131.59	641	152.44	712	171.35	783	190.20
427	113.95	497	116.65	568	132.50	642	152.81	713	171.99	785	190.57
429	114.07	499	116.71	570	132.91	644	153.55	715	172.06	786	190.59
431	114.14	501	116.77	572	132.98	646	154.49	717	172.48	788	190.65
433	114.23	502	116.83	573	133.67	648	155.00	719	173.26	790	190.88
434	114.38	504	116.89	575	134.12	649	155.97	720	174.12	792	191.10
436	114.53	506	116.95	579	134.53	651	156.44	722	175.07	793	191.20
438	114.60	508	117.01	581	135.01	653	156.59	724	175.20	795	191.57
439	114.62	509	117.26	582	136.07	654	156.24	726	175.94	797	191.80
441	114.73	511	116.53	584	136.71	656	156.68	727	176.12	799	191.95
443	114.87	513	117.71	586	137.14	658	156.92	729	176.11	800	192.58
445	114.94	515	117.85	588	137.86	660	156.62	731	176.37	802	192.98
446	115.00	516	117.53	589	138.50	661	156.61	733	177.03	804	194.14
448	115.06	518	117.94	591	139.41	663	157.60	734	177.26	806	194.47
450	115.12	520	118.27	593	139.75	665	157.19	736	178.41	807	196.26
452	115.19	521	118.84	595	139.25	667	157.84	738	179.13	809	196.55
453	115.23	523	119.22	596	139.39	668	158.12	739	179.54	811	196.78
455	115.27	525	119.98	598	140.99	670	159.73	741	179.62	812	197.06
457	115.32	527	120.73	600	141.16	672	160.04	743	179.65	814	197.17
458	115.36	528	121.13	601	141.60	674	160.15	745	180.84	816	197.30
460	115.40	530	121.65	603	142.01	675	161.07	746	180.45	818	197.16
462	115.45	532	122.48	605	142.05	677	161.07	748	182.24	819	197.32
464	115.49	534	122.05	607	142.48	679	161.32	750	182.18	821	198.22
465	115.52	535	122.29	608	143.43	681	161.66	752	182.37	823	199.11
467	115.56	537	123.08	610	144.10	682	162.61	753	182.47	825	199.16
468	115.70	539	125.35	612	144.96	684	163.00	755	182.18	826	199.36
470	115.75	541	124.33	614	145.77	686	164.12	757	183.00	828	199.38
471	115.80	542	125.43	615	145.10	687	165.07	759	183.03	830	199.40
473	115.83	544	125.61	617	145.15	689	165.83	760	183.47	832	199.45
475	115.88	546	125.83	619	145.50	691	167.71	762	183.55	833	199.57
477	115.92	547	126.16	621	145.83	693	168.31	764	183.58	835	199.67
478	115.97	549	126.51	622	145.84	694	169.12	766	183.61	837	199.76
480	116.06	551	126.80	624	145.85	696	170.53	767	184.05	839	199.96
482	116.11	553	127.29	626	146.87	698	171.23	769	184.21	841	200.00
483	116.17	554	127.53	627	147.01	700	171.46	771	184.02		
485	116.23	556	127.58	629	147.32	701	171.48	772	184.78		

APPENDIX C

Matlab Codes

```
%-----------------------------------------------------------------------------------------------------------------------------------
%Matlab program to solve the axisymmetric transient heat transfer during heat up and cyclic injera baking

% N.B:  the boundary condition varies depending on the power source used (electric or heated oil)
%-----------------------------------------------------------------------------------------------------------------------------------

% T,rr + (T,r)/r + T,zz =a T,t, 0< r < 0.3, 0 < z < 0.02

% T,r(0,z) = 0, T,r(0.3,z) = (20/0.8)*(T-20)

% using linear triangular elements
% Variable descriptions
% k = element matrix
% f = element vector
% kk = system matrix
% ff = system vector
% gcoord = coordinate values of each node
% nodes = nodal connectivity of each element
% index = a vector containing system dofs associated with each element
% bcdof = a vector containing dofs associated with boundary conditions
% bcval = a vector containing boundary condition values
%-----------------------------------------------------------------------------------------------------------------------------------
clear all
%-----------------------------------------------------------------------------------------------------------------------------------
% input data for control parameters
%-----------------------------------------------------------------------------------------------------------------------------------
 nel=260;                                                    % number of elements

nnel=3;                                                      % number of nodes per element

ndof=1;                                                      % number of dofs per node

nnode=154;                                                   % total number of nodes in system

sdof=nnode*ndof;                                             % total system dofs

deltt=1;                                                     % time step size for transient analysis

stime=0.0;                                                   % initial time

ftime=1585;                                                  % termination time

ntime=fix((ftime-stime)/deltt);                              % number of time increment

iel=1:nel;

for nel=1:200

   rho=2400;                                                 % Density of the material[kg/m3]
```

```
    cp=960;                                                    % heat capacity of the material[J/kg.K]
    k=0.8;                                                     % thermal conductivity of material [W/m.K]
   a=(rho*cp)/k;                                               % coefficient for the transient term
end
for nel=201:260
    sigma=0.56;                                                % thermo-gradient coefficient [degree M/K]
   lamda=2.257*10^(6);                                         % latent heat of vaporization of water vapor [J/kg]
    epsilon=0.3;                                               % ratio of vapordiffussion coefficient to diffusion of moisture
   D=0.288 *10^(-4);                                           %Diffusion coefficient between air and water [m2/s]
    rho=1160.29;                                               % Density of Injera[kg/m3]
    cp=3440.1;                                                 % heat capacity of Injera[J/kg.K]
   k=0.655;                                                    % thermal conductivity of Injera pest initial[W/m.K]
% a= (rho*cp)/ (k+ (epsilon*lamda*rho*sigma* D))
end
hc1=15.9;                  % convective + radiative heat transfer coefficient of air[W/m2.K] over the surface of pan
b1=hc1/k; d1=20;                                               % Constants for Cauchy-type BC (dT/dn=b(T-d))
%-------------------------------------------------------------------------------------------------------------------------
%boundary condition for only heated oil baking pans
%-------------------------------------------------------------------------------------------------------------------------
 hc2=354.532;                                                  %convective heat transfer coefficient of Thermia oil B[W/m2.K]
 b2=hc2/k; d2=275;                                             %Constants for Cauchy-type BC (dT/dn=b(T-d))
%-------------------------------------------------------------------------------------------------------------------------
%boundary condition for only electric baking pans
%-------------------------------------------------------------------------------------------------------------------------
%hc2=2.5;                                                      % convective transfer coefficient of air [W/m2.K]
%b2=hc2/k; d2=20;                                              %Constants for Cauchy-type BC (dT/dn=b(T-d))
%-------------------------------------------------------------------------------------------------------------------------
 hc4=2000; b4=hc4/k; d4=90;                                    % boiling heat transfer coefficient
 % teta=0;                                                     % Forward difference method for time scheme
teta=1;                                                        % Back ward difference method for time scheme
 % teta=0.5;                                                   %Crank-Nicolson method for time scheme
% teta=2/3;                                                    % Galerkin's method for time scheme
 nf=40;                                                        % number of element boundaries with flux
nnels=2;                                                       % number of nodes per side of each element
```

```
%-------------------------------------------------------------------------------------------------------------------------------------------------
%input data for nodal coordinate values, gcoord (i,j) wherei->node no, andj->x/y
%-------------------------------------------------------------------------------------------------------------------------------------------------
gcoord=[
0.0 0.0; 0.03 0.0; 0.06 0.0; 0.09 0.0; 0.12 0.0; 0.15 0.0; 0.18 0.0; 0.21 0.0; 0.24 0.0; 0.27 0.0; 0.30 0.0;
0.0 0.0008;0.03 0.0008;0.06 0.0008;0.09 0.0008;0.12 0.0008;0.15 0.0008;0.18 0.0008;0.21 0.0008;0.24
0.0008;0.27 0.0008;0.30 0.0008; 0.00 0.0016;0.03 0.0016;0.06 0.0016;0.09 0.0016;0.12 0.0016;0.15
0.0016;0.18 0.0016;0.21 0.0016;0.24 0.0016;0.27 0.0016;0.30 0.0016; 0.00 0.0024;0.03 0.0024;0.06 0.0024;0.09
0.0024;0.12 0.0024;0.15 0.0024;0.18 0.0024;0.21 0.0024;0.24 0.0024;0.27 0.0024;0.30 0.0024;0.00 0.0032;0.03
0.0032;0.06 0.0032;0.09 0.0032;0.12 0.0032;0.15 0.0032;0.18 0.0032;0.21 0.0032;0.24 0.0032;0.27 0.0032;0.30
0.0032; 0.00 0.004;0.03 0.004;0.06 0.004;0.09 0.004;0.12 0.004;0.15 0.004;0.18 0.004;0.21 0.004;0.24
0.004;0.27 0.004;0.30 0.004; 0.00 0.0048;0.03 0.0048;0.06 0.0048;0.09 0.0048;0.12 0.0048;0.15 0.0048;0.18
0.0048;0.21 0.0048;0.24 0.0048;0.27 0.0048;0.30 0.0048; 0.00 0.0056;0.03 0.0056;0.06 0.0056;0.09 0.0056;0.12
0.0056;0.15 0.0056;0.18 0.0056;0.21 0.0056;0.24 0.0056;0.27 0.0056;0.30 0.0056; 0.00 0.0064;0.03
0.0064;0.06 0.0064;0.09 0.0064;0.12 0.0064;0.15 0.0064;0.18 0.0064;0.21 0.0064;0.24 0.0064;0.27 0.0064;0.30
0.0064; 0.00 0.0072;0.03 0.0072;0.06 0.0072;0.09 0.0072;0.12 0.0072;0.15 0.0072;0.18 0.0072;0.21 0.0072;0.24
0.0072;0.27 0.0072;0.30 0.0072; 0.00 0.008;0.03 0.008;0.06 0.008;0.09 0.008;0.12 0.008;0.15 0.008;0.18
0.008;0.21 0.008;0.24 0.008;0.27 0.008;0.30 0.008;

0 0.009; 0.03 0.009; 0.06 0.009; 0.09 0.009; 0.12 0.009; 0.15 0.009; 0.18 0.009; 0.21 0.009; 0.24 0.009; 0.27 0.009;
0.3 0.009; 0 0.01; 0.03 0.01; 0.06 0.01; 0.09 0.01; 0.12 0.01; 0.15 0.01; 0.18 0.01; 0.21 0.01; 0.24 0.01; 0.27
0.01; 0.3 0.01; 0 0.011; 0.03 0.011; 0.06 0.011; 0.09 0.011; 0.12 0.011; 0.15 0.011; 0.18 0.011; 0.21 0.011; 0.24
0.011; 0.27 0.011; 0.3 0.011];
%-------------------------------------------------------------------------------------------------------------------------------------------------
% input data for nodal connectivity for each element ,nodes(i,j) where i-> element no. and j-> connected nodes
%-------------------------------------------------------------------------------------------------------------------------------------------------
nodes=[
1 2 13 ;2 3 14;3 4 15;4 5 16;5 6 17;6 7 18;7 8 19; 8 9 20;9 10 21;10 11 22; 1 13 12; 2 14 13;3 15 14 ;4 16 15;5 17
16;6 18 17;7 19 18; 8 20 19;9 21 20;10 22 21;12 13 24; 13 14 25;14 15 26; 15 16 27;16 17 28;17 18 29; 18 19 30;19
20 31;20 21 32;21 22 33; 12 24 23;13 25 24; 14 26 25;15 27 26; 16 28 27;17 29 28; 18 30 29;19 31 30;20 32 31;21
33 32; 23 24 35;24 25 36; 25 26 37;26 27 38;27 28 39;28 29 40; 29 30 41;30 31 42;31 32 43; 32 33 44; 23 35 34;24
36 35;25 37 36;26 38 37;27 39 38; 28 40 39; 29 41 40; 30 42 41;31 43 42;32 44 43; 34 35 46;35 36 47;36 37 48;37
38 49;38 39 50; 39 40 51; 40 41 52;41 42 53;42 43 54;43 44 55; 34 46 45;35 47 46;36 48 47; 37 49 48; 38 50 49;39
51 50; 40 52 51;41 53 52;42 54 53;43 55 54; 45 46 57;46 47 58; 47 48 59;48 49 60;49 50 61;50 51 62; 51 52 63;52
53 64;53 54 65; 54 55 66; 45 57 56;46 58 57;47 59 58;48 60 59;49 61 60;50 62 61; 51 63 62; 52 64 63; 53 65 64;54
66 65; 56 57 68;57 58 69;58 59 70;59 60 71;60 61 72; 61 62 73; 62 63 74;63 64 75;64 65 76;65 66 77; 56 68 67;57
69 68;58 70 69; 59 71 70; 60 72 71;61 73 72; 62 74 73;63 75 74;64 76 75;65 77 76; 67 68 79;68 69 80; 69 70 81;70
71 82;71 72 83;72 73 84; 73 74 85;74 75 86;75 76 87; 76 77 88; 67 79 78;68 80 79;69 81 80;70 82 81;71 83 82;72 84
83; 73 85 84; 74 86 85; 75 87 86;76 88 87; 78 79 90;79 80 91;80 81 92;81 82 93;82 83 94; 83 84 95; 84 85 96;85 86
97;86 87 98;87 88 99; 78 90 89;79 91 90;80 92 91; 81 93 92; 82 94 93;83 95 94;84 96 95;85 97 96;86 98 97;87 99
```

```
98;89 90 101;90 91 102;91 92 103;92 93 104;93 94 105; 94 95 106; 95 96 107; 96 97 108; 97 98 109; 98 99 110; 89
101 100; 90 102 101;  91 103 102;  92 104 103;  93 105 104;  94 106 105;95 107 106; 96 108 107;  97 109 108; 98
110 109;  100 101 112; 101 102 113;102 103 114;103 104 115;104 105 116; 105 106 117; 106 107 118; 107 108
119;108 109 120;109 110 121; 100 112 111;101 113 112; 102 114 113; 103 115 114;104 116 115; 105 117 116; 106
118 117;107 119 118;108 120 119;109 121 120;111 112 123;112 113 124;113 114 125;114 115 126;115 116
127;116 117 128;117 118 129;118 119 130;119 120 131;120 121 132;111 123 122;112 124 123;113 125 124;114
126 125;115 127 126;116 128 127;117 129 128;118 130 129;119 131 130;120 132 131;122 123 134;123 124135;124
125 136;125 126 137;126 127 138;127 128 139;128 129 140;129 130 141;130 131 142;131 132 143;122 134133;123
135 134;124 136 135;125 137 136;126 138 137;127 139 138;128 140 139;129 141 140;130 142 141;131 143 42;133
134 145;134 135 146;135 136 147;136 137 148;137 138 149;138 139 150;139 140 151;140 141 152;141 142
153;142 143 154;133 145 144;134 146 145;135 147 146;136 148 147;137 149 148;138 150 149;139 151 150;140
152 151;141 153 152;142 154 153];
%-------------------------------------------------------------------------------------------------------------------------------------------
% input for flux boundary conditions nflx(i,j) where i-> element no. and j-> two side nodes
%-------------------------------------------------------------------------------------------------------------------------------------------
nflx(1,1)=111; nflx(1,2)=112;                                   % nodes on 1st element side with flux
nflx(2,1)=112; nflx(2,2)=113;                                   % nodes on 2nd element side with flux
nflx(3,1)=113; nflx(3,2)=114;                                   % nodes on 3rd element side with flux
nflx(4,1)=114; nflx(4,2)=115;                                   % nodes on 4th element side with flux
nflx(5,1)=115; nflx(5,2)=116;                                   % nodes on 5th element side with flux
nflx(6,1)=116; nflx(6,2)=117;                                   % nodes on 6th element side with flux
nflx(7,1)=117; nflx(7,2)=118;                                   % nodes on 7th element side with flux
nflx(8,1)=118; nflx(8,2)=119;                                   % nodes on 8th element side with flux
nflx(9,1)=119; nflx(9,2)=120;                                   % nodes on 9th element side with flux
nflx(10,1)=120;nflx(10,2)=121;                                  % nodes on 10th element side with flux
nflx(11,1)=1; nflx(11,2)=2;                                     % nodes on 11th element side with flux
nflx(12,1)=2; nflx(12,2)=3;                                     % nodes on 12th element side with flux
nflx(13,1)=3; nflx(13,2)=4;                                     % nodes on 13th element side with flux
nflx(14,1)=4; nflx(14,2)=5;                                     % nodes on 14th element side with flux
nflx(15,1)=5; nflx(15,2)=6;                                     % nodes on 15th element side with flux
nflx(16,1)=6; nflx(16,2)=7;                                     % nodes on 16th element side with flux
nflx(17,1)=7; nflx(17,2)=8;                                     % nodes on 17th element side with flux
nflx(18,1)=8; nflx(18,2)=9;                                     % nodes on 18th element side with flux
nflx(19,1)=9; nflx(19,2)=10;                                    % nodes on 19th element side with flux
nflx(20,1)=10; nflx(20,2)=11;                                   % nodes on 20th element side with flux
nflx(21,1)=11; nflx(21,2)=22;                                   % nodes on 21th element side with flux
nflx(22,1)=22; nflx(22,2)=33;                                   % nodes on 22th element side with flux
nflx(23,1)=33; nflx(23,2)=44;                                   % nodes on 23th element side with flux
```

```
nflx(24,1)=44; nflx(24,2)=55;                                   % nodes on 24th element side with flux
nflx(25,1)=55; nflx(25,2)=66;                                   % nodes on 25th element side with flux
nflx(26,1)=66; nflx(26,2)=77;                                   % nodes on 26th element side with flux
nflx(27,1)=77; nflx(27,2)=88;                                   % nodes on 27th element side with flux
nflx(28,1)=88; nflx(28,2)=99;                                   % nodes on 28th element side with flux
nflx(29,1)=99; nflx(29,2)=110;                                  % nodes on 29th element side with flux
nflx(30,1)=110; nflx(30,2)=121;                                 % nodes on 30th element side with flux
nflx(31,1)=144; nflx(31,2)=145;                                 % nodes on 31st element side with flux
nflx(32,1)=145; nflx(32,2)=146;                                 % nodes on 32nd element side with flux
nflx(33,1)=146; nflx(33,2)=147;                                 % nodes on 33rd element side with flux
nflx(34,1)=147; nflx(34,2)=148;                                 % nodes on 34th element side with flux
nflx(35,1)=148; nflx(35,2)=149;                                 % nodes on 35th element side with flux
nflx(36,1)=149; nflx(36,2)=150;                                 % nodes on 36th element side with flux
nflx(37,1)=150; nflx(37,2)=151;                                 % nodes on 37th element side with flux
nflx(38,1)=151; nflx(38,2)=152;                                 % nodes on 38th element side with flux
nflx(39,1)=152; nflx(39,2)=153;                                 % nodes on 39th element side with flux
nflx(40,1)=153; nflx(40,2)=154;                                 % nodes on 40th element side with flux
%-------------------------------------------------------------------------------------------------------------------------------
% initialization of matrices and vectors
%-------------------------------------------------------------------------------------------------------------------------------
ffo=zeros(sdof,1);                                              % initialization of system vector
fn=zeros(sdof,1);                                               % initialization of effective system vector
fsol=zeros(sdof,1);                                             % initialization of solution vector
kko=zeros(sdof,sdof);                                           % initialization of system matrix
mm=zeros(sdof,sdof);                                            % initialization of system matrix
index=zeros(nnel*ndof,1);                                       % initialization of index vector
f1=zeros(nnels*ndof,1);                                         % element flux vector
k1=zeros(nnels*ndof,nnels*ndof);                                % flux matrix
index1=zeros(nnels*ndof,1);                                     % flux index vector
%-------------------------------------------------------------------------------------------------------------------------------
% computation of element matrices and vectors and their assembly
%-------------------------------------------------------------------------------------------------------------------------------
for iel=1:nel                                                   % loop for the total number of elements
   nd(1)=nodes(iel,1);                                          % 1st connected node for (iel)-th element
   nd(2)=nodes(iel,2);                                          % 2nd connected node for (iel)-th element
   nd(3)=nodes(iel,3);                                          % 3rd connected node for (iel)-th element
   r1=gcoord(nd(1),1); z1=gcoord(nd(1),2);                      % coord values of 1st node
   r2=gcoord(nd(2),1); z2=gcoord(nd(2),2);                      % coord values of 2nd node
```

```
   r3=gcoord(nd(3),1); z3=gcoord(nd(3),2);                    % coord values of 3rd node
%-------------------------------------------------------------------------------------------------------------------------------
%the following power changing factor and heat load distribution should be included for electric baking pans
%-------------------------------------------------------------------------------------------------------------------------------
 %    factor for changing the power source
%-------------------------------------------------------------------------------------------------------------------------------
%qr=3/3;                                                    % factor for changing the power source
%P1=qr*32.8956;                                            % power distribution per circumference in the 1st loop
%P2=qr*72.3720;                                            % power distribution per circumference in the 2nd loop
%P3=qr*111.8400;                                           % power distribution per circumference in the 3rd loop
%P4=qr*151.3200;                                           % power distribution per circumference in the 4th loop
%P5=qr*190.80;                                             % power distribution per circumference in the 5th loop
%P6=qr*230.280;                                            % power distribution per circumference in the 6th loop
%P7=qr*269.760;                                            % power distribution per circumference in the 7th loop
%P8=qr*309.2400;                                           % power distribution per circumference in the 8th loop
%P9=qr*348.7200;                                           % power distribution per circumference in the 9th loop
%P10=qr*388.2000;                                          % power distribution per circumference in the 10th loop
%P11=qr*427.6320;                                          % power distribution per circumference in the 11th loop
%P12=qr*467.1600;                                          % power distribution per circumference in the 12th loop
%-------------------------------------------------------------------------------------------------------------------------------
%boundary condition due to heat load from the resistors
%-------------------------------------------------------------------------------------------------------------------------------
%ffo(56)=0.416667*P1;                                      % heat generation rate at inside node
%ffo(57)=0.583333*P1+0.25*P2;                              % heat generation rate at inside node
%ffo(58)=0.75*P2+0.083333*P3+0.916667*P4;                  % heat generation rate at inside
%ffo(59)=0.916667*P3+0.08333*P4+0.75*P5;                   % heat generation rate at inside
%ffo(60)=0.25*P5+0.583333*P6;                              % heat generation rate at inside node
%ffo(61)=0.416667*P6+0.41667*P7;                           % heat generation rate at inside node
%ffo(62)=0.58333*P7+0.25*P8;                               % heat generation rate at inside node
%ffo(63)=0.75*P8+0.083333*P9+0.916667*P10;                 % heat generation rate at inside
%ffo(64)=0.916667*P9+0.08333*P10+0.75*P11;                 % heat generation rate at inside
%ffo(65)=0.25*P11+0.583333*P12;                            % heat generation rate at inside node
%ffo(66)=0.416667*P12;                                     % heat generation rate at outside node
%-------------------------------------------------------------------------------------------------------------------------------
index=feeldof(nd,nnel,ndof);                               % extract system dofs associated with element
ko=felpaxt3(r1,z1,r2,z2,r3,z3);                            % compute element matrix
m=a*felpt2t3(r1,z1,r2,z2,r3,z3);                           % compute element matrix
```

```
   kko=feasmbl1(kko,ko,index);                                   % assemble element matrices
   mm=feasmbl1(mm,m,index);                                      % assemble element matrices
end
%-------------------------------------------------------------------------------------------------------------------------
                                                % initial conditions
%-------------------------------------------------------------------------------------------------------------------------
for in=1:sdof
   fsol(in)=20;                                                  % initial condition
end
   sol(1,1)=fsol(8);                                          % sol contains time-history solution at node 8
   sol(2,1)=fsol(30);                                        % sol contains time-history solution at node 30
   sol(3,1)=fsol(63);                                        % sol contains time-history solution at node 63
   sol(4,1)=fsol(74);                                        % sol contains time-history solution at node 74
   sol(5,1)=fsol(96);                                        % sol contains time-history solution at node 96
   sol(6,1)=fsol(118);                                      % sol contains time-history solution at node 118
   sol(7,1)=fsol(149);                                      % sol contains time-history solution at node 149
%-------------------------------------------------------------------------------------------------------------------------
% additional computation due to convection boundary condition
%-------------------------------------------------------------------------------------------------------------------------
for it=1:deltt:ntime
      kk=kko; ff=ffo;
%-------------------------------------------------------------------------------------------------------------------------
%additional computation due to flux BC on bottom surface and side of the pan
%-------------------------------------------------------------------------------------------------------------------------
for ifx=11:30
   nds(1)=nflx(ifx,1);                                       % extract node with flux BC for (ifx)-th element
   nds(2)=nflx(ifx,2);                                       % extarct node with flux BC for (ifx)-th element
   r1=gcoord(nds(1),1); z1=gcoord(nds(1),2);                                    % nodal coordinate
   r2=gcoord(nds(2),1); z2=gcoord(nds(2),2);                                    % nodal coordinate
   eleng=sqrt((r2-r1)*(r2-r1)+(z2-z1)*(z2-z1));                                 % element side length
   index1=feeldof(nds,nnels,ndof);                                              % find related system dofs
   b=b2; d=d2;
   k1=b*feflxl2(eleng,r1,r2);                              % compute element matrix due to convection bound.
   f1=b*d*fef1l(eleng,r1,r2);                              % compute element vector due to convection bound.
   [kk,ff]=feasmbl2(kk,ff,k1,f1,index1);                                        % assembly
end
%-------------------------------------------------------------------------------------------------------------------------
% additional computation due to flux BC on top surface of the pan
%-------------------------------------------------------------------------------------------------------------------------
for ifx=1:10
```

```
nds(1)=nflx(ifx,1);                                  % extract node with flux BC for (ifx)?th element
nds(2)=nflx(ifx,2);                                  % extarct node with flux BC for (ifx)?th element
r1=gcoord(nds(1),1); z1=gcoord(nds(1),2);            % nodal coordinate
r2=gcoord(nds(2),1); z2=gcoord(nds(2),2);            % nodal coordinate
eleng=sqrt((r2-r1)*(r2-r1)+(z2-z1)*(z2-z1));         % element side length
index1=feeldof(nds,nnels,ndof);                      % find related system dofs
 if it<=355                                          %heat up period
   nel=200; nnode=121;
   b=b1; d=d1;
elseif it>355 & it <=505                             %baking period
   nel=260;nel=260;   nnode=154;
   b=b4; d=d4;
   b1=0;  d1=0;
elseif it>505 & it <=625                             % idle period
   nel=200; nnode=121;
   b=b1; d=d1;
elseif it>625 & it <=775                             %baking period
   nel=260;   nnode=154;
   b=b4; d=d4;
   b1=0;  d1=0;
elseif it>775 & it <=895                             % idle period
   nel=200; nnode=121;
   b=b1; d=d1;
elseif it>895 & it <=1045                            %baking period
   nel=260;   nnode=154;
   b=b4; d=d4;
   b1=0;  d1=0;
elseif it>1045 & it <=1165                           % idle period
   nel=200; nnode=121;
   b=b1; d=d1;
elseif it>1165& it <=1315
   nel=260;   nnode=154;                             %baking period
   b=b4; d=d4;
   b1=0;  d1=0;
elseif it>1315 & it <=1435                           % idle period
   nel=200; nnode=121;
   b=b1; d=d1;
   b1=0;  d1=0;
```

```
    else
       nel=260;   nnode=154;                                          %baking period
       b=b4; d=d4;
       b1=0;  d1=0;
    end
k1=b*feflxl2(eleng,r1,r2);                          % compute element matrix due to convection bound.
f1=b*d*fef1l(eleng,r1,r2);                          % compute element vector due to convection bound.
[kk,ff]=feasmbl2(kk,ff,k1,f1,index1);                                  % assembly
end
for ifx=31:40
    nds(1)=nflx(ifx,1);                          % extract node with flux BC for (ifx)?th element
    nds(2)=nflx(ifx,2);                          % extarct node with flux BC for (ifx)?th element
    r1=gcoord(nds(1),1); z1=gcoord(nds(1),2);                          % nodal coordinate
    r2=gcoord(nds(2),1); z2=gcoord(nds(2),2);                          % nodal coordinate
    eleng=sqrt((r2-r1)*(r2-r1)+(z2-z1)*(z2-z1));                       % element side length
    index1=feeldof(nds,nnels,ndof);                                % find related system dofs
    if it<=355                                                             %heat up period
       nel=200; nnode=121;
       b=0; d=0;
    elseif it>355 & it <=505                                               %baking period
       nel=260;   nnode=154;
       b=b1;  d=d1;
    elseif it>505 & it <=625                                               % idle period
       nel=200; nnode=121;
       b=0; d=0;
    elseif it>625 & it <=775                                               %baking period
       nel=260;   nnode=154;
       b=b1;  d=d1;
    elseif it>775 & it <=895                                               % idle period
       nel=200; nnode=121;
       b=0; d=0;
    elseif it>895 & it <=1045                                              %baking period
       nel=260;   nnode=154;
       b=b1;  d=d1;
    elseif it>1045 & it <=1165                                             % idle period
       nel=200; nnode=121;
       b=0; d=0;
```

```
   elseif it>1165 & it <=1315                                        %baking period
      nel=260;   nnode=154;
      b=b1;  d=d1;
   elseif it>1315 & it <=1435                                        % idle period
      nel=200; nnode=121;
      b=0; d=0;
   else
      nel=260;   nnode=154;                                          %baking period
      b=b1;  d=d1;
   end
   k1=b*feflxl2(eleng,r1,r2);                                        % compute element matrix due to convection bound.
   f1=b*d*fef1l(eleng,r1,r2);                                        % compute element vector due to convection bound.
   [kk,ff]=feasmbl2(kk,ff,k1,f1,index1);                             % assembly
end
aa=mm+deltt*teta*kk;
vv=deltt*ff+(mm-deltt*(1-teta)*kk)*fsol;                             % compute effective column vector
fsol=aa\vv;                                                          % solve the matrix equation
if it<=355
   nel=200; nnode=121;
   sol(1,it+1)=fsol(8);                                              % sol contains time history solution at node 8
   sol(3,it+1)=fsol(63);                                             % sol contains time history solution at node 63
   sol(6,it+1)=fsol(118);                                            % sol contains time history solution at node 118
   fsol(149)=20;
   sol(7,it+1)=20;
elseif it>355 & it <=505
   nel=260;   nnode=154;
   sol(1,it+1)=fsol(8);                                              % sol contains time history solution at node 8
   sol(3,it+1)=fsol(63);                                             % sol contains time history solution at node 63
   sol(6,it+1)=fsol(118);                                            % sol contains time history solution at node 118
   sol(7,it+1)=fsol(149);                                            % sol contains time history solution at node 151
elseif it>505 & it <=625
   nel=200; nnode=121;
   sol(1,it+1)=fsol(8);                                              % sol contains time history solution at node 8
   sol(3,it+1)=fsol(63);                                             % sol contains time history solution at node 63
   sol(6,it+1)=fsol(118);                                            % sol contains time history solution at node 118
   fsol(149)=20;
   sol(7,it+1)=20;
elseif it>625 & it <=775
```

```
    nel=260;   nnode=154;
    sol(1,it+1)=fsol(8);                    % sol contains time history solution at node 8
    sol(3,it+1)=fsol(63);                   % sol contains time history solution at node 63
    sol(6,it+1)=fsol(118);                  % sol contains time history solution at node 118
    sol(7,it+1)=fsol(149);                  % sol contains time history solution at node 151
elseif it>775 & it <=895
    nel=200; nnode=121;
    sol(1,it+1)=fsol(8);                    % sol contains time history solution at node 8
    sol(3,it+1)=fsol(63);                   % sol contains time history solution at node 63
    sol(6,it+1)=fsol(118);                  % sol contains time history solution at node 118
    fsol(149)=20;
    sol(7,it+1)=20;
elseif it>895 & it <=1045
    nel=260;   nnode=154;
    sol(1,it+1)=fsol(8);                    % sol contains time history solution at node 8
    sol(3,it+1)=fsol(63);                   % sol contains time history solution at node 63
    sol(6,it+1)=fsol(118);                  % sol contains time history solution at node 118
    sol(7,it+1)=fsol(149);                  % sol contains time history solution at node 151
elseif it>1045& it <=1165
    nel=200; nnode=121;
    sol(1,it+1)=fsol(8);                    % sol contains time history solution at node 8
    sol(3,it+1)=fsol(63);                   % sol contains time history solution at node 63
    sol(6,it+1)=fsol(118);                  % sol contains time history solution at node 118
    fsol(149)=20;
    sol(7,it+1)=20;
elseif it>1165 & it <=1315
    nel=260;   nnode=154;
    sol(1,it+1)=fsol(8);                    % sol contains time history solution at node 8
    sol(3,it+1)=fsol(63);                   % sol contains time history solution at node 63
    sol(6,it+1)=fsol(118);                  % sol contains time history solution at node 118
    sol(7,it+1)=fsol(149);                  % sol contains time history solution at node 151
elseif it>1315& it <=1435
    nel=200; nnode=121;
    sol(1,it+1)=fsol(8);                    % sol contains time history solution at node 8
    sol(3,it+1)=fsol(63);                   % sol contains time history solution at node 63
    sol(6,it+1)=fsol(118);                  % sol contains time history solution at node 118
    fsol(149)=20;
```

```
   sol(7,it+1)=20;
else
   nel=260;   nnode=154;
   sol(1,it+1)=fsol(8);                                    % sol contains time history solution at node 8
   sol(3,it+1)=fsol(63);                                   % sol contains time history solution at node 63
   sol(6,it+1)=fsol(118);                                  % sol contains time history solution at node 118
   sol(7,it+1)=fsol(149);                                  % sol contains time history solution at node 151
end
end
%-------------------------------------------------------------------------------------------------------------------------------
%updating and correcting thermal conductivity as a function of time and temperature
%-------------------------------------------------------------------------------------------------------------------------------
for iel=201:260
   a(iel)=(rho*cp)/k;
   M=0.73-(9.9*10^-4)*it;                                  %moisture content as linear function of baking time
   elmcon =[nodes(:,1) nodes(:,2) nodes(:,3)];
   Te(iel) = (1/3)*(fsol(elmcon(iel,1))+ fsol(elmcon(iel,2))+  fsol(elmcon(iel,3)));
   a(iel)=(rho*cp)/(0.18587871+(0.001275388*Te(iel)) + (0.57109*M) + (1.7625*10^-
    3*Te(iel)*M)+(epselon*lamda*rho*sigma*D));
   m=a(iel)*felpt2t3(r1,z1,r2,z2,r3,z3);                   % compute element matrix
   mm=feasmbl1(mm,m,index);                                % assemble element matrices
end
%-------------------------------------------------------------------------------------------------------------------------------
% print fem solutions
%-------------------------------------------------------------------------------------------------------------------------------
store3=[ sol(6,:)]
store4=[ sol(7,:)]
%-------------------------------------------------------------------------------------------------------------------------------
% plot the solution at selected nodes
%-------------------------------------------------------------------------------------------------------------------------------
time=0:deltt:ntime*deltt;
plot(time,sol(1,:),'Color','b','LineWidth',1.75);grid on; hold on;
plot(time,sol(3,:),'Color','g','LineWidth',1.75);hold on;
plot(time,sol(6,:),'Color','r','LineWidth',1.75);hold on;
plot(time,sol(7,:),'Color','b','LineWidth',1.75);hold off;
axis([0,1585,0,320]);set(gca,'xtick',[0:100:1585]);set(gca,'ytick',[0:20:320]);
xlabel('Time (s)','color','b')
```

```
ylabel('Temperature  (\circC)','color','b')
 gtext('node 8');gtext('node 63'); gtext('node 118'); gtext('node 149');
 gtext('inj-1'); gtext('inj-2'); gtext('inj-3'); gtext('inj-4'); gtext('inj-5');

%----------------------------------------------FEM  FUNCTIONS-----------------------------------------------------
%-----------------------------------------------------------------------------------------------------------------
function [m]=felpt2t3(r1,z1,r2,z2,r3,z3)-
%-----------------------------------------------------------------------------------------------------------------
% Purpose:
% element matrix for transient term of two-dimensional
% Laplace's equation using linear triangular element
% Synopsis:
% [m]=felpt2t3(r1,z1,r2,z2,r3,z3)
% Variable Description:
% m - element stiffness matrix (size of 3x3)
% r1, y1 - x and y coordinate values of the first node of element
% r2, y2 - x and y coordinate values of the second node of element
% r3, y3 - x and y coordinate values of the third node of element
%-----------------------------------------------------------------------------------------------------------------
% element matrix
A=0.5*(r2*z3+r1*z2+r3*z1-r2*z1-r1*z3-r3*z2); % area of the triangle
m = (A/60)* [ 6*r1+2*r2+2*r3 2*r1+2*r2+r3 2*r1+r2+2*r3;
2*r1+2*r2+r3 2*r1+6*r2+2*r3 r1+2*r2+2*r3;
2*r1+r2+2*r3 r1+2*r2+2*r3 2*r1+2*r2+6*r3 ];
%-----------------------------------------------------------------------------------------------------------------
function [kk]=feasmbl1(kk,k,index)
%-----------------------------------------------------------------------------------------------------------------
% Purpose:
% Assembly of element matrices into the system matrix
% Synopsis:
% [kk]=feasmbl1(kk,k,index)
% Variable Description:
% kk - system matrix
% k - element matrix
% index - d.o.f. vector associated with an element
%-----------------------------------------------------------------------------------------------------------------
edof = length(index);
for i=1:edof
        ii=index(i);
for j=1:edof
```

```
        jj=index(j);
        kk(ii,jj)=kk(ii,jj)+k(i,j);
end
end
%-------------------------------------------------------------------------------------------------------------------
function [kk,ff]=feasmbl2(kk,ff,k,f,index)
%-------------------------------------------------------------------------------------------------------------------
% Purpose:
% Assembly of element matrices into the system matrix &
% Assembly of element vectors into the system vector
% Synopsis:
% [kk,ff]=feasmbl2(kk,ff,k,f,index)
% Variable Description:
% kk - system matrix
% ff - system vector
% k - element matrix
% f - element vector
% index - d.o.f. vector associated with an element
%-------------------------------------------------------------------------------------------------------------------
edof = length(index);
for i=1:edof
        ii=index(i);
        ff(ii)=ff(ii)+f(i);
for j=1:edof
        jj=index(j);
        kk(ii,jj)=kk(ii,jj)+k(i,j);
end
end
%-------------------------------------------------------------------------------------------------------------------
function [index]=feeldof(nd,nnel,ndof)
%-------------------------------------------------------------------------------------------------------------------
% Purpose:
% Compute system dofs associated with each element
% Synopsis:
% [index]=feeldof(nd,nnel,ndof)
% Variable Description:
% index - system dof vector associated with element "iel"
% iel - element number whose system dofs are to be determined
% nnel - number of nodes per element
```

```
% ndof - number of dofs per node
%-----------------------------------------------------------------------------------------------------------------------
edof = nnel*ndof;
k=0;
for i=1:nnel
        start = (nd(i)-1)*ndof;
for j=1:ndof
        k=k+1;
        index(k)=start+j;
end
end
%-----------------------------------------------------------------------------------------------------------------------
function [f]=fef1l(eleng,r1,r2)
%-----------------------------------------------------------------------------------------------------------------------
% Purpose:
% element vector for f(x)=1
% using linear element
% Synopsis:
% [f]=fef1l(eleng,r1,r2)
% Variable Description:
% f - element vector (size of 2x1)
% xl - coordinate value of the left node
% xr - coordinate value of the right node
%-----------------------------------------------------------------------------------------------------------------------
% element vector
eleng=r2-r1; % element length
f=(eleng/6)*[ 2*r1+r2; r1+2*r2];
%-----------------------------------------------------------------------------------------------------------------------
function [k]=feflxl2(eleng,r1,r2)
%-----------------------------------------------------------------------------------------------------------------------
% Purpose:
% element matrix for Cauchy-type boundary such as du/dn=a(u-b)
% using linear element where a and b are known constants.
% Synopsis:
% [k]=feflxl2(eleng)
% Variable Description:
% k - element vector (size of 2x2)
% eleng - length of element side with given flux
```

```
%-------------------------------------------------------------------------------------------------------------------
% element matrix
=(eleng/12)*[ 3*r1+r2 r1+r2;r1+r2 r1+3*r2];
%-------------------------------------------------------------------------------------------------------------------
function [k]=felpaxt3(r1,z1,r2,z2,r3,z3)
%-------------------------------------------------------------------------------------------------------------------
% Purpose:
% element matrix for axisymmetric Laplace equation
% using three-node linear triangular element
% Synopsis:
% [k]=felpaxt3(r1,z1,r2,z2,r3,z3)
% Variable Description:
% k - element stiffness matrix (size of 3x3)
% r1, z1 - r and z coordinate values of the first node of element
% r2, z2 - r and z coordinate values of the second node of element
% r3, z3 - r and z coordinate values of the third node of element

%-------------------------------------------------------------------------------------------------------------------
% element matrix
%-------------------------------------------------------------------------------------------------------------------
A=0.5*(r2*z3+r1*z2+r3*z1-r2*z1-r1*z3-r3*z2); % area of the triangle
rc=(r1+r2+r3)/3; % r coordinate value of the centroid
k(1,1)=((r3-r2)*((r3-r2))+(z2-z3)*((z2-z3)))/(4*A);
k(1,2)=((r3-r2)*(r1-r3)+(z2-z3)*(z3-z1))/(4*A);
k(1,3)=((r3-r2)*(r2-r1)+(z2-z3)*(z1-z2))/(4*A);
k(2,1)=k(1,2);
k(2,2)=((r1-r3)*(r1-r3)+(z3-z1)*(z3-z1))/(4*A);
k(2,3)=((r1-r3)*(r2-r1)+(z3-z1)*(z1-z2))/(4*A);
k(3,1)=k(1,3);
k(3,2)=k(2,3);
k(3,3)=((r2-r1)*(r2-r1)+(z1-z2)*(z1-z2))/(4*A);
k=rc*k;
```

Declaration

I hereby declare that the work which is being presented in this thesis entitled “Heat Transfer Analysis During the Process of Injera Baking by the Finite Element Method ” is original work of my own, has not been presented for a degree of any other university and all the resource of materials used for this thesis have been duly acknowledged.

_____ _____

Gashaw Getenet Date

This is to certify that the above declaration made by the candidate is correct to the best of my Knowledge.

_____ _____

Dr.-Ing. Demiss Alemu (Advisor) Date